INHIBITION OF CARDIAC ALLOGRAFT ARTERIOSCLEROSIS BY NOS (ENOS OR INOS) SPECIFIC EXPRESSION IN SMOOTH MUSCLE OR ENDOTHELIAL CELLS

by

Jing Lei

Environmental Engineering, BS, Dalian University of Technology, 1993

Biochemical Engineering, MS, Dalian University of Technology, 1996

Submitted to the Graduate Faculty of

School of Medicine in partial fulfillment

of the requirements for the degree of

Doctor of Philosophy

University of Pittsburgh

2008

UNIVERSITY OF PITTSBURGH

School of Medicine

This thesis/dissertation was presented

by

Jing Lei

It was defended on

December 5, 2007

and approved by

Bruce Pitt, PhD, Professor, Department of Environmental and Occupational Health

Anthony J. Demetris, MD, Professor, Cellular and Molecular Pathology Department

Yoram Vodovotz, PhD, Associate Professor, Department of Surgery & Cellular and Molecular Pathology Department

Yifan Dai, MD, PhD, Associate Professor, Department of Surgery

Thesis Director/Dissertation Advisor: Timothy R. Billiar, MD, Professor, Departmental of Surgery & Cellular and Molecular Pathology Department

Inhibition of cardiac allograft arteriosclerosis by specific expression of NOS (eNOS or iNOS) in smooth muscle or endothelial cells

Jing Lei, PhD

University of Pittsburgh, 2008

Cardiac allograft arteriosclerosis (CAA) is the leading cause of death in cardiac transplantation recipients. Nitric oxide (NO) produced by NO donors or nitric oxide synthase (NOS) inhibits smooth muscle cell proliferation and migration, promotes endothelial cell proliferation, blocks endothelial cell apoptosis, prevents platelet and leukocyte adhesion and platelet aggregation. NO has been shown to inhibit intimal hyperplasia and suppress the development of cardiac allograft arteriosclerosis. Conversely, induction of NO in cardiomyocytes leads to myocardial apoptosis and suppresses cardiac function, mainly represented by decreased cardiac contractility. Based on these studies, we hypothesize that cell type-specific overexpression of eNOS or iNOS, in smooth muscle or endothelial cells, will inhibit the development of cardiac allograft arteriosclerosis without suppressing cardiac function. To test this hypothesis, we developed two gene delivery systems that specifically express NO in smooth muscle or endothelial cells. One system we constructed is adenoviral vectors that employed the *fms*-like tyrosine kinase-1 (Flt-1, -748 ~ +284 bp), or the intercellular molecule 2 (ICAM2, -292 ~ +44 bp) promoters to drive the human iNOS specific expression in endothelial cells. Another system we developed is vascular-specific iNOS inducible transgenic mice that employed the GeneSwitch system (Invitrogen) and vascular –specific promoter. We obtained two iNOS transgenic lines, in which iNOS can be induced by the ligand mifepristone with the supply of the Switch protein. To determine the efficacy of eNOS endothelial-specific expression on suppression of cardiac allograft arteriosclerosis, we employed

eNOS transgenic mice in which the human eNOS promoter was driving the human eNOS expression. In a mouse heterotopic transplantation model, the male transgenic and female wild-type counterparts were used as donor and recipient, respectively. The donor grafts were harvested 60 days after transplantation and the percentage of vessel occlusion was determined. The vessel occlusion developed in the transegenic donor did not show significant difference compared to the wild-type control. As an alternative approach, the eNOS/GTPCH double transgenic mice will be used as donor and its efficacy will be determined. We hope that these proof-of -principle studies will serve as the basis for the development of an effective treatment strategy to prevent cardiac allograft arteriosclerosis.

TABLE OF CONTENTS

LIST OF TABLES

LIST OF FIGURES

ACKNOWLEDGEMENT

First, I sincerely thank my mentor, Dr. Timothy R. Billiar, for his scientific tutoring, research guidance, support and patience for these six years. I also sincerely thank my Ph.D committee professors, Drs Bruce Pitt, Yoram Vodovotz, Yifan Dai and Anthony J. Demetris for their research navigation and generous help for these six years. I sincerely thank Dr. Noriko Murase, Dr. Shinichi Kanno, Dr. Hong Sun, Dr. Atsunori Nakao, Dr. Koji Tomiyama, Dr. Eizaburo Sasatomi, Dr. Wentao Gao, Richard Shapiro and Huijie Sun for their research guidance and technical help. I sincerely thank Surgery lab, Dr. Andrea Gambotto's lab, Dr. Simmon Watkin's lab, Dr. Yifan Dai's lab and Dr. Noriko Murase's lab for their generous help.

I sincerely thank Drs Ann Thompson, John Horn, Wendy Mars and Sandra Honick to help me to finish the last piece of melody in my thesis and grow up. I sincerely thank Drs Harvey Borovetz, Stephen Phillips, Savio Woo and Mainak Mazumdar to give me generous help and introduce me from Benedum Hall to Scaif Hall.

Last but not the least, I sincerely thank my parents, Zudi and Xihui, and my bother, Ming, to give me tremendous support for these years. I sincerely thank my friends to bring me warmth and share life with me.

ABBREVIATIONS

murine Tie2 promoter with a 1.6 kb enhancer: defined as Tie2SE in this thesis

murine Tie2 promoter with a 10 kb enhancer: defined as Tie2LE

human intercellular adhesion molecular 2 promoter (-292 ~ +44 bp): ICAM2

human von Willebrand factor promoter (-487 ~ +246 bp): vWF

human *fms*-like tyrosine kinase-1 promoter(-748 ~ +284 bp): Flt-1

rat smooth muscle myosin heavy chain promoter with enhancer (-4229 ~ +11600 bp): defined as SMMHCL

rabbit smooth muscle myosin heavy chain promoter with enhancer (-2305 ~ -4 bp): defined as SMMHCS

bovine aortic endothelial cell: BAEC

smooth muscle cell: SMC

endothelial cell: EC

sodium dodecyl sulphate: SDS

(6*R*)-5,6,7,8-tetrahydrobiopterin: BH_4

superoxide dismutase: SOD

inducible nitric oxide synthase: iNOS

endothelial nitric oxide synthase: eNOS

neuronal nitric oxide synthase: nNOS

sodium nitroprusside: SNP

isosorbide dinitrate: ISDN

S-nitroso-N-acetylpenicillamine: SNAP

N^G-monomethyl-L-arginine: L-NMMA

N(omega)-nitro-L-arginine: L-NNA

N^G-nitro-L-arginine methyl ester: L-NAME

verhoeff's Van Geison staining: vVG staining

1.0 INTRODUCTION

Cardiac transplantation has become an effective treatment for the end-stage cardiac diseases. Current immunosuppressive regimens control acute rejection and has achieved greater than 90% of one year survival (1). However, cardiac allograft arteriosclerosis constitutes the major limitation to long-term survival of the recipients. This disease can be detected by coronary angiography in 6-18% of cardiac recipients at 1 year and in 50% of recipients at 5 years (2, 3). The development of cardiac allograft arteriosclerosis has become the principle cause of late death and allograft dysfunction (4-6). At present, effective treatments for this disease have not yet been found. Retransplantation remains the only alternative, but this is not an effective option given the shortage of organs and only 48% of patients are alive 1-year after retransplantation (7). In addition, cardiac allograft arteriosclerosis can still develop in the second allograft.

1.1 CHARACTERISTICS AND PROPOSED MECHANISM OF CARDIAC ALLOGRAFT ARTERIOSCLEROSIS

Cardiac allograft arteriosclerosis is characterized by a diffuse, concentric form of arteriosclerosis that affects both small intramyocardial and large coronary arteries and veins (8). It is hallmarked by intimal thickening resulting from smooth muscle cell proliferation and migration from the tunica media to the intimal layer and by a paucity of collateral neovascularization (9). This

process appears along the entire length of the affected vessels. This process is not unique to cardiac allograft coronary vessels, but is seen in all solid organ allograft vascular beds (190). The intimal elastic lamina is usually inact, with occasional deposition of calcium (191).

The mechanism for cardiac allograft arteriosclerosis is still not clear. It is proposed that both immunological factors and non-immunological factors contribute to cardiac allograft arteriosclerosis. The immunological factors include histocompatibility (199, 200, 201), acute rejection (202-205) and chronic inflammation. Non-immunological factors are related to ischemia/referfusion injury (206), cytomeganovirus infection (207, 208), age (205, 209), sex (209), hypertension (209), hyperlipidemia (210, 211), heperhomocysteinemia (212-215), insulin restistance (216), obesity and smoking (192). The endothelium functions to regulate vascular tone, prevent coagulation and inhibit thrombosis. Endothelial injury likely initiates the development of cardiac allograft arteriosclerosis. During transplantation, the first injury to the donor allograft is perfusion and ischemia, which injures and activates endothelial cells to express major histocompatibility complex (MHC) class I and II antigens (196, 217, 218). These antigens activate recipient T cells to secrect cytokines, including interlekin-2 (IL-2), IL-4, IL-5, IL-6, interferon-γ (INF-γ), tumor necrosis factor-α (TNF-α) and TNF-β (218). These cytokines promote proliferation of alloreactive T cells and stimulate donor endothelial cells to upregulate adhesion molecules, including vascular cell adhesion molecule-1 (VCAM-1) and intercellular adhesion molecule-1 (ICAM-1) (195, 218). The upregulated adhesion molecules recruit leukocytes, platelets and macrophages which adhere to endothelium and initiate a localized and sustained inflammatory response. Some inflammatory cells transmigrate across the endothelial barrier into the intima. The inflammatory response activates endothelial cells to express endothelin-1, a vessel constrictor that perpetuates the development of cardiac allograft

arterioslerosis (219, 220). The inflammatory response stimulates smooth muscle cells to secret C-reactive protein-1 (CRP-1) (221), which downregulates eNOS expression in endothelial cells (222) and upregulates angiotensin-1 receptor in smooth muscle cells (223). The inflammatory response also stimulates caridomyocytes and the vascular wall to release vascular endothelial growth factor (VEGF) (14), aFGF (12), PDGF-AA (11, 12), thrombospondin-1 (197) and matrix metalloproteinase family: MMP2, MMP3, MMP9 and MMP13 (224-226). Other growth factors and cytokines that are upregulated include PDGF-BB (11, 227), bFGF (11), TNF-α (10, 11, 13), HB-EGF (13) and TGF-β (228). Some of the growth factors and cytokines, including PDGF-AA, PDGF-BB, TGF-β, TNF-α, EGF, FGF, bFGF and IGF-1, thrombosponding-1 and CRP, initiate the transformation of vascular smooth muscle cells from the normal non-proliferative contractile phenotype to a proliferative and synthetic phenotype (15), leading to the proliferation and migration of smooth muscle cells from tunica media to intima layer (10, 16, 17) as well as matrix deposition (18-20). The upregulated matrix metalloproteinases promote the degradation of matrix proteins and faciliates smooth muscle cell migration (229).

The development of cardiac allograft arteriosclerosis is not only associated with a cellular immune response, but also is the result of humoral rejection. The majority of patients produce anti-human leukocyte antigen antibodies (anti-HLA) after transplantation (230-233). The production of anti-HLA antibodies is significantly associated with graft survivral rate and the severity of graft vasculopathy (234, 235).

The extent of cardiac allograft arteriosclerosis is determined by the balance of two inter-related processes: positive and negative remodeling of coronary vessels. Positive remodeling leads to vessel lumen enlargement while negative remodeling means the process of intimal hyperplasia. Some studies (193, 194) showed even though intimal hyperplasia develops at 1 to 3

years after transplantation, positive remodeling offsets the negative remodeling. In these cases, vessel lumen enlarges to a greater extent than the intimal hyperplasia area. However, over time after transplantation, negative remodeling typically dominates and coronary vessel lumen exhibits shrinkage. Gradually, cardiac allograft arteriosclerosis develops.

.

1.2 BIOLOGICAL CHARACTERISTICS OF NO

Nitric Oxide (NO) is an intra- and intercellular signaling molecule that plays important roles in many physiological and pathological processes, including vasodilatation, neuronal transmission, immunomodulation, and cardiac contraction (21-26). In 1992, NO was named as "molecule of the year" by *Science*. In 1998, Nobel Prize in Physiology and Medicine was awarded to Drs Robert F. Furchgott, Louis J. Ignarro and Ferid Murad for their discoveries of NO as a signaling molecule in the cardiovascular system. Over the last two decades, NO has been studied extensively.

NO has a half life of about 6 seconds in biological systems. NO is highly diffusible and can reach adjacent cells quickly. NO can be converted from NO donor, *e.g.* S-nitroso-N-acetylpenicillamine (SNAP), or synthesized from substrate L-arginine under the catalysis of nitric oxide synthase (NOS). There are three NOS isoforms: endothelial NOS (eNOS), neuronal NOS (nNOS) and inducible NOS (iNOS). eNOS is mainly expressed in endothelial cells and is also found in smooth muscle cells, cardiomyocytes, bone cells and neurons. nNOS is mainly expressed in neurons and is also found in skeletal muscle, the pancreas and the kidneys. In contrast, iNOS is not expressed under normal condition but can be induced in almost every cell

type by a variety of stimuli such as inflammatory cytokines, microbes, microbial products (LPS) and mechanical perturbation (27-30).

eNOS and nNOS are constitutively expressed and the activity of these isoforms is activated by increasing intracellular Ca^{2+} fluxes that results in calmodulin binding to the enzyme. In contrast, iNOS activity is not dependent on Ca^{2+} fluxes. eNOS and nNOS generates NO in nanomolar level (25, 31, 32), while iNOS generates NO in micromolar concentration range for long periods of time (22, 23, 25).

1.3 VASOPROTECTIVE ROLES OF NO

NO has been shown to exert many vasoprotective roles in vascular system, including inhibition of smooth muscle cell proliferation and migration, enhancement of endothelial cell proliferation and migration, inhibition of endothelial cell apoptosis, suppression of platelet aggregation and inhibition of platelet, leukocyte and monocyte adhesion to endothelium. These protective roles will be described in detail in the following section.

1.3.1 No inhibits SMC proliferation and migration

The inhibitory effect of NO on SMC proliferation was first demonstrated in 1989 by Garg *et al.* (33). Three NO donors, SNAP, sodium nitroprusside (SNP), and isosorbide dinitrate (ISDN), inhibited SMC proliferation in a dose-dependent pattern. SMC proliferation was assayed by serum-induced [^{3}H] thymidine incorporation. This inhibitory effect was also exhibited by 8-bromo-cGMP. However, SNAP-induced inhibition of proliferation was prevented when

hemoglobin, which scavenges NO, was present. In contrast, SNAP-induced antiproliferation was accelerated when superoxide dismutase (SOD) was added. SOD catalyzes the degradation of superoxide, while superoxide oxidizes NO to form peroxynitrite $ONOO^{\cdot-}$.

Cornwell *et al.* (34) further showed that the cytokine IL-1β or the NO donor, SNAP or SNP, inhibited PDGF-induced SMC proliferation. NO increased cyclic GMP (cGMP) levels, which activated cAMP kinase. However, NO did not change cAMP levels. The cyclic AMP kinase inhibitor (R) p-bromoadenosine 3', 5'-cyclic monophosphorothioate (Rp-8-BrcAMP[S]) reversed NO induced inhibition of SMC proliferation. However, the cyclic GMP kinase inhibitor [(R) p-bromoguanosine 3', 5'-cyclic monophosphorothioate (Rp-8-BrcGMP[S]) did not exhibit this inhibitory effect. Garg and Cornwell's results demonstrated that NO inhibits SMC proliferation through cGMP and cAMP kinase dependent pathways, but not cAMP and cGMP kinase dependent pathway. In 1995, Guo *et al.* also confirmed that SMC proliferation was inhibited by an NO donor 4-hydroxymethyl-furazan-3-carboxylic acid-2-oxide (CAS 1609), but not by the non-NO donating control compound 4-hydroxymethyl-furazan-3-carboxylic acid (C93-4845) (35).

NO has also been shown to inhibit SMC migration (36, 37). In 1995, Dubey *et al.* reported the antimigratory effect of NO on SMC cells (36). SMC migration was induced by angiotensin II in a dose-dependent pattern, which was evaluated using a modified Boydens Chamber. Angiotensin II induced SMC migration was suppressed by the NO donor SNAP or SNP, or 8-bromo cGMP in a dose-dependent pattern. This suppression was reversed by hemoglobin and exaggerated by SOD. The antimigratory effect exhibited by SNAP was partially reversed by the cGMP-dependent protein kinase inhibitor, KT5832, or the inhibitor of soluble

guanylate cyclase LY 83583. However, this antimigratory effect was not changed in the presence of the adenylate cyclase inhibitor, DDA, or the cAMP-dependent protein kinase inhibitor Rp-cAMP. This antimigratory effect was also exhibited when L-arginine was present in SMC in which iNOS was induced by IL-1β. In contrast, the presence of D-arginine did not show any antimigratory effect. Moreover, the NOS inhibitor L-NAME completely abrogated this antimigratory effect. These data suggest that NO inhibits SMC migration partially through a cGMP-dependent pathway. This inhibitory effect of NO was also confirmed by Sarkar *et al.* in 1996 when three other NO donors, diethylamine NONOate, S-nitrosoglutathione and Spermine NONOate, suppressed SMC migration (37).

These studies demonstrate that NO inhibits SMC proliferation and migration partially through the cGMP-dependent pathway.

1.3.2 NO enhances proliferation and migration of endothelial cells and inhibits apoptosis

In 1994, Ziche *et al.* reported that NO promoted endothelial cell proliferation and migration (95). Three NO donors, SNP, ISDN and glyceryl trinitrate, enhanced proliferation of coronary venular endothelial cells, which was determined by [^{3}H]-thymidine incorporation and couting cell number. These NO donors also increased the migration of endothelial cells. In contrast, these promoting effects were reversed by the NOS inhibitor L-NMMA, L-NNA or L-NAME. In 1995, Guo *et al.* also showed that NO promoted endothelial cell proliferation in both cultured endothelial cells and injured carotid arteries (35). NO donor 4-hydroxymethyl-furazan-3-carboxylic acid-2-oxide (CAS-1609) increased proliferation of rat aortic endothelial cells, which was determined by counting the cell number and incorporating 5-bromo-2'-deoxy-uridine (BrdU) into DNA. However, this increase was not observed when cells were treated by a non-

NO-donating control compound, 4-hydroxymethyl-furazan-3-carboxylic acid (C93-4845). Moreover, endothelial regeneration was accelerated in a rat carotid artery injury model when treated by the NO donor CAS-1609, but not by its control compound C93-4845 without the NO moiety.

In 1997, Tzeng *et al.* demonstrated that NO attenuated LPS-induced endothelial cell apoptosis (96). Infection by adenoviral vector AdCMV-iNOS in sheep arterial endothelial cells resulted in a significant enhancement of endothelial cell proliferation without cytotoxicity when assayed by ^{51}Chromium release compared to the AdCMV-lacZ control. Moreover, AdCMV-iNOS infection did not induce endothelial cell apoptosis. In contrast, it inhibited LPS-induced apoptosis, which was detected by internucleosomal DNA fragmentation. These data demonstrate that NO enhances endothelial cell proliferation and migration and inhibits apoptosis.

1.3.3 No suppresses platelet aggregation

In 1983, Mellion *et al.* demonstrated that NO suppressed human platelet aggregation (38). When human platelets were induced to aggregate by aggregating agents, including ADP, collagen, U46619, or sodium arachidonate, three NO donors, SNAP, S-nitrosocysteine, or S-nitroso-β–D-thioglucose inhibited platelet aggregation in a dose-dependent fashion. In contrast, this antiaggregatory effect was attenuated when methemoglobin, a hemoprotein with a high affinity for NO, was present. Concomitantly, the three NO donors also induced a rapid and marked increase in the cGMP levels. This increase was partially reversed by hemoproteins. Meanwhile, cAMP levels were not changed. Moreover, guanylate cyclase that was purified from platelets, was significantly activated by the three NO donors while this activation was attenuated by hemoproteins. This antiaggregatory effect of NO was also confirmed by McCall *et al.* (39).

1.3.4 NO inhibits platelet, leukocyte and monocyte adhesion to endothelium

In 1987, Radomski *et al.* demonstrated that NO supppressed human platelet adhesion to the vascular endothelium (40). Human platelets were radiolabelled with indium-111-oxine and added onto cultured bovine aortic endothelial cell monolayers. Exogenous NO, or bradykinin, which induced NO production and prostacyclin, significantly inhibited platelet adhesion. Addition of aspirin to bradykinin-treated cells, which completely abrogated prostacyclin synthesis, did not affect the adhesion of platelets to the endothelium. In contrast, addition of haemoglobin into bradykinin-treated cells, significantly increased the adhesion. On the contrary, this enhancement of adhesion was not observed when the cells were pretreated with methaemoglobin, which does not scavenge NO. These results clearly indicate that suppression of platelet adhesion is NO-dependent. In 1996, Yan *et al.* further confirmed the inhibitory effect of NO (41) in a rat carotic artery injury model. Platelets were prelabelled with ^{111}In-oxine and injected intraveneously. This was followed by injection of the NOS inhibitor L-NAME. iNOS was strongly induced in the neointima and media layer of the injured segment, but not in the control intact segment. L-NAME significantly increased the deposition of platelets on the injured segment, but not on the control segment. This deposition was L-NAME dose-dependent and was not observed when using its inactive enantiomer, D-NAME. L-NAME treatment also significantly decreased blood flow by 32%, which indicates that NO plays an important role on regulating local blood flow.

In 1991, Kubes *et al.* reported that NO inhibits leukocyte adhesion to vascular endothelium (42). Inhibition of endogenous NO production in postcapillary venules by L-NMMA or L-NAME, increased leukocyte adhesion to the endothelium by 15 times and reduced wall shear rate by half compared to the control. Leukocytes adhesion was observed in single

venules by intravital video microscopy. Leukocyte adhesion was completely reversed by L-arginine and by a leukocyte adhesion glycoprotein CD18-specific antibody IB_4, while D-arginine had no effect. Moreover, SOD, which prevents NO inactivation, has been reported to reverse the adhesion of leukocytes to mesenteric venules (43). To further elucidate the role of NO on leukocytes adhesion, Hickey *et al.* compared adhesion of leukocytes to endothelium between iNOS-deficient and wild-type mice (44). Between 2 and 4 hours after LPS administration, the speed of leukocyte rolling and the number of adherent leukocytes in cremasteric postcapillary venules of the iNOS-deficient mice was significantly higher than that of wild-type mice. The number of leukocytes adherent to postsinusoidal venules in liver was also significantly elevated in iNOS-deficient mice relative to the wild-type mice. Moreover, the number of leukocytes interacting with E-selectin in iNOS-deficient mice was significantly higher than that of the wild-type mice.

In 1998, Peng *et al.* demonstrate that NO inhibited monocyte-endothelial cell interaction (45). When human saphenous vein endothelial cells were treated with the NOS inhibitor LNMA, eNOS activity was inhibited by greater than 85% and this resulted in a significant increase in monocyte adhesion to endothelial cells. When endothelial cells were co-cultured with RAW264.7 cells stimulated by LPS and IFN-γ, NO generated from the RAW264.7 cells significantly prevented monocyte adhesion to the endothelial monolayers. This inhibition is through downregulation of VCAM-1 expression and decrease of NF-κB activity in endothelial cells.

These studies clearly demonstrated that NO inhibits platelet, leukocyte and monocyte adhesion to endothelium.

The information presented in sections 1.3.1, 1.3.2, 1.3.3 and 1.3.4 serves as the basis to view NO as a vasoprotective molecule.

1.4 NO INHIBITS THE DEVELOPMENT OF INTIMAL HYPERPLASIA IN VASCULAR INJURY

1.4.1 Mechanisms for the development of intimal hyperplasia

Intimal hyperplasia is a feature of the healing process following vascular injury. Endothelial dysfunction by either physical force (e.g. balloon angioplasty) or by immune mechanisms (e.g. allograft rejection) initiates the injury response. Platelets immediately adhere to the injured site and aggregate (46). Then leukocytes are recruited to endothelial cells or platelets in the vessel wall. P-selectin glycoprotein ligand-1 (PSGL-1) that is expressed on leukocytes interacts with P-selectin that is expressed on platelets, which facilitates attaching and rolling of leukocytes along the vessel wall (47). β2-integrin Mac-1 (CD11b/CD18) that is expressed on leukocytes and ICAM2, an important β-integrin ligand present on platelets (48), also play an important role in mediating leukocyte-platelet interactions (49). Activated platelets secret PDGF, which initiates SMC migration and proliferation (50, 51). Activated leukocytes, monoctyes, macrophages and mast cells secret growth factors and cytokines, including PDGF, bFGF, IGF-1, EGF, FGF, TNF-α, TGF-β and IL-1β (52), which further perpetuate vascular injury. Next, SMC in the tunica media layer are stimulated to convert from a contractile nonproliferative phenotype to a synthetic proliferative phenotype (53-57) and SMC proliferation and migration from the tunica media layer to the intimal layer are initiated. Numerous extracellular stimuli and intracellular signal

transduction pathways are proposed to be involved. As mentioned above, following vascular injury, many growth factors and cytokines are released, which stimulate SMC to proliferate and migrate to the intimal layer. Faries *et al.* showed that within hours after epigastric vein was interposed into femoral artery, PDGF-AA, bFGF, IGF-1, IL-1β, TNF-α were upregulated and released and this persisted for 2 weeks (58). Tanaka *et al.* showed that TNF-α expression was remarkably induced in SMC of the tunica medial layer in cardiac allografts (59). IL-1α (60), IL-1β (61), IGF-1 (62, 63), EGF (64) and bFGF (65) have been shown to enhance SMC proliferation *in intro*. bFGF has also been shown to strongly induce SMC proliferation in balloon-injured carotid arteries from 11.5 % in the control vessel to 54.8% in the bFGF-treated counterpart (66). PDGF is a strong mitogen to induce SMC migration *in vitro* (67). In balloon expansion induced carotid artery injury, PDGF-BB infused arteries showed significant intimal hyperplasia compared to the vehicle control (68). IGF-1 has been shown to exacerbate intimal hyperplasia in aortic allografts (69). In contrast, inhibition or knockdown of expression of TGF-β (70), TNF-α (71, 72) and bFGF (73) significantly suppressed intimal hyperplasia. SMC begin to proliferate within 24 hours after injury (74) and SMC migration to the intimal layer is seen within 1 to 3 days after injury. Following vascular injury, some of matrix-degrading enzymes, such as plasminogen activator (75) and matrix metalloproteinase (76), are upregulated, which activates the degradation of cellular matrix and facilitates SMC migration. In contrast, a matrix metalloproteinase inhibitor decreased the number of SMC in the intimal layer by 97% compared to the vehicle control (76).

1.4.2 NO inhibits intimal hyperplasia

Based on the vasoprotective actions of NO, it is easy to appreciate that exogenous delivery of NO would inhibit the development of intimal hyperplasia. In 1993, McNamara *et al.* administered the NO substrate, L-arginine to rabbits following catheter-induced injury to the thoracic aorta and observed a drop in intimal hyperplasia by 39% compared to the untreated controls. This reduction in intimal hyperplasia was reversed by co-administration of NOS inhibitor L-NAME (77). Chemical NO donors such as SPM-5185 (78), NO protein adduct S-nitrososerum albumin (79), molsidomine (80), 4-hydroxymethyl-furazan-3-carboxylic acid-2-oxide (81), or direct inhalation of NO (82), were also shown to inhibit intimal hyperplasia in balloon injury models. In 1996, Tzeng *et al.* delivered human iNOS gene to isolated porcine arterial segments by *ex vivo* gene transfer using a retroviral vector. Although only 1% transfection efficiency was obtained, intimal thickening by balloon catheter injury was completely inhibited (83). In another balloon injury model, transfection of rat carotid artery using an adenoviral vector AdiNOS reduced intimal hyperplasia by >95% in the rat carotid artery at 6 weeks post-injury and by 51.8% in the pig iliac artery at 21 days post-injury (84). Not only AdiNOS, but AdeNOS transduced carotid artery also showed reduced intimal hyperplasia at 14 days after injury (85). Moreover, transfection of carotid artery using liposome-DNA plasmid with the iNOS gene also suppressed the development of intimal hyperplasia by 81% at 6 months after injury (86). Moreover, adenoviral-mediated iNOS expression inhibited intimal hyperplasia in the vein grafts by 30% at 21 days after bypass surgery (87). Furthermore, in an aortic transplantation model, when aortic allografts from eNOS knockout mice were transplanted into wild-type mice, intimal hyperplasia was significantly exacerbated at 30 days after transplantation (88). However, overexpression of iNOS by *ex vivo* AdiNOS gene transfer almost completely

prevented the development of aortic allograft arteriosclerosis at 4 weeks after transplantation (88, 89). In contrast, inhibition of iNOS expression by the iNOS inhibitor L-N^6-(l-iminoethyl)-lysine (L-NIL) or cyclosporine A (CsA) increased intimal thickening by 57.2% and 65% respectively (89). The inhibitory effect of NO on intimal hyperplasia was also shown in the jugular vein grafts which were interposed into the carotid artery (90-94). Fulton *et al.* delivered SNAP locally to the vein grafts by mixing SNAP with 30% of pluronic gel and coating the gel on the periadventitial vein surface. The local delivery of SNAP resulted in a 36% decrease in intimal thickness compared to the gel-only treated control (90) at 28 days after transplantation. Other NO donors, spermine/nitric oxide or L-arginine polymer, also showed similar inhibitory effect (91, 92). Using the same transplantation model, West *et al.* showed that AdnNOS gene transfer significantly suppressed the acute inflammation that was represented by the suppressed expression of the leukocyte marker CD18 and RAM11 at 3 days after transplantation. At 28 days post-transplantation, this transient AdnNOS gene transfer decreased intimal thickness by 40% compared to the sham or the Adβgal-treated control (94).

1.5 NO AND CARDIAC ALLOGRAFT ARTERIOSCLEROSIS

Cardiac allograft arteriosclerosis is characterized by intimal thickening resulting from smooth muscle cell proliferation and migration from the tunica media to the intimal layer. It affects the entire coronary tree, including both arteries and veins. Based on the extensive studies that show that NO inhibits intimal hyperplasia in balloon injury models as well as aorta and vein transplantation models, it is reasonable to hypothesize that NO/iNOS plays an inhibitory role on the development of cardiac allograft arteriosclerosis. This has been substantiated in cardiac

transplantation models. For example, in 1996, Lou *et al.* showed that supplying 2.5% L-arginine in the drinking water to rabbit heart transplantation recipients from day 7 to day 42 after transplantation significantly reduced intimal hyperplasia in the donor graft from 44% +/- 4% in the non-L-arginine group to 16% +/- 2% in the L-arginine group ($p < 0.002$) (97). Kown *et al.* have shown that the incubation of donor hearts in L-arginine polymer solution *ex vivo* before transplantation led to the attenuation of intimal hyperplasia even 90 days after transplantation (98). The inhibitory role of NO has also been demonstrated in a previous study where wild-type hearts transplanted into $iNOS^{-/-}$ mice exhibited 25% higher intimal thickening compared to the wild-type controls at 55 days after transplantation (99). One of the characteristics of cardiac allograft arteriosclerosis is the widespread involvement of small, medium and large sizes myocardial vessels. In the $iNOS^{-/-}$ recipients, 97% of the graft vessels were affected, which was significantly higher than the 79% seen in the wild-type controls (99). Furthermore, commonly used immunosuppressants such as FK506, cyclosporine and steroids inhibited the induction of iNOS gene (100-102) and this inhibition can be associated with greater allograft arteriosclerosis (89). Rapamycin, on the other hand, has similar immunosuppressant activities but does not inhibit the expression of iNOS and has been shown to prevent the development of cardiac allograft arteriosclerosis (103, 104).

1.6 NO AND CARDIAC FUNCTION

Exogenous NO has a concentration-dependent effect on myocardial contractility under basal conditions (25). As shown in Figure 1 (25), NO has positive or negative inotropic effects on myocardial contractility, which is dependent on NO concentration. Low concentrations of NO

improved cardiac contractility both *in vitro* (105-107) and *in vivo* (108-110) while high concentrations of NO (> 10^{-7}M) exhibit negative inotropic effects. For example, after iNOS expression was induced in cardiomyocytes by cytokines or *E. Coli.* lipopolysaccharide, the reactivity of the myocardial muscle changed and myocardial contractility decreased (111-115, 166, 236). Here, the response to β-adrenergic stimulation was diminished (114, 115) and higher cardiac myocyte death was observed (116). In contrast, adding an iNOS inhibitor reversed these changes. Overexpression of iNOS in mouse myocardium led to a mild inflammatory cell infiltrate, cardiac fibrosis, hypertrophy, dilatation and a high incidence of sudden cardiac death. This cardiac phenotype was rescued by specific attenuation of iNOS activity (117).

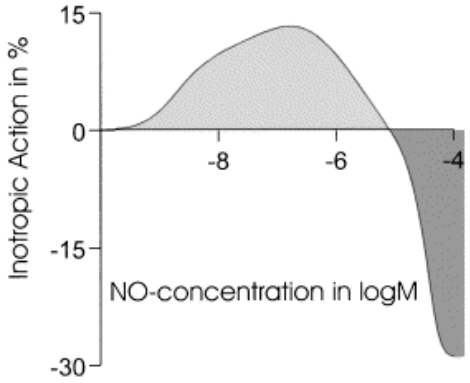

Figure 1 Scheme of the effects of exogenous NO on myocardial contractility under basal conditions.

In contrast to the beneficial effect of iNOS on inhibition of cardiac allograft arteriosclerosis during chronic rejection, there is some evidence that iNOS contributes to the suppression of cardiac function. In cardiac transplant patients, iNOS was shown to be upregulated in cardiomyocytes from initial stage up to 180 days after transplantation (118-120) and this induction was correlated to cardiomyocyte apoptosis (118, 119), and systolic and diastolic left ventricular contractile dysfunction (120). Myocardial iNOS gene expression level

was significantly correlated with the abbreviation of left ventricle electromechanical systole time and the fall of left ventricle end-systolic pressure (121). However, in an animal model of cardiac transplantation, inhibition of iNOS by aminoguanidine or dexamethasone attenuated acute rejection, which was represented by significantly prolonged graft survival (122, 123), reduced inflammatory cell infiltrate, interstitial edema and myocyte injury (122, 123), improved contractile function of papillary muscle (122, 124) and increased left ventricular diastolic filling (125). In addition, when iNOS was knocked out in both donor and recipient mice, cardiac allograft survival was significantly increased along with significant reductions in inflammatory infiltrate, rejection score, total number of apoptotic nuclei and of apoptotic cardiomyocytes during the acute rejection stage (126). Therefore, substantial induction of iNOS in cardiomyocytes appears to be toxic to cardiac function.

Based on these studies, we hypothesize that **specific overexpression of eNOS/iNOS in smooth muscle or endothelial cells will inhibit the development of cardiac allograft arteriosclerosis without suppressing cardiac function.**

1.7 PRELIMINARY DATA: ADCMV-INOS TRANSDUCTION OF DONOR HEART

Our preliminary data support our hypothesis. In a rat heterotopic heart transplantation model, PVG and ACI rats were used as donor and recipient, respectively. Donor hearts were transduced using an adenoviral vector AdCMV-iNOS *ex vivo* for 20 min, and were then transplanted into an ACI recipient heterotopically. AdCMV-EGFP was used as a negative control. The adenoviral transduction method adopted involved recirculating adenoviral vector in the donor heart as described in **2.1.1**. The donor graft was harvested at day 4, day 14 or day 28. The grafts were

harvested at 28 days after transplantation, embedded in paraffin and the tissue sections were stained by verhoeff's Van Geison (vVG) staining. Cardiac allograft arteriosclerosis was determined by measuring the extent of vessel occlusion in the graft from the vVG staining slides as described in **2.18**. Cardiac function was measured for the grafts harvested at 4 and 14 days after transplantation using Langendorff perfusion as described in **2.3**.

1.7.1 AdCMV-EGFP mediated universal EGFP expression in the donor graft

We first determined how the transgene was expressed in the allografts when it was driven by the universal promoter cytomegavirus (CMV). Donor PVG rat hearts were transduced by AdCMV-EGFP, at a dose of 5×10^9 PFU *ex vivo*, and then transplanted into ACI recipients. The allografts were harvested at 4 days after transplantation. As shown in Figure 2, driven by the universal promoter CMV, EGFP was universally expressed in all of the cardiac tissues, including vasculature and cardiomyocytes.

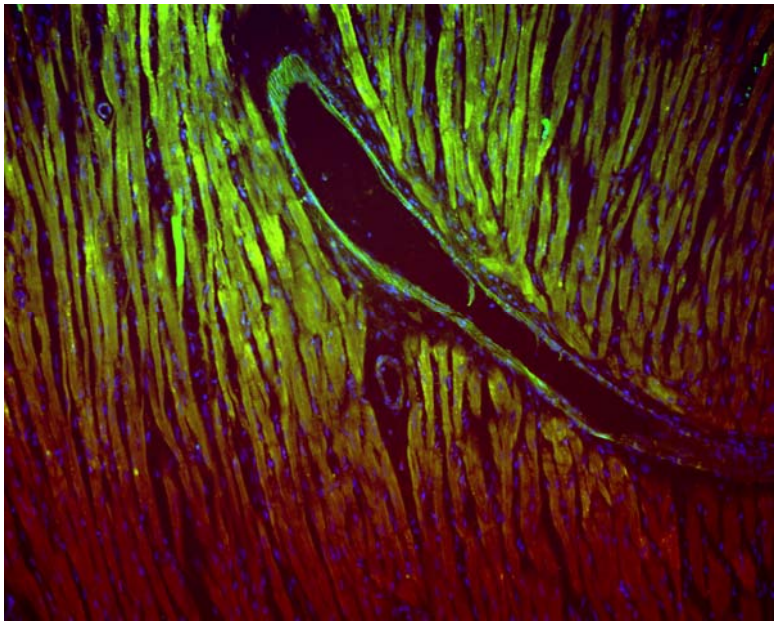

Figure 2 The CMV promoter led to global expression of EGFP in cardiomyocytes and vasculature when donor heart was transduced by AdCMV-EGFP.

1.7.2 AdCMV-iNOS mediated iNOS expression inhibited cardiac allograft arteriosclerosis

From Figure 2, we can assume that iNOS will be expressed both in cardiomyocytes and blood vessels when non-targeting vector AdCMV-iNOS is used to transduce the hearts.

Using the same transplantation model, donor hearts were transduced by AdCMV-iNOS *ex vivo*, at a dose of 10^8, 10^9, or 10^{10} PFU, prior to transplantation. As shown in Figure 3, at 28 days after transplantation, 10^{10} PFU of AdCMV-iNOS significantly suppressed the development of cardiac allograft arteriosclerosis while lower titers did not.

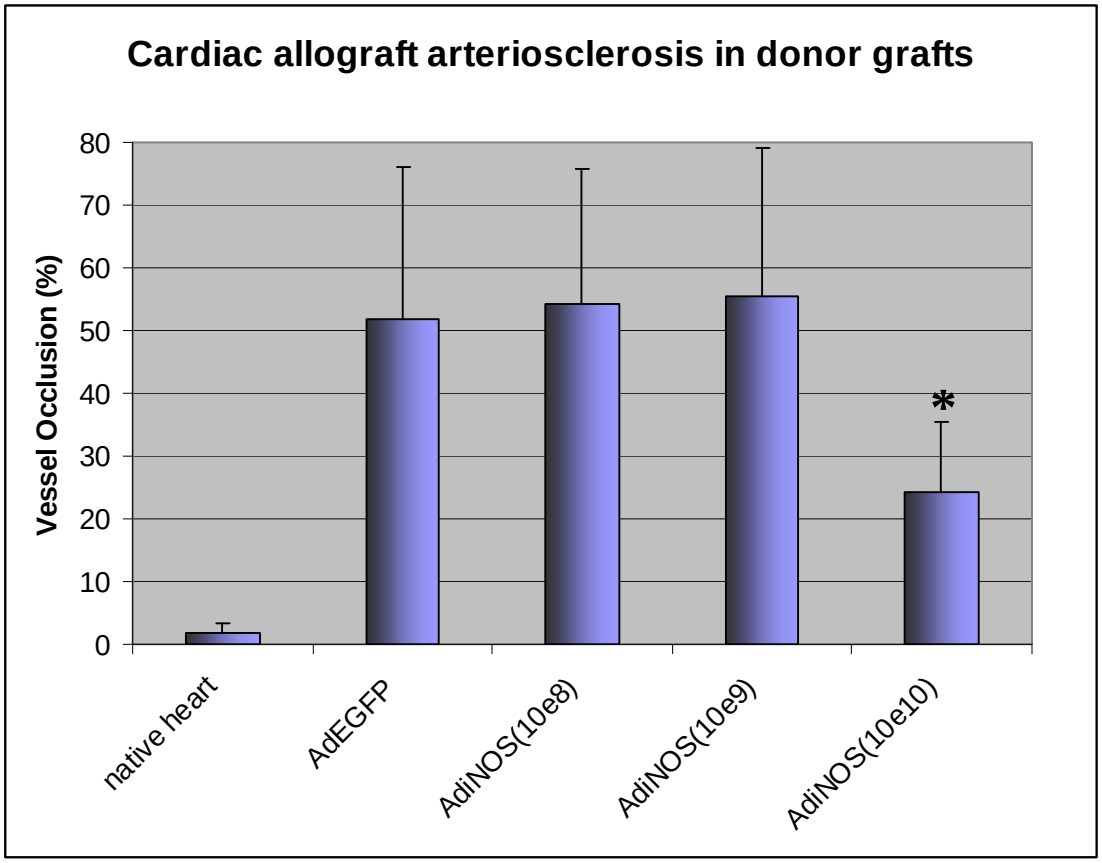

Figure 3 iNOS expression by Ad-CMV-iNOS inhibits cardiac allograft arteriosclerosis in donor allogrfts.

Cardiac allograft arteriosclerosis was evaluated by planimetric analysis. At 28 days after transplantation, Ad-CMV-iNOS transduction with 10^{10} PFU significantly suppresses CAA. n=1 for each group. *: $p<0.05$

1.7.3 AdCMV-EGFP mediated iNOS expression impaired cardiac function

Next, we determined whether AdCMV-iNOS mediated iNOS expression in the allografts impaired cardiac contractility. As shown in Figure 4, at 4 days after transplantation, AdCMV-iNOS transduction led to a dose-dependent decrease in the left ventricle systolic pressure (LVSP) and left ventricle diastolic pressure (LVDP). Moreover, with the titer of 10^{10} PFU, AdCMV-iNOS transduction significantly decreased LVSP, LVDP, maximal rate of left ventricular pressure development (max dP/dt) or decline (-min dP/dt), heart rate (HR) and coronary flow

(CF), compared to the AdCMV-EGFP control. Mean arterial pressure and left ventricular end diastolic pressure were not affected (data not shown). However, at 14 days after transplantation, the above cardiac hemodynamic parameters were not significantly different between AdCMV-iNOS treatment and AdCMV-EGFP control (data not shown).

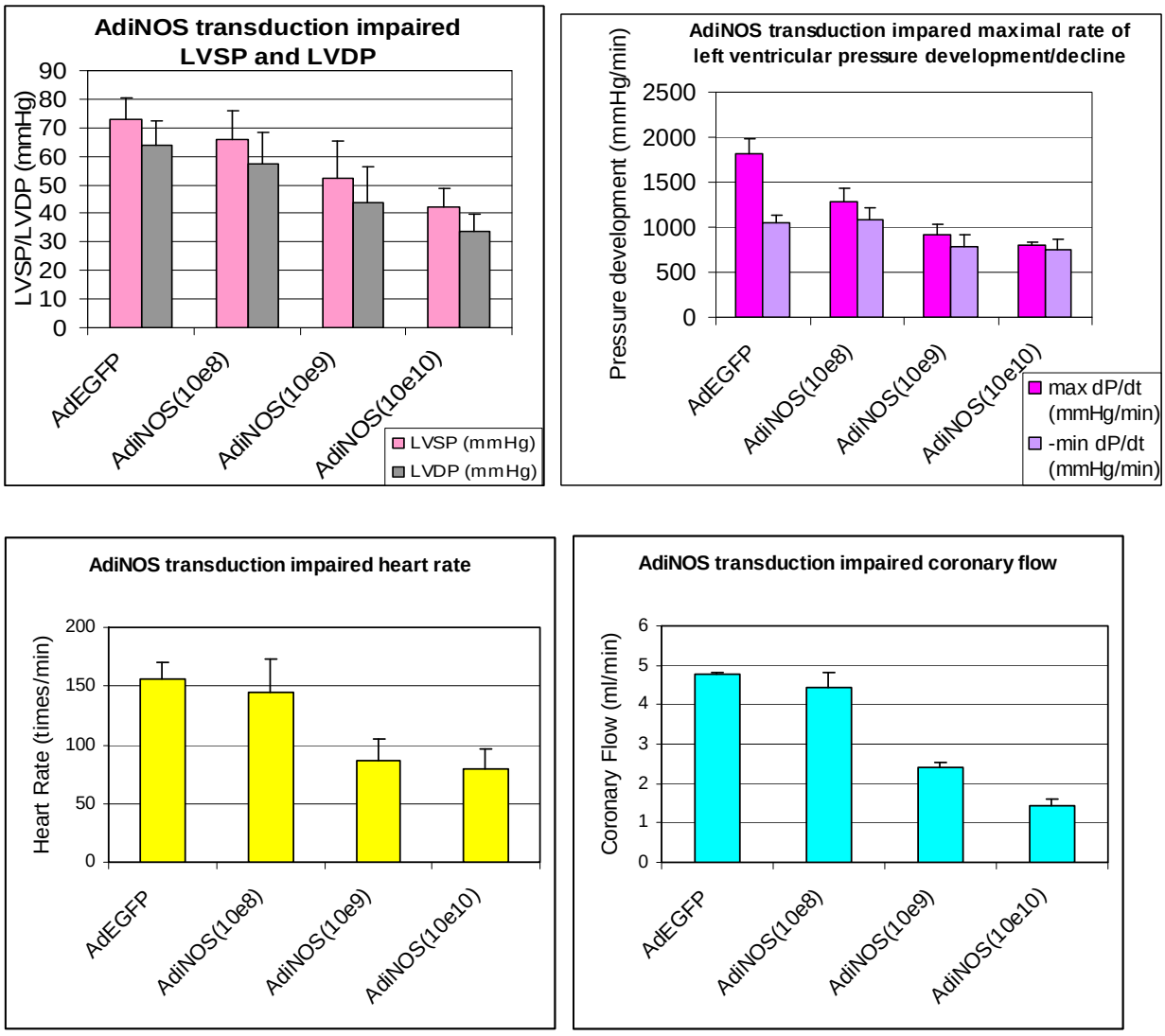

Figure 4 AdiNOS transduction (1010 PFU) impaired cardiac function of donor grafts.

N=4 for each group.

These preliminary data indicate that global expression of iNOS in the donor graft inhibited cardiac allograft arterioscleroiss but also suppressed cardiac function. Vascular-specific expression of iNOS may avoid the inhibitory effect of excessive NO production on cardiac function while preserving its protective effects on vessel injury.

1.8 VASCULAR-SPECIFIC TARGETING

Vascular-targeted gene therapy is a promising option for vascular diseases, including tumor angiogenesis, atherosclerosis, and the processes leading to intimal hyperplasia (127). However, the major limitation in this field has been the lack of endothelial- or smooth muscle cell-specific targeting in the vessel wall. To facilitate vascular-specific targeting, different approaches have been investigated, including modification of the adenoviral fiber coat proteins (139), insertion of a specific peptide into the fiber knob (184) or hexon (185) to permit recognition by specific cell receptors, or mixing the vector with tissue-specific antibody (186-188). However, many of these are still in the early stage of development with limited success.

An alternative strategy is to identify promoters capable of directing endothelial- or smooth muscle cell-specific expression. The recent development of transgenic mouse technology has proven to be a powerful tool to identify cell type-specific promoters since the exogeneous promoter and reporter gene is integrated into the host genome. With this technology, several endothelial- or smooth muscle cell-specific promoters have been identified in the past decade. The endothelial cell-specific promoters include the murine Tie2 promoter with a 1.6 kb enhancer (128), the murine Tie2 promoter with a 10 kb enhancer (128), the human intercellular adhesion molecular 2 promoter (ICAM2, -292 ~ +44 bp) (129), the human von Willebrand factor promoter

with enhancer (vWF, -487 ~ +246 bp) (130), the murine vascular endothelial cadherin promoter with enhancer (-2486 ~ +24 bp) (131), the murine preproendothelin-1 promoter with small enhancer (5.9kb 5' flank region + first exon and first intron) (132), and the murine preproendothelin-1 promoter with large enhancer (9.2kb 5'flank region + first exon and first intron) (133) (9.2 kb 5'flank region + first exon and first intron). The smooth muscle cell-specific promoters include rat smooth muscle myosin heavy chain promoter with large enhancer (SMMHC, -4229 ~ +11600 bp) (134), rabbit smooth muscle myosin heavy chain promoter (SMMHC, -2305 ~ -4 bp) (135) and murine smooth muscle 22α promoter (SM22α, -441 ~ +41 bp) (136). The vascular-specificity of these promoters, was established in transgenic mice (128-133). Another endothelial cell-specific promoter, the human *fms*-like tyrosine kinase-1 promoter (Flt-1, -748 ~ +284 bp) (137), was identified *in vitro* by serial deletions of the promoter region of the Flt-1 gene. The specificity of this promoter was also confirmed in two other studies *in vitro* and *in vivo* (138, 139), in which the Flt-1 promoter was utilized in adenoviral vectors.

In this study, we proposed to identify a smooth muscle or endothelial cell-specific promoter for vascular-specific expression of iNOS in the heart.

1.9 GENE DELIVERY SYSTEM

Based on the protective effects of NO on vascular injury and the destructive role of NO at high level on cardiac function, we propose to develop a gene delivery system to express iNOS specifically in smooth muscle or endothelial cells, but not in cardiomyocytes. Which gene delivery system can achive this? We first chose to contruct an adenoviral vector.

1.9.1 Adenoviral vector

For the past decade, viral and nonviral vectors have been the most widely used tools to deliver transgene into tissue, among which adenoviral vectors are the most popular gene delivery vectors. Adenoviruses are well characterized biochemically and genetically. Decades of studies have produced a relatively clear picture of the viral life cycle and the functions of most of the viral proteins (140). Adenoviruses have been modified with the deletion of some or all of the viral genes to accommodate foreign genes with a wide range of sizes. The E1, E3 deleted adenovirus can accommondate foreign genes up to 7~8kb. The most recent generation of adenovirus, gutless adenovirus, can carry foreign genes up to 38kb. In contrast, adeno-associated viruses can accommondate foreign genes up to 4.5kb. With the deletion of viral genes, the immune response in the host is also significantly reduced. Adenoviruses are easily manipulated and can be grown to high titers (141). They infect both resting and dividing cells (142, 143) and transduce most types of cells with high efficiency while non viral vectors are limited by low transfection efficiency. Unlike retroviruses, adenoviruses do not integrate into host genome and long-term therapeutic safety is less of a concern.

Our preliminary data also supports the notion that an adenoviral vector designed for vascular-specific targeting would be a good choice to inhibit cardiac allograft arteriosclerois while preserving cardiac function. Considering these advantages, we decided to construct adenoviral vectors using cell type-specific promoters to restrict iNOS expression to the vessel wall, as shown in Figure 5.

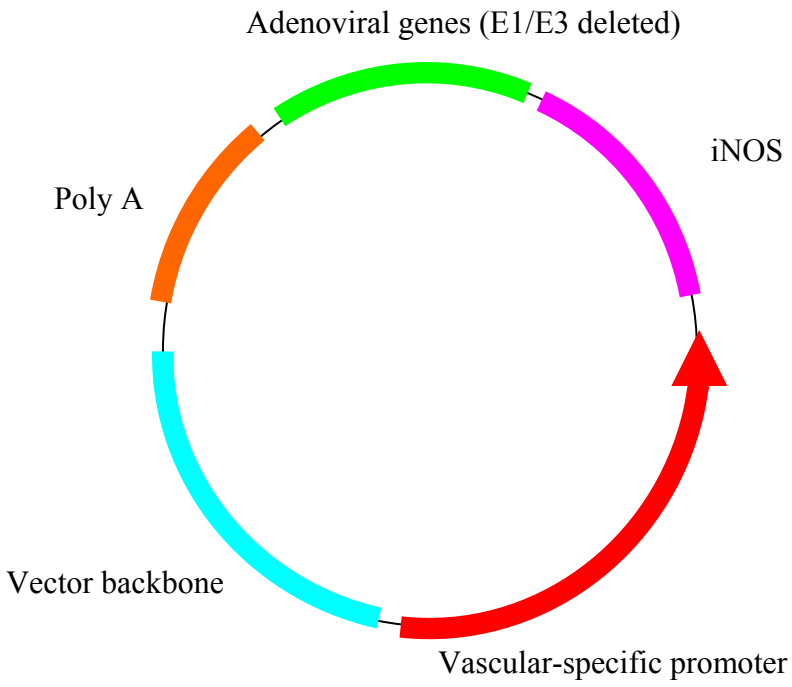

Figure 5 Structure of adenoviral vector with vascular-specific promoter and the iNOS gene.

1.9.2 Vascular-specific iNOS inducible transgenic mice

Although adenoviruses have many advantages, great variation, poor reproducibility, and lack of control of transgene expression levels and duration limit their applicability. Other approaches may be required to test our hypothesis. For example, inducible regulation of transgene expression in a transgenic animal model could circumvent these limitations and may serve as a good alternative option to investigate the therapeutic effect of transgene (144, 145).

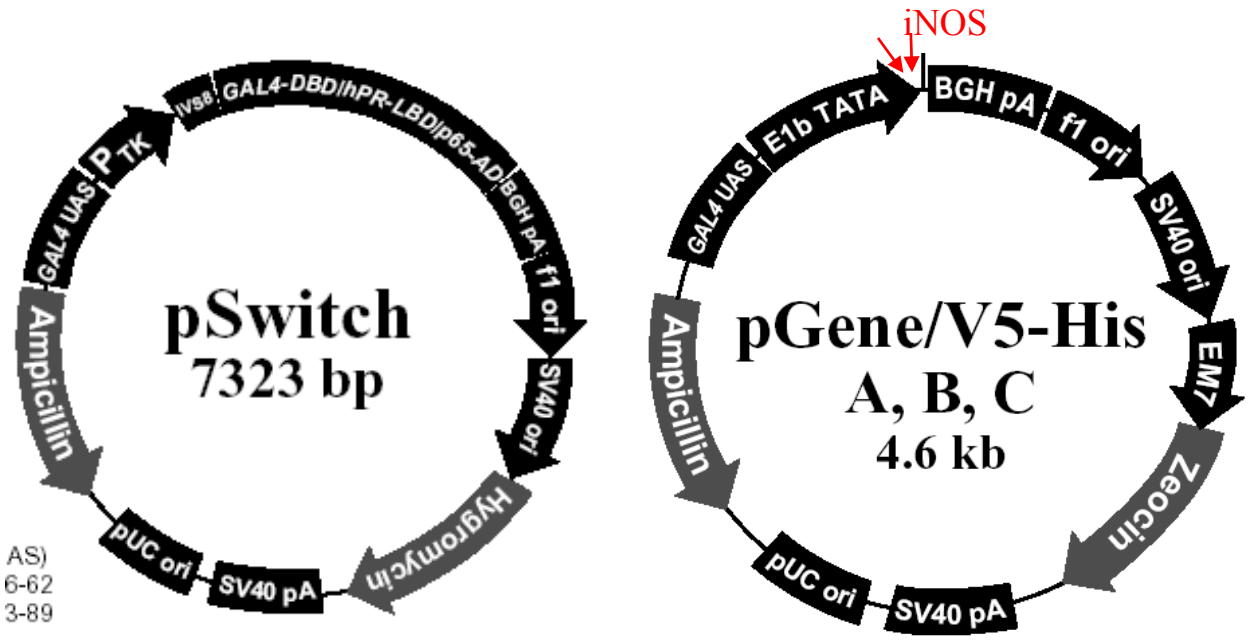

Figure 6 GeneSwitch system is composed of two DNA plasmids: regulatory plasmid pSwitch and responsive plasmid pGene/V5-his.

An advantage of the inducible system is that transgene is silent until a ligand is given to induce its expression or *vice versa*. Based on ligand type, there are four inducible regulation systems currently available: tetracycline (Tet on/off), ecdysone (Complete Control), mifepristone (GeneSwitch) and RL1 (RheoSwitch). These systems can be best explained by describing two DNA plasmids: a regulatory and a responsive DNA plasmid. For example, in the GeneSwitch system (Figure 6), pSwitch is the regulatory plasmid and pGeneV5/His is the responsive plasmid. Transgene (iNOS) would be inserted into the multiple cloing site of the responsive plasmid between the E1A TATA minimal promoter and BGH pA sequence. The DNA plasmid pSwitch regulates the expression of the Switch protein, which is composed of two domains: a ligand-binding domain and a response element-binding domain. Only after the ligand, mifepristone, binds to its ligand-binding domain, does a conformational change occure in the

Switch protein. This change promotes its element-binding domain binds to an element-binding sequence GAL4 USA which is located upstream of the transgene in the pGeneV5/His DNA plasmid. This binding activates the transcription and translation of the transgene. The regulation of inducible transgene expression in GeneSwitch is shown in Figure 7. The level and duration of the transgene expression can be regulated by the dose and time of the ligand administration (146). Cell-type specific expression of the transgene can also be achieved by using a cell-type specific promoter to drive the Switch expression (146-149).

In the inducible system, it is critical whether the transgene can be tightly regulated. Tet on/off system exhibited leaky expression of the transgene (150, 151). In contrast, GeneSwitch has been reported to regulate transgene stringently *in vitro* and *in vivo* (146, 148). As shown in Table 1 (from Invitrogen Catalog 2004), Invitrogen Corp. compared the two systems and concluded that the leaky expression of GeneSwitch is much lower than that of Tet-on in HEK293 cells. As a stringent test of leakiness *in vivo*, Osterwalder *et al.* inserted TeTxLC, a potent neurotoxin, into GeneSwitch and made a transgenic *Drosophila*. Expression of TeTXLC results in complete embryonic paralysis and failure to hatch *Drosophila* offspring. Their results showed that without mifepristone induction, embryonic survival of the TeTxLC-transgenic *Drosophila* was 77.8%, which was similar to the EGFP-transgenic control (71.5%). With 1μg/ml mifepristone, the survival rate of TeTXLC-transgenic *Drosophila* dropped to 7% (Figure 8, 146). These data solidly validated that the transgene is tightly regulated in GeneSwitch system.

Table 1 Comparison of regulated mammalian expression systems (From Invitrogen Catalog 2004).

system	Basal expression	Induced expression level	Response time to maximal	Transgenic application
Tet-Regulated Expression	Low	Highest	24hrs	Suitable
Flp-in Tet-Regulated Expression	Lower	High	24~48 hrs	Suitable
GeneSwitch System	Lowest	Low	24hrs	Suitable

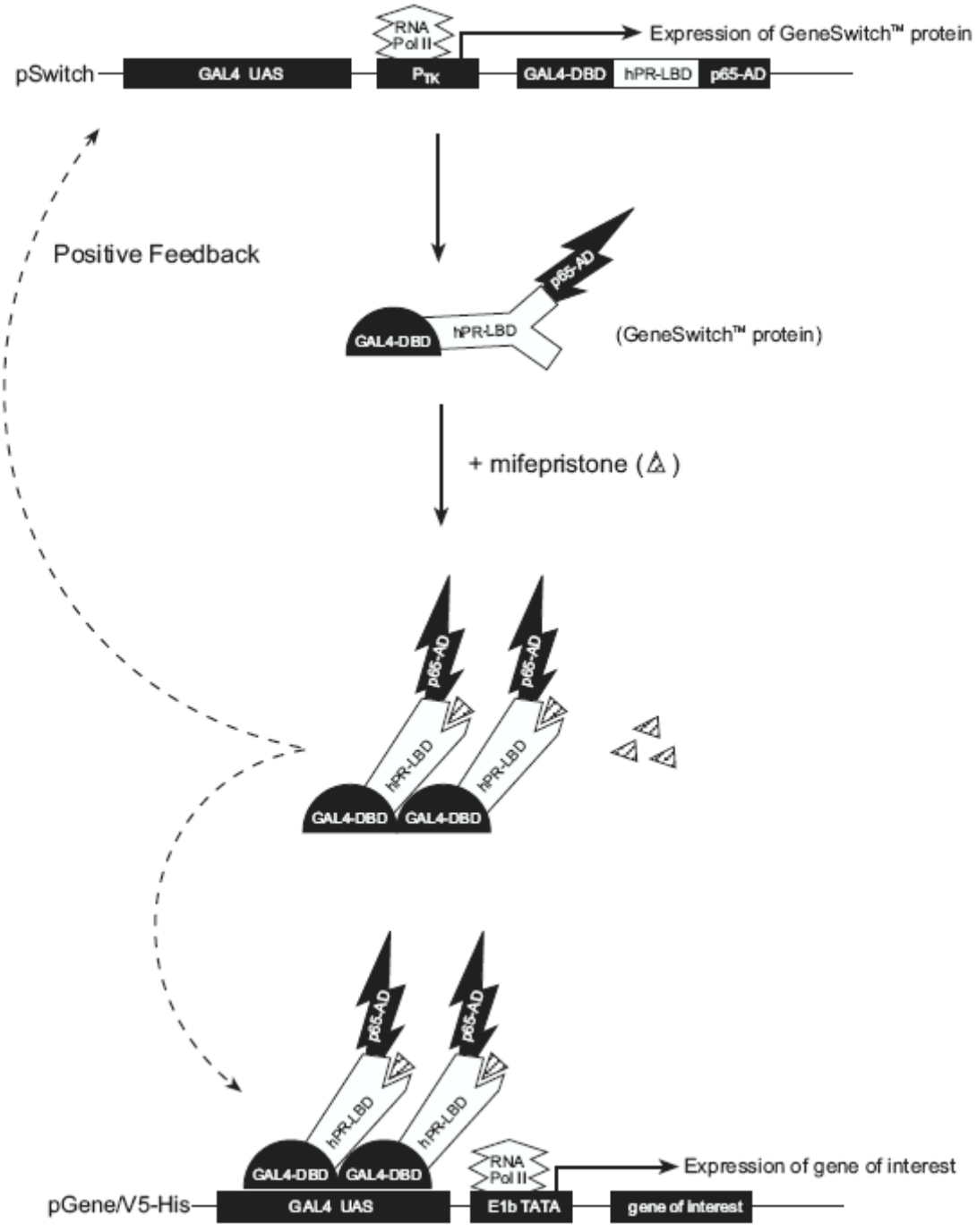

Figure 7 Regulation of transgene inducible expression by GeneSwitch.

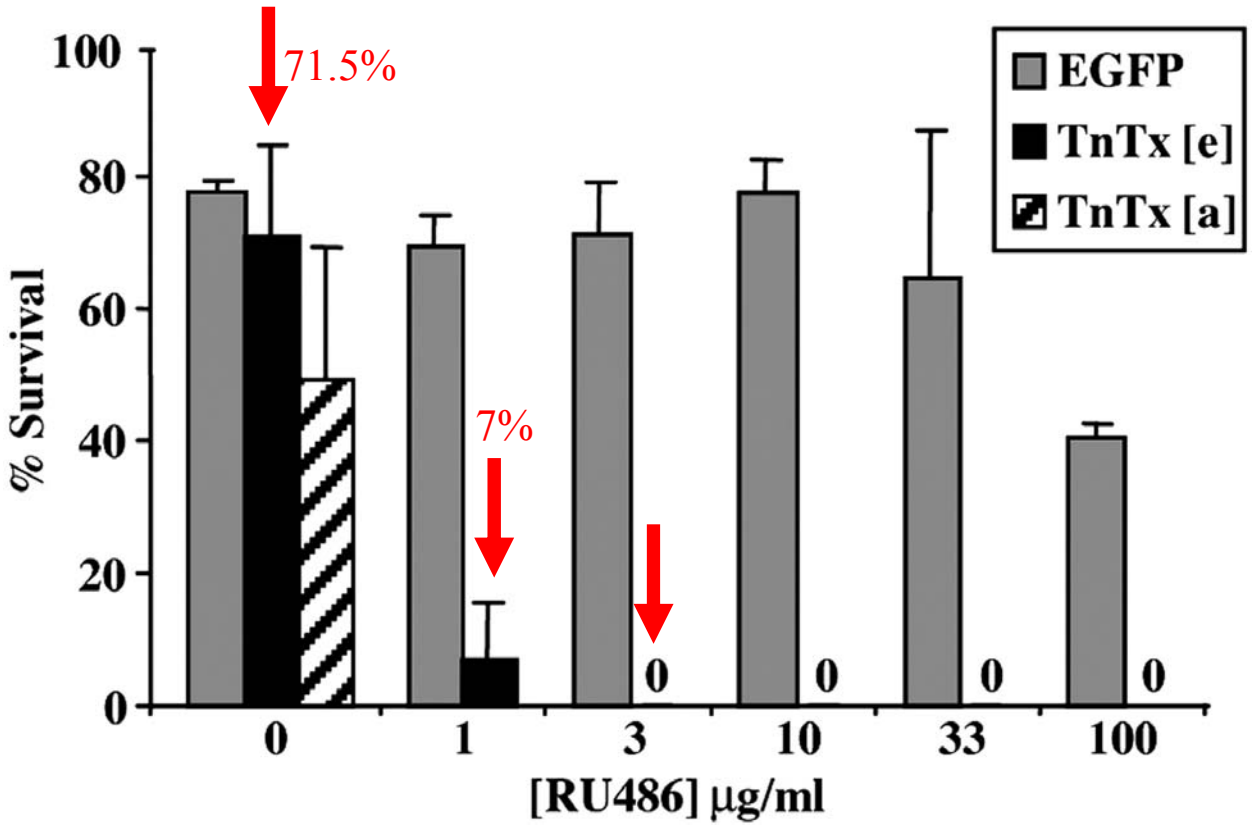

Figure 8 GeneSwitch exhibited low basal expression in transgenic *drosophila*.

Besides near absent basal transgene expression, GeneSwitch demonstrated several other advantages. First, the regulatory protein Switch is a fusion protein and composed of a ligand binding domain and a response element binding domain. One universal promoter, herpes simplex virus thymidine kinase mimimal promoter and its upstream GAL4UAS sequence, regulates the expression of Switch universally. To achieve vascular-specific expression of iNOS, we will replace this universal promoter with a smooth muscle or endothelial cell-specific promoter. In contrast, in RheoSwitch, the regulatory protein is composed of two proteins, whose expression is manipulated by two universal promoters. For cell type-specific expression of iNOS, we need to substitute the vascular-specific promoter for these two promoters. Therefore, modification of the GeneSwitch system is easier. Second, the ligand mifepristone in GeneSwitch, also named as

RU486 (a French name), is a synthetic steroid. The combinational use of mifepristone/misoprostol was approved as an abortion drug by FDA in 2000. Mifepristone binds to progesterone receptor as an antagonist of progesterone. Studies have demonstrated that progesterone neither affected the development of intimal hyperplasia in a balloon-injured carotid artery (152) nor the progress of arteriosclerosis in coronary artery (153-155) in rat, rabbit and monkey models regardless of gender. Therefore, we assume that a progesterone antagonist, mifepristone, will not affect the development of intimal hyperplasia in our heart transplantation model. Third, mifepristone does not affect cardiac function. Lutucuta S *et al.* (156) showed that administration of mifepristone into wild-type or geneswitch transgenic mice for 16 days did not significantly change cardiac function, including heart rate, left ventricular ejection fraction, left-ventricular end-diastolic diameter, left-ventricular end-systolic diameter, fractional shortening, aortic maximum velocity, circumference per second, deceleration time, mitral valve inflow E velocity, mitral valve inflow E/A ratio and velocity of circumferential fiber shortnening. Mifepristone also did not induce morphological change, including body weight, left ventricular mass, left ventricular mass/body weight ratio, posterior wall thickness and septal thickness. Therefore, we assume that mifepristone will not affect cardiac function in the donor heart. From these studies, we propose that GeneSwitch is an optimal option for our cardiac allograft arteriosclerosis project.

Considering the possible failure of adenoviral vector for vascular-specific expression of iNOS, as a back up strategy, we employed the GeneSwitch system to develop iNOS inducible transgenic mice. iNOS transgenic mice have not been successfully generated yet because transgenic mice with constitutively expressed iNOS do not survive to the adult stage (117). Inducible iNOS transgenic mice serve a better model to determine the effect and function of

iNOS. We propose to use the iNOS inducible transgenic mice as donor and determine the efficacy of vascular-specific iNOS overexpression on the suppression of cardiac allograft arteriosclerosis and the effects on cardiac function.

1.10 ENOS TRANSGENIC MICE

We hypothesize that smooth muscle- or endothelial-specific NOS (eNOS or iNOS) expression will inhibit cardiac allograft arteriosclerosis without affecting cardiac function. To achieve iNOS specific expression in smooth muscle or endothelial cells, we proposed to develop two gene delivery systems: adenoviral vector and vascular-specific iNOS inducible transgenic mice. In case these approaches fail, we imported eNOS transgenic mice from Dr. Rini De Crom (Netherland) as a backup strategy to test our hypothesis. In this eNOS transgenic mice line, the human eNOS promoter regulates the human eNOS endothelial-specific expression (159). The schematic structure of this transgenic mice transgene is shown in Figure 9.

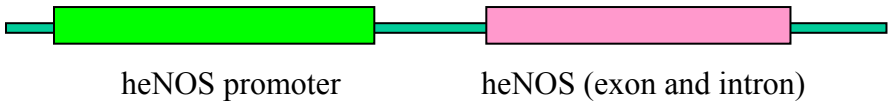

Figure 9 Schematic structure of eNOS transgenic mice.

eNOS has been shown to play a protective role in vascular injury. Overexpression of eNOS in balloon-injured carotid artery by administration of sendi virus/liposome-DNA plasmid complex (157) or by AdeNOS gene delivery (85) significantly suppressed intimal hyperplasia at 14 days after injury. In a murine aortic transplantation model, aortic allograft arteriosclerosis was

accelerated in aortic allografts of eNOS knock-out mice (88). Iwata A *et al.* showed that liposome-DNA-mediated gene transfer of eNOS into donor heart decreased ischemia-reperfusion injury by inhibiting NF-κB activation, reduced expression of adhesion molecules ICAM-1 and VCAM-1 as well as leukocytes infiltration in the donor heart (158). The consequence of eNOS overexpression in eNOS transgenic mice on atherosclerosis has been elucidated by van Haperen *et al. (*159). Crossing the eNOS transgenic mice with apo E knockout mice resulted in a suppression of the atherosclerotic lesion formation. **We hypothesize that endothelial-specific overexpression of eNOS would inhibit cardiac allograft arteriosclerosis.**

2.0 MATERIALS AND METHODS

2.1 *EX VIVO* TRANSDUCTION OF DONOR HEART BY ADENOVIRAL VECTOR

We adopted two methods to transduce donor heart using adenoviral vector: one is to recirculate the adenoviral vector in donor heart at 4°C; the other is to inject adenoviral vectors into donor heart and incubate for two hours at 4°C in a static system.

2.1.1 *Ex vivo* transduction of donor heart by recirculating adenoviral vector in donor heart

Donor hearts were arrested with cold cardioplegia solution (University of Wisconsin), then perfused with 5 ml of cold (4°C) UW solution containing varying concentrations from 2×10^7 to 2×10^{10} pfu adenoviral vector. The perfusate was directed into the aortic root for 20 minutes using a recirculating circuit that collects the viral effluent from the coronary sinus to the pulmonary artery and allowed for the continuous reperfusion of the vector in the coronary vessels. The perfusion pressure was kept at 70 cm H_2O, and the graft and the perfusate was kept at 4°C during the infection. This infection technique provides homogenous transfer throughout the ventricular mass and additionally leads to high efficiency of transfer to the coronary artery endothelial cells.

2.1.2 *Ex vivo* transduction of donor heart by single injection of adenoviral vector into donor heart

In a syngeneic heart transplantation model, PVG rats (200~250g, Harlan Sprague Dawley) were used as both donor and recipient. The abdomen and chest of the donor rat were opened and the heart was perfused with 10ml of Lactated Ringer's solution (Rxveterinary Products, Porterville, CA). The inferior vena vein, superior vena vein, left lung, right lung, and the three river veins were ligated. The adenoviral vectors, AdFlt-1-lacZ or AdICAM2-lacZ (dose of 10^{10}PFU) were diluted in Lactated Ringer's solution to make the total volume 1000 μl and injected slowly into the coronary arteries through the brachiocelephilic artery. After injection, the aortic root and the pulmonary artery were clamped and the donor heart was harvested. The donor heart was kept in the Lactated Ringer's solution at 4ºC for two hours. Next, it was transplanted into a syngeneic PVG rat heterotopically as described in **2.2**.

2.2 RODENT HETEROTOPIC HEART TRANSPLANTATION

Male PVG (RT1-A^c) and ACI (RT1-A^a) rats, 2-3 months old and weighing 200-250 grams, were purchased from Harlan Sprague Dawley (Indianapolis, IN). PVG and ACI rats were used as donor and recipient, respectively. Heterotopic heart transplantation was performed as previously described by Ono and Linsay (160). Briefly, after induction of general anesthesia with inhaled isofluorane, a laparotomy was performed under clean conditions. The donor heart was heterotopically transplanted into the recipient by end-to-side anastomoses of the aorta and the pulmonary artery to the abdominal aorta and inferior vena cava, respectively using 10/0

monofilament sutures. The abdominal wall was closed by continuous suture using 4-0 silk after hemostasis was obtained. After transplantation, recipient rats received a 10 day course of cyclosporine (CsA: 100mg/ml, Sandoz Pharmaceuticals, Holzkirchen, Germany) at a dose 5mg/kg/day, IP (intraperitoneal) injection. Graft function was assessed by daily palpation of beating.

The mouse heterotopic heart transplantation was performed in a similar manner.

2.3 MEASURRMENT OF CARDIAC FUNCTION USING LANGENDORFF PERFUSION

Langendorff perfusion is a well-accepted method to measure cardiac function in rodents. In this preparation, the heart was perfused using a physiologic solution at a constant physiologic preload. Specifically, the rats were anesthetized with pentobarbital (50mg/kg IP) and anti-coagulated by injection of heparin (1000U/kg IV). The graft was excised and immediately submerged in iced Krebs-Henseleit solution, then mounted on an isolated heart perfusion apparatus with a retrograde perfusion pressure of 80 cmH_2O. The left atrium was cannulated and antegrade perfusion was started at a constant pressure of 10 cm H_2O. The solution was kept at 37°C and bubbled with 95%O_2-5%CO_2. A fluid-filled latex balloon was inserted into the left ventricle and connected to a transducer for measurement of left ventricle pressures. The graft was permitted to stabilize for 15 minutes, at which time cardiac performance was measured, including heart rate (HR), left ventricle systolic pressure (LVSP), left ventricular developed pressure (LVDP), left ventricle end systolic pressure (LVESP), arterial pressure (AP), maximal

rate of left ventricular pressure development (+dP/dt max), maximal rate of left ventricular pressure decline (-dP/dt min), and coronary flow (CF).

2.4 DNA PLASMIDS AND ADENOVIRUSES

The DNA plasmids pTie2SE-lacZ and pTie2LE-lacZ were kindly provided by Dr. Thomas N. Sato **(**University of Texas Southwestern Medical Center), and are referred to the original name used by this laboratory pHHSDKXK and pT2HLacZpA1I.7, respectively. The ICAM2, vWF, Flt-1 and cytomegalovirus (CMV) promoters were constructed in E1-deleted adenoviruses referred to as AdICAM2-lacZ, AdvWF-lacZ, AdFlt-1-lacZ, and AdCMV-lacZ, respectively. The Flt-1 promoter was also constructed in a DNA plasmid upstream of the luciferase gene, referred to as pFlt-1-luc. The four adenoviruses and the DNA plasmid pFlt-1-luc were kindly provided by Dr. Andrew H Baker (University of Glasgow) with the permission of the original authors. The Tie2SE, ICAM2, vWF, and CMV promoters were constructed in DNA plasmids upstream of the FretMT gene and are referred to as pTie2SE-FretMT, pICAM2-FretMT, pvWF-FretMT, and pCMV-FretMT, respectively. FretMT is a fusion protein that is composed of Enhanced Cyan Fluorescent Proteins (ECFP) human metallothionein (MT) and Enhanced Yellow Fluorescent Proteins (EYFP) genes. The four DNA plasmids were kindly provided by Dr. Bruce Pitt (University of Pittsburgh). The Rous sarcoma virus promoter (RSV) was constructed in a DNA plasmid upstream of the luciferase gene and is referred to as pRSV-luc. The DNA plasmid pCMV-EGFP was purchased from Clontech (Mountain view, CA) with the original name of pEGFP N1. The adenovirus AdCMV-EGFP was kindly provided by Dr. Andrew Gambotto (University of Pittsburgh). The DNA plasmid pSMMHCL-luc was kindly provided by Dr. Gary

K. Owens (University of Virginia) with the original name of pPI Myo-luc. The DNA plasmid pSMMHCS-EGFP was kindly provided by Dr. Wolfgang M. Franz (University of Lübeck, Germany) with the original name of pSMHC-EGFP. The GeneSwitch^{TM} core kit, including the DNA plasmids pSwitch, pGene/V5-hisA, pGene/V5-hisB, pGene/V5-hisC and pGene/V5-his-lacZ were purchased from Invitrogen. The adenoviral vectors AdSwitch and Ad5xGal4-luc were kindly provided by Dr. Ramesh A Bhat (Weyth Research).

2.5 CONSTRUCTION OF ADENOVIRAL VECTOR ADFLT-1-INOS, ADICAM2-INOS AND ADTIE2-INOS

To make E1, E3 deleted adenoviral vectors, shuttle DNA plasmids with the insertion of cell type-specific promoter Flt-1, ICAM2, or Tie2SE and the target gene iNOS were constructed first. The adenoviral shuttle plasmid pAdlox (SwaI modified) used for the construction of E1/E3 deleted adenoviral vector was kindly offered by our collaborator, Dr. Andrea A. Gambotto (U. Pittsburgh). The CMV promoter in this plasmid was replaced by the endothelial-specific promoter Flt-1, ICAM2 or Tie2SE. To construct the shuttle DNA plasmid pAdloxFlt-1, the Flt-1 promoter was subcloned from viral DNA extracted from adenovirus AdFlt-1-lacZ. Fifty microliters of AdFlt-1-lacZ (10^9 PFU) was degraded in 150 μl of protein degrading buffer with a final concentration of 0.1% SDS and 0.03 μg/μl protein kinase K at 37°C for 1h. Next, the viral DNA was extracted using Qiaquick gel extraction kit (Qiagen, Valencia, CA). Two hundred microliters of the degrading mixture was incubated with 600 μl of QG buffer on heat-block at 50°C for 5min, was then applied to a Qia quick column. The column was washed using 750 μl of PE buffer and spun for 30 sec. The liquid was cleaned out and the residual of PE buffer in the

column was spinned down for 2 more min. The column was inserted into a new microfuge tube and the viral DNA was eluted using dH_2O. Thirty-five microliters of dH_2O was preheated to 70°C and added into the column. The column was incubated on heat-block at 70°C for 2 min, then spun down for 2 min and the viral DNA pAdFlt-1-lacZ was collected.

The Flt-1 promoter was amplified from pAdFlt-1-lacZ by PCR using 5' primer CCCCTCGAGCTTCTAGGAAGCAGAAGACTGAGGA and 3' primer CAACAAGCTTGTGAGCGCGACGCGGCCTGCTCGCC. The PCR condition is 94°C, 5 min; 94°C, 45 sec, 60°C, 30 sec, 72°C, 80 sec, 30 cycles; 72°C, 7 min. The PCR product of the Flt-1 promoter was separated from other non-specific bands by running 0.9% of agarose gel and extracted using QIAquick gel extraction kit. The Flt-1 promoter was codigested by restriction enzyme XhoI (5') and HindIII (3') (New England Biolabs, IpSwich, MA) and the Flt-1 promoter fragment was ready to be subcloned. If no specific indication, all of the restriction enzymes used in this thesis were purchased from New England Biolabs. The CMV promoter was removed from the DNA plasmid pAdlox by XhoI (5') and HindIII (3'). Then the Flt-1 promoter fragment was ligated with the pAdlox fragment by T4 DNA ligase (Rapid ligation kit, Gene Choice, Frederick, MD) and the DNA plasmid pAdloxFlt-1 was constructed (Figure 10).

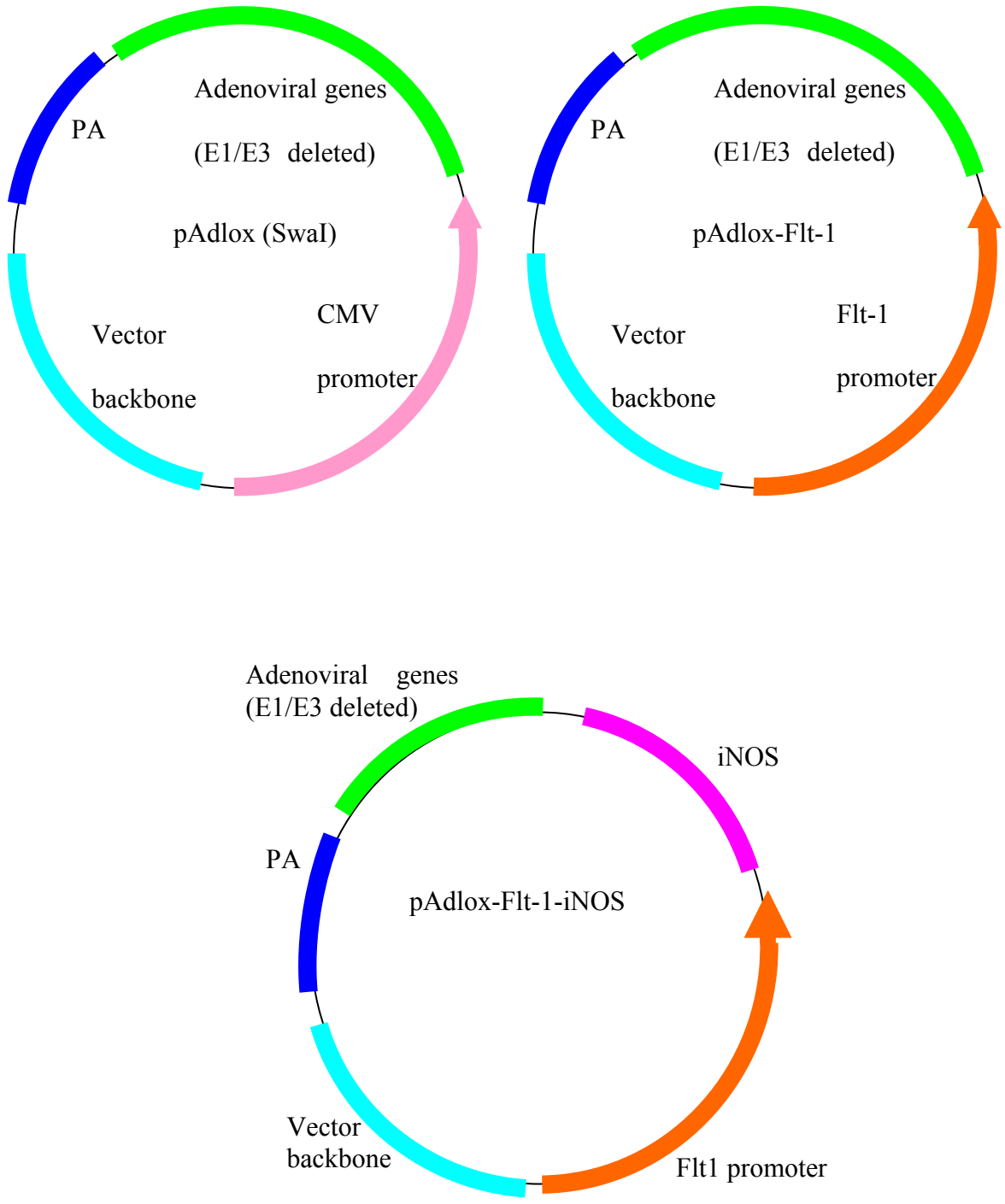

Figure 10 Construction of DNA plasmids pAdlox-Flt-1 and pAdloxFlt-1-iNOS from pAdlox (Swa I).

To construct the shuttle plasmid pAdloxFlt-1-iNOS, the DNA plasmid pAdloxFlt-1 was digested using restriction enzyme Sma I and Hind III sequentially and then incubated with

alkaline phosphatase (Roche Diagnostics, Indianapolis, IN) at 37°C for 60 min to remove the phosphate group from the 5' end to prevent self-ligation. To release the human iNOS cDNA from the DNA plasmid pcDNA3-iNOS, pcDNA3-iNOS was digested using XbaI. Then the DNA fragment was blunted by DNA end-repair enzymes T4 DNA polymerase and T4 polynucleotide kinase with the supply of dNTP and ATP (End-it DNA End-Repair kit, Epicentre, Madson, WI) at room temperature for 45 min. Next, the linearized DNA fragment was digested with Hind III and the 3.5 kb human iNOS cDNA was released. The vector pAdlox Flt-1 fragment was ligated with the insertion of human iNOS fragment by T4 DNA ligase at room temperature for 30 min and finally pAdloxFlt-1-iNOS was constructed (Figure 10).

AdICAM2-iNOS and AdTie2-iNOS were generated similarly.

2.6 CELL CULTURE

Rat smooth muscle cells were isolated from Lewis rat (Harlan Sprague-Dawley, Indianapolis, IN) aortic strips as previously described (18). Cultured cells had the characteristic "hills and valleys" appearance and were routinely more than 95% pure by SMC α-actin staining (data not shown). Cells were grown in Dulbecco's Modified Eagles medium (low glucose)/Ham's F12 (1:1 vol:vol; BioWhittaker; Walkersville, MD) supplemented with 10% FBS, 100 U/mL penicillin, 100 μg/mL streptomycin, and 4 mmol/L L-glutamine. The cells from passages 3 to 7 were used for transfection. Bovine aortic endothelial cells (BAEC) were purchased from BioWhittaker and were cultured in EGM2-MV medium. Rat hepatocytes were isolated from Lewis male rats (200-250g, Harlan Sprague-Dawley) by a modification of the *in situ* collagenase perfusion technique of Seglen (19). Hepatocytes were plated onto gelatin-coated dishes and maintained using cell

culture medium consisting of Williams' medium E (GIBCO, Carlsbad, CA) supplemented with L-arginine (0.5 mM), insulin (1 μM), Hepes (15 mM), L-glutamine, penicillin, streptomycin, and 10% low endotoxin calf serum (Hyclone, Logan, UT). HEK293 cells were kindly offered by Dr. Andrea Gambotto (University of Pittsburgh). HEK293 cells were cultured in Dulbecco's Modified Eagles medium (high glucose, Cellgro, Herndon, VA) supplemented with 10% FBS and 100 U/mL penicillin, and 100 μg/mL streptomycin.

2.7 TRANSFECTION OF CELLS USING LIPOSOME-DNA PLASMIDS COMPLEX

The transfection conditions of BAEC, rat smooth muscle cells, rat hepatocytes and HEK293 cells were optimized for each cell line.

2.7.1 Transfection of BAEC and rat hepatocytes

To transfect BAEC and rat hepatocytes, cells were plated in 12-well plates at a density of 5×10^4 cells/well. 1.6 μg of DNA plasmids was mixed with 100 μl of Opti-MEM (Invitrogen, Carlsbad, CA). Five microliters of Lipofectin (Invitrogen) were mixed with 100 μl of Opti-MEM and incubated for 35 minutes at room temperature. The DNA plasmids were then mixed with Lipofectin and incubated for 15 minutes at room temperature. Next, 800 μl of Opti-MEM was added into the mixture and mixed gently. The transfection mixture was added into cells and the cells were incubated at 37°C for 5 hours. The transfection mixture was aspirated and the cells were incubated in normal culture medium for 48 hours. Finally, reporter gene expression was

determined by checking green fluorescence, performing X-gal staining, or measuring luciferase activity as appropriate to each reporter construct assessed as described below.

2.7.2 Transfection of primary rat SMC

To transfect primary rat smooth muscle cells, cells were plated in 12-well plates at a density of 5×10^4 cells/well. 1.6 μg of DNA plasmids was mixed with 100 μl of Opti-MEM. Four microliters of Lipofectamine 2000 (Invitrogen) was mixed with 100 μl of Opti-MEM and incubated for 5 minutes at room temperature. Then the DNA plasmids were mixed with Lipofectamine 2000 and incubated for 20 minutes. Next, 800 μl of Opti-MEM was added into the mixture, mixed gently, and the total 1000 μl of mixture was added to the cells. After 6 hours, FBS was added into the transfection medium to a final concentration of 10%, and the cells were incubated for 16 hours. The transfection medium was replaced by the cell culture medium. Fourty-eight hours later, the cells were analyzed for reporter gene expression as described below.

2.7.3 Transfection of HEK293 cells

To transfect HEK293 cells, the cells were plated in 12-well plates at a density of 5×10^5 cells/well. Next, 3.2 μl of TransIT Express™ (Mirus Bio, Madison, WI) was mixed with 40 μl of Opti-MEM and incubated at room temperature for 15 minutes. Then, 0.4 μg of DNA plasmids was added into the mixture and incubated for 15 minutes. Next, 460 μl of Opti-MEM was added into the mixture and the total 500 μl of the mixture was added to the cells for transfection. One hour later, 500 μl of the cell culture medium was added into the transfection mixture and

incubated for 24 hours. The transfection medium was replaced by fresh culture medium. Thirty-six hours later, reporter gene expression was assessed as described below.

2.8 DETECTION OF REPORTER GENE EXPRESSION

FretMT expression was detected by green fluorescence using an Olympus Provis AX70 microscope (Tokyo, Japan) and the percentage of the cells demonstrating green fluorescence was calculated. *LacZ* expression was detected by X-gal staining (beta-galactosidase staining kit, Mirus Bio) according to manufacturer's protocol, and the percentage of the cells with blue staining was calculated. Luciferase activity was measured using a Luciferase assay system (Promega, San Luis Obispo, CA). Briefly, cells were washed with PBS for three times and 150 μl of reporter lysis buffer was added (for a 12-well plate). Cells were lysed at room temperature for 15 minutes by shaking. The cell lysates were then microcentrifuged (13000 rpm × 5 min) and 20 μl of the clear supernatants were added to 100 μl of luciferase assay buffer (Promega). The activity was measured in an AutoLumat LB 953 Luminometer (Berthold, Bad Wildbad, Germany) over a 30-second period. Luciferase activity was normalized to the amount of protein and expressed as relative luciferase activity (LU/μg protein).

2.9 *EX VIVO* TRANSDUCTION OF RAT AORTA, CARDIAC AND SKELETAL MUSCLE

Rat aortas were cut into 5 mm-long strips. Rat cardiac and skeletal muscles were also cut into 3 mm × 3 mm pieces. The aorta, cardiac muscle, and skeletal muscle samples were washed with Opti-MEM medium three times. 2×10^9 PFU of AdFlt-1-lacZ, AdICAM2-lacZ, AdvWF-lacZ, AdCMV-lacZ, or AdCMV-EGFP were diluted in 200 μl of Opti-MEM. The tissues were rinsed in the adenoviral mixture and incubated at 37°C for 2 hours. The tissues were then washed with PBS three times and rinsed in 5 ml of culture medium (Dulbecco's Modified Eagles medium (low glucose)/Ham's F12, 1:1 vol:vol; BioWhittaker; Walkersville, MD) supplemented with 10% FBS, 100 U/mL penicillin, 100 μg/mL streptomycin, and 4 mmol/L L-glutamine) in 30-mm dishes. The tissues were incubated in cell culture incubator for 72 hours with daily changes of culture medium.

2.10 X-GAL STAINING OF ADENOVIRAL VECTOR TRANSDUCED RAT AORTA, CARDIAC AND SKELETAL MUSCLE

Seventy-two hours after culture, rat aortas, cardiac and skeletal muscles were fixed in 2% of paraformaldehyde, washed with PBS and stained with the X-gal staining reagents (Mirus Bio) in a humid dark box for 16 hours. Then the stained tissues were frozen in OCT compound (Sakura Tissue-Tek, McGaw Park, IL,) and cryostat sections were cut to a thickness of 6 μm. At every 10 cuts, the specimen was collected and checked for positive staining using a reflected light differential interference contrast microscope (Olympus Provis AX70, Tokyo, Japan).

2.11 TRANSFECTION OF HEK293 CELLS USING GENESWITCH

To determine the induction of *lacZ* gene by GeneSwitch, HEK293 cells were seeded in a 12-well plate at a density of 3.5×10^6 cells/well. Eight microliters of transfection reagent TransIT Express™ (Mirus Bio) were gently mixed with 100 μl of Opti-MEM and incubated for 15 min at room temperature. 0.25 μg of DNA plasmid pSwitch and 1μg of pGenev5His-lacZ were added into TransIT Express™ mixture, gently mixed and incubated for 15 min at room temperature. Subsequently, 400 μl of Opti-MEM was added into the mixture, mixed gently and the total volume of 500 μl of the transfection mixture was added into HEK293 cells and incubated for 1 hr. Then 500 μl of the cell culture media was added into cells and incubated for 24 hrs. Next, the cells were induced by the ligand mifepristone at a concentration gradient from10^{-12} M to10^{-7} M for 48 hrs. Finally, X-gal staining was performed to detect the *lacZ* expression. Pictures were taken for the cells using a reflected light differential interference contrast microscope (Olympus Provis AX70, Tokyo, Japan) and the percentage of blue stained cells was calculated using Metamorph software.

To detect the iNOS expression, the method is the same as above, but the DNA plasmid pGeneA-iNOS replaced pGenev5His-lacZ. Twenty-four and 48 hrs after mifepristone induction, Greiss assay was applied to measure the nitrite level in the cell culture media. Cells were harvested and western blot was performed to detect the iNOS expression. A rabbit anti-iNOS polyclonal antibody (BD Biosciences, San Jose, CA) was used to detect the iNOS expression.

2.12 HARVESTING FIBROBLAST CELLS FROM MOUSE TAIL AND CULTURE

Wild-type mice C3B6F1 were purchased from Charles River (Wilmington, MA). Mouse tail (3~5 cm long) was sterilized with betadine and vortexed for 3~5 sec in 100% ethanol for sterilization and infused in sterilized PBS. The tail was cut into 5mm long small pieces. Each piece was split in the middle to expose the connective tissue. The bone was removed and the connective tissue side was attached to the bottom of a 6-well culture dish. The cell culture medium (Dulbecco's Modified Eagle Medium (high glucose, Invitrogen) supplied with 20% FBS and 1% antimyocotic (Invitrogen)) was added and changed daily. Fibroblasts started to migrate out of the connective tissue within 3 days and continued to migrate and proliferate in the dish for 10 days.

2.13 TRANSFECTION OF C3B6F1 MOUSE TAIL FIBROBLASTS USING DNA-LIPOSOME MIXTURE OR BY ELECTROPORATION

To optimize the transfection effiency in primary adult mouse tail fibroblast, different transfection reagents were used to transfect fibroblast that was extracted from C3B6F1 mice tail, including lipofectamine LTX with Plus (Invitrogen), lipofectamine 2000 with Plus (Invitrogen), GenePORTER (Genelantis, San Diego, CA), TransIT express (Mirus Bio) and Fugene 6 (Roche Diagnostics). The fibroblasts were also transfected by electroporation.

2.13.1 Transfection of primary mice tail fibroblasts with lipofectamine LTX and Plus

Primary fibroblasts were seeded in a 24-well plate at a density of 5×10^4 cells/well. 0.5μg of DNA plasmid pCMV-lacZ was gently mixed with 100 μl of Opti-MEM. 0.5 μl of Plus was added, gently mixed and the mixture was incubated at room temperature for 10 min. Next, 1.25 μl of lipofectamine LTX was added, gently mixed and the mixture was incubated at room temperature for 30 min. 150 μl of Opti-MEM was added into mixture, mixed gently, and the total 250 μl of the DNA-liposome mixture was added into the cells and incubated for 6 hrs. Next, 250 μl of DMEM medium (Dulbecco's Modified Eagle Medium (high glucose, Invitrogen)) with 40% FBS was added into cells, mixed with the transfection medium and the cells were incubated for 16 hrs. Subsequently, the tranfection mixture was aspirated and fresh cell culture media was added to incubate cells for 48 hrs. Finally, X-gal staining was performed to detect the lacZ expression.

2.13.2 Transfection of primary mice tail fibroblasts with lipofectamine 2000 and Plus

Primary fibroblasts were seeded in a 24-well plate at a density of 5×10^4 cells/well. 0.8 μg of DNA plasmid pCMV-lacZ was gently mixed with 50 μl of Opti-MEM. Eight microliters of Plus was added, gently mixed and the mixture was incubated at room temperature for 15 min. At the same time, two microliters of lipofectamine 2000 was mixed with 50 μl of Opti-MEM and incubated for 15 min. Next, the DNA and lipofectamine 2000 mixture were combined together, mixed gently and incubated for 15 min. 150 μl of Opti-MEM was added, mixed gently, and the total 250 μl of transfection media was added into cells and the cells were incubated for 6 hrs.

Subsequently, the tranfection mixture was aspirated and 500 μl of DMEM with 20% FBS was added into cells and the cells were incubated for 48 hrs. Finally, X-gal staining was performed to detect the lacZ expression.

2.13.3 Transfection of primary mice tail fibroblasts with GenePORTER

Primary fibroblasts were seeded in a 24-well plate at a density of 5×10^4 cells/well. Two micrograms of the DNA plasmid pCMV-lacZ was gently mixed in 125 μl of DMEM. Five microliters of GenePORTER was mixed with 125 μl of DMEM and incubated for 3~5 min. Next, the DNA and GenePORTER mixture were mixed gently and was incubated for 40 min at room temperature. The DNA-liposome mixture was added into cells and the cells were incubated for 5.5 hrs. Subsequently, 250 μl of DMEM with 20% FBS was added into cells, mixed gently with the transfection media and the cells were incubated for 16 hrs. Next, the fresh cell culture media substituted the transfection media and the cells were incubated for 48 hrs before X-gal staining was performed.

2.13.4 Transfection of primary mice tail fibroblasts with Fugene 6

Primary fibroblasts were seeded in a 24-well plate at a density of 5×10^4 cells/well. Ninety-seven microliters of the DMEM media was pipetted into a mirofuge tube. Three microliters of Fugene 6 was pipetted into the DMEM media directly without allowing contact with the plastic wall of the tube and mixed gently. One microgram of the DNA plasmid pCMV-lacZ was added into the tube, mixed gently and the DNA-Fugene 6 mixture were incubated at room temperature for 30 min. 150 μl of the DMEM media was added into the mixture, mixed gently and the total 250 μl

of DNA-Fugene 6 mixture was added into cells in a drop-wise manner and the cells were incubated for 6 hrs. Next, 250 μl of DMEM with 20% FBS was added into cells, mixed with the tranfection media gently and the cells were incubated for 48 hrs before X-gal staining.

2.13.5 Transfection of primary mice tail fibroblasts with TransIT Express™

Primary fibroblasts were seeded in a 24-well plate at a density of 5×10^4 cells/well. Eight microliters of TransIT Express™ was diluted in 100 ul of Opti-MEM, mixed gently and incubated at room temperature for 15 min. One microgram of the DNA plasmid pCMV-lacZ was added into the mixture, pipetted gently and mixed gently. The liposome-DNA mixture was incubated at room temperature for 15 min. Subsequently, 150 μl of Opti-MEM was added into DNA-TransIT Express™ mixture, mixed gently, and the total of 250 μl of mixture was added into the cells and incubated for 1 hr. Next, 250 μl of fresh culture media was added into the transfection mixture and the cells were incubated for 48 hrs. Finally, X-gal staining was performed.

2.13.6 Transfection of primary mice tail fibroblasts by electroporation

Primary fibroblasts were seeded in a 6-well plate at a density of 1×10^6 cells/well. Before electroporation, the cultured fibroblasts were trypsinized and resuspended in 0.8 ml of PBS. The suspension was transferred into a 0.2 cm electroporation cuvett, and 5 μg of the DNA plasmid pCMV-lacZ was added into cells and were mixed gently by pipetting. The cells were incubated on ice for 10 min. Next, the cells were electroporated in GenePulser Xcell (Bio-Rad Laboratories, Hercules, CA) with the following condition. Pulse type: exponential decay;

Voltage: 160V; C: 500 μF; PC ohm: ∞. After electroporation, the cells were incubated on ice again for recovery for 10 min and were then seeded into a 6-well plate. The cells were incubated for 48 hrs before X-gal staining was performed.

2.14 INDUCTION OF INOS EXPRESSION IN FOUNDER MICE FIBROBLASTS USING PSWITCH-LIPOFECTAMINE LTX TRANSFECTION

Founder fibroblasts were seeded in 6-well plates at a density of 1×10^5 cells/well or 2×10^5 cells/well according to the available number of cells. Each line of cells was seeded in three wells. One well of cells was transfected using the DNA plasmid pSwitch but not induced by mifepristone. The other two wells of cells were transfected using the DNA plasmid pSwitch and induced by mifepristone. pSwitch (2.5 μg) was gently mixed with 500 μl of Opti-MEM. Plus (2.5 μl) was added, gently mixed and the mixture was incubated at room temperature for 10 min. Next, 6.25 μl of lipofectamine LTX was added, gently mixed and the mixture was incubated at room temperature for 30 min. Five hundred microliters of Opti-MEM were added into mixture, mixed gently, and the total 1000 μl of the DNA-liposome mixture was added into the cells and incubated for 6 hrs. Next, 2000 μl of DMEM medium (Dulbecco's Modified Eagle Medium (high glucose, Invitrogen)) with 20% FBS was added into cells, mixed with the transfection medium and the cells were incubated for 24 hrs. Subsequently, the media in one well was replaced by 2 ml of fresh cell culture media and the media in other two wells was replaced by 2 ml of fresh cell culture media with 10^{-7} M mifepristone. The cells were incubated for 48 hrs. At the time points of 24 and 48 hrs, nitrite levels were measured in the culture media.

2.15 INDUCTION OF LUCIFERASE ACTIVITY IN FIBROBLASTS BY COINFECTION OF ADSWITCH AND AD5XGAL4-LUC

Wild type C3B6F1 tail fibroblasts were seeded in 6-well plates at a density of 3×10^5 cells/well. Adenoviral vectors AdSwitch and Ad5xGal4-luc were mixed with 1000 μl of Opti-MEM at a MOI of 500, respectively, and were used to infect cells for 18 hrs. Subsequently, the infection media were replaced by 2 ml of fresh culture media and the cells were allowed to recover for 24 hrs. Next, the cells were induced by mifepristone for 24 hrs in 2 ml of fresh culture media with addition of 10^{-7}M mifepristone. Subsequently, the cells were induced again for another 24 hrs in fresh culture media with 10^{-7}M mifepristone. Finally, the cell lysate was harvested and protein concentration was determined. Luciferase activity was measured and relative luciferase activity was obtained.

2.16 CONSTRUCTION OF THE DNA PLASMIDS PICAM2-SWITCH, PSMMHCS-SWITCH AND PGENEA-INOS

To develop vascular-specific iNOS inducible transgenic mice, we modified the GeneSwitch system (Invitrogen). In the DNA plasmid pSwitch, either the smooth muscle cell-specific promoter SMMHCS (-2305 ~ 4 bp) or the endothelial cell-specifc promoter ICAM2 (-292 ~ 44 bp) was used to replace the universal promoter herpes simplex virus tyrosine kinase, to regulate the Swich expression. The constructed DNA plasmids were named as pSMMHCS-Switch and pICAM2-Switch. We also inserted the human iNOS gene into the response plasmid pGenev5-His A and constructed the iNOS basal expression DNA plasmid pGeneA-iNOS.

To construct the DNA plasmid pSMMHCS-Swtich, the DNA plasmid pSwitch was cut by the restriction enzymes Mlu I and Sbf I sequentially to remove the Gal4DBD binding sequence and the universal promoter herpes simplex virus thyminding kinase minimal promoter, and then this vector fragment was dephosphated by alkine phosphatase (Roche Applied Sciences). To clone the rabbit SMMHCS promoter, the DNA plasmid pSMMHCS-EGFP was linearized by the restriction enzyme Apa I. The SMMHCS promoter was cloned from the linerized pSMMHCS-EGFP by PCR. The primers used for PCR were: 5': AATACCTGCAGGGTCGACCTGCAGGTCAACGGATCCTT; 3': AATAACGCGTGCGCGCCTCGGACGCTGCTCTTTATA. The PCR condition was: 94°C , 15min; 94°C, 30 sec, 70°C, 30 sec, 72°C, 180 sec (35 cycles); 72°C, 10 min. The PCR product of the SMMHCS promoter was cut by restriction enzymes Mlu I and Sbf I sequentially. Next, the SMMHC promoter fragment and the vector pSwitch fragment were ligated at 16°C overnight and the DNA plasmid pSwitch-SMMHCS was constructed.

The procedure to construct the DNA plasmid pSwitch-ICAM2 is similar as above. The ICAM2 promoter was cloned from the DNA plasmid pAdloxICAM2, which was constructed as described in **2.5**. The primers used to clone the ICAM2 promoter were: 5': AATACCTGCAGGCCATGGGATTTGGGGTTCCCCAGATCTG 3': AATAACGCGTCCAAGGGCTGCCTGGAGGGAGATG. The PCR condition was: 94°C , 15min; 94°C, 30 sec, 54°C, 30 sec, 72°C, 60 sec (35 cycles); 72°C, 10 min.

To construct the DNA plasmid pGeneA-iNOS, the DNA plasmid pGene/V5-hisA was codigested by the restriction enzymes Hind III (Roche Diagnostics) and Not I at 5' and 3' end, respectively. To release the human iNOS gene from the DNA plasmid pcDNA3-iNOS, pcDNA3-iNOS was codigested by Hind III (Roche Diagnostics) and Not I. Next, the vector pGene/V5-

hisA fragment was ligated with the insert (human iNOS fragment) by T4 DNA ligase and the DNA plasmid pGeneA-iNOS was constructed.

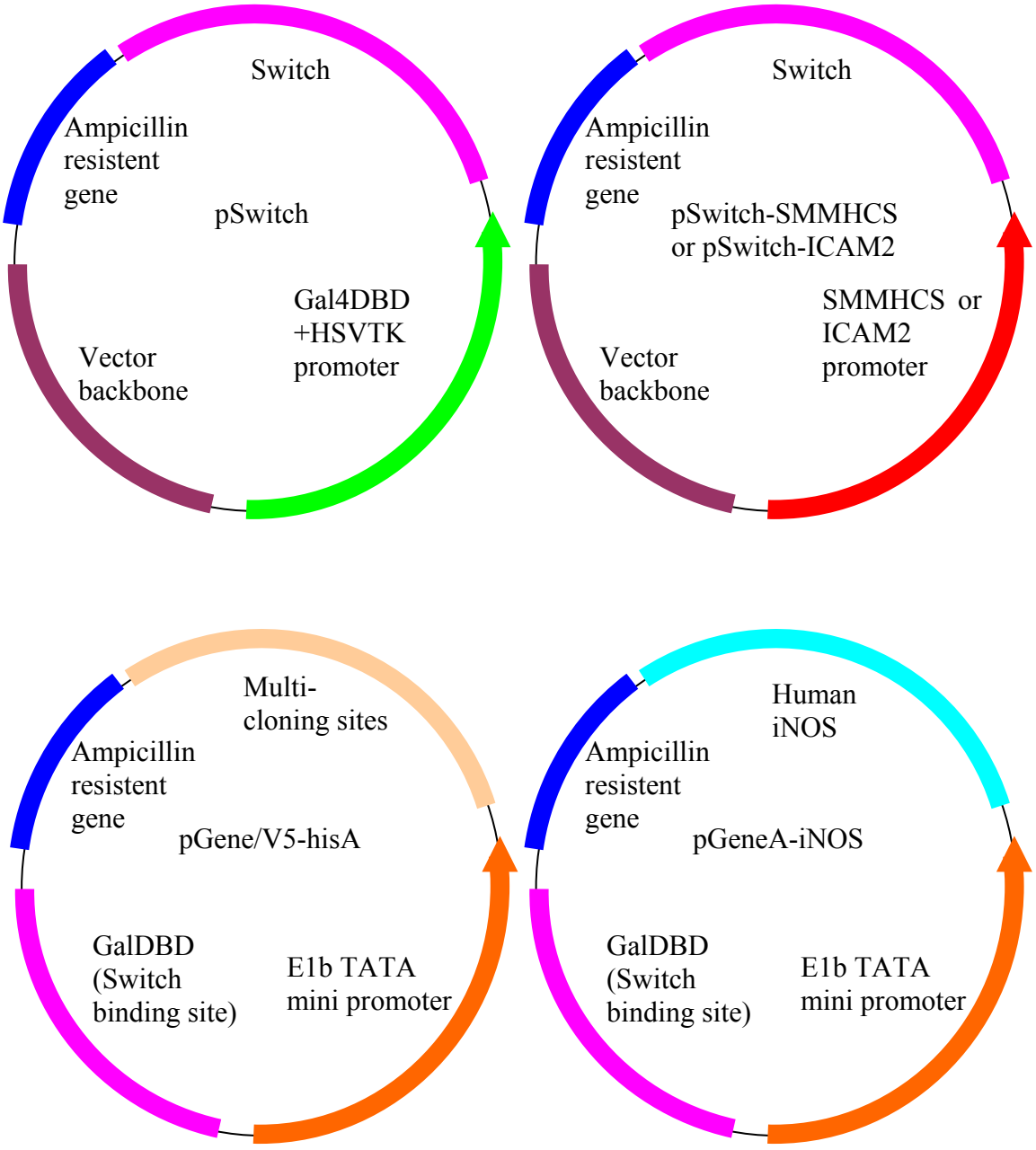

Figure 11 Construction of pSwitch-SMMHC, pSwitch-ICAM2, pGeneA-iNOS from pSwitch and pGene/v5-hisA.

Figure 11 shows the structure of the DNA plasmids pSwitch-SMMHCS, pSwitch-ICAM2 and pGeneA-iNOS.

2.17 DETERMINATION OF GLOBAL INFLAMMATION IN DONOR GRAFTS

To determine the global inflammation grade in the donor graft, the donor graft was harvested and cut into two to four sections from apex to base and each section was embedded in paraffin. The graft tissue in each paraffin block was cut at two levels, which were 40 μm apart. Altogether, there were 4 to 8 levels of graft sections from apex to base. At each level, the tissue section was stained by the H&E staining in the pathohistology lab. The staining slides were evaluated blindly by Dr. Eizaburo Sasatomi (U. Pittsburgh) to grade the acute rejection in the donor heart. Grading is according to the criteria made by the International Heart and Lung Transplantation Society (IHLTS) in 1990 as following:

Grade 0: Negative for acute rejection

Grade 1A: focal mild acute rejection

Grade 1B: Diffuse mild acute rejection

Grade 2: Focal moderate acute rejection

Grade 3A: Multifocal moderate acute rejection

Grade 3B: Diffuse moderate acute rejection

Grade 4: Diffuse aggressive polymorphous infiltrate with necrosis.

2.18 DETERMINATION OF CARDIAC ALLOGRAFT ARTERIOSCLEROSIS IN DONOR GRAFTS

Cardiac allograft arteriosclerosis was determined by measuring the percentage of vessel occlusion in the donor grafts. As described in **2.17**, after harvested, the donor grafts were divided into 2 to 4 sections and each section was embedded in paraffin. Graft tissue in each paraffin block was cut at two levels, which were 40 μm away. Altogether, there were 4 to 8 levels of graft section from apex to base. At each level, the tissue section was stained by verhoeff's Van Geison (vVG) staining. Pictures were taken for arteries in the tissue section using a reflected light differential interference contrast microscope (Olympus Provis AX70, Tokyo, Japan). Vessel occlusion was measured using Metamorph software. Figure 10 represents a vVG staining section of a human coronay artery with severe cardiac allograft arteriosclerosis (183). Metamorph estimated the areas of the internal elastic lamina and lumen. The percentage of the vessel occlusion was calculated using the following formula:

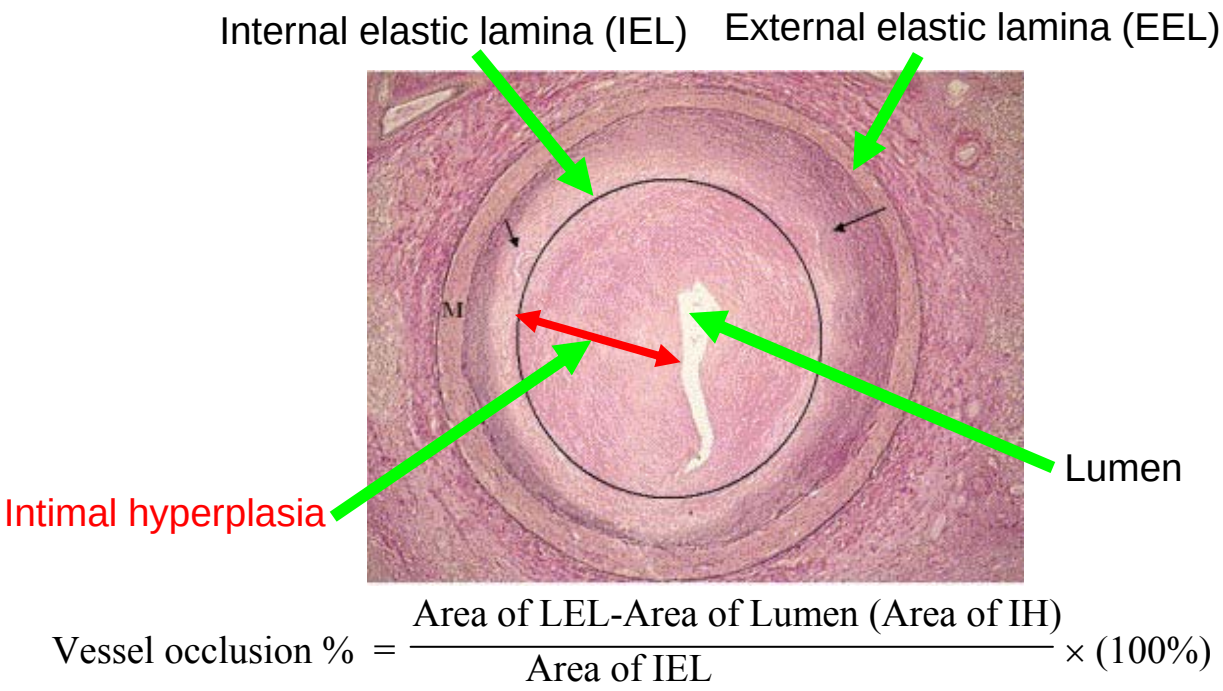

$$\text{Vessel occlusion \%} = \frac{\text{Area of LEL-Area of Lumen (Area of IH)}}{\text{Area of IEL}} \times (100\%)$$

Figure 12 Determination of the percentage of vessel occlusion.

To get the mean and stardard deviation of vessel occlusion in the donor graft, we established our criteria to count vessels in the tissue section: 1. The vessel diameter ≥30μm; 2. The vessel should be an artery, not vein. 3. The vessel should have an identifiable internal elastic lamina; 4. The vessel should be represented cross section, but not the mix of cross and tangential section.

We also employeed the grading system described by Dr. Anthony J. Demetris to grade cardiac allograft arteriosclerosis (175). The grade criteria are as following:

Grade 0: no occlusion

Grade 1: Vessel occlusion >0 and ≤10%;

Grade 2: Vessel occlusion >10% and ≤ 25%.

Grade 3: Vessel occlusion >25% and ≤ 50%.

Grade 4: Vessel occlusion >50% and ≤ 75%.

Grade 5: Vessel occlusion > 75%.

2.19 SEQUENTIAL INJECTION OF LIPOSOME-ADCMV-LACZ OR ADCMV-EGFP

Liposomes containing DOTAP and cholesterol in a 1:1 molar ratio were prepared as follows. The lipid mixture in chloroform was dried under a stream of nitrogen as a thin layer in a 100-ml round-bottomed flask, which was further desiccated under vacuum for 2 h. The lipid film was hydrated in 5% dextrose in water to give a final concentration of 10 mg DOTAP/ml. Preparation of small unilamellar vesicles by extrusion was performed as follows. The lipid solution was briefly sonicated, followed by incubation at 50°C for 10 min, and then sequentially extruded through polycarbonate membranes with the following pore sizes: 1.0, 0.6 and 0.2 μm. The size of liposomes was around 150 nm as measured by dynamic laser scattering using a Coulter N4SD particle sizer (Hialeah, FL, USA).

The amount of DOTAP:cholesterol liposomes and adenoviral vector per mouse was 900 nmol and 10^{11} viral particles, respectively. All of the dilutions were made in saline. Four mice received an injection of 150 μl of liposome through the tail vein. Five minutes later, 150 μl of adenoviral vector AdCMV-lacZ was injected via the tail vein again. In another group, four mice received 150 μl of liposome and then 150 μl of adenoviral vector AdCMV-EGFP. Control mice only received AdCMV-lacZ or AdCMV-EGFP (n=4).

Three days later, the mice were sacrificed. Heart and lung were harvested and transgene expression was determined.

3.0 RESULTS: DEVELOPMENT OF GENE DELIVERY SYSTEM FOR INOS SPECIFIC EXPRESSION

3.1 DEVELOPMENT OF ENDOTHELIAL-SPECIFIC ADENOVIRAL VECTOR

NO has been shown to play an inhibitory role on the development of cardiac allograft arteriosclerosis. NO inhibits intimal hyperplasia by suppressing smooth muscle cell proliferation and migration, preventing leukocyte and platelet adhesion to endothelium & platelet aggregation, promoting endothelial cell proliferation and blocking endothelial cell apoptosis. NO donors, arginine or arginine polymer, suppressed intimal hyperplasia in the cardiac allografts even 90 days after transplantation (97, 98). Despite these promising results, our preliminary data showed that iNOS expression mediated by adenoviral vector with the CMV promoter lacked tissue-specific targeting. Consequently, the induction of iNOS in cardiomyocytes suppressed cardiac contractility, as supported by our preliminary data and by many other studies (111-115, 166, 236). Furthermore, the induction of iNOS in cardiomyocytes led to apoptosis and exacerbated acute rejection after transplantation (117-119, 126).

Based on these studies, we want to take an advantage of the inhibitory effect of iNOS on cardiac allograft arteriosclerosis while avoiding its detrimental role on cardiac function by vascular-specific expression. In this chapter, we describe the establishment of two vascular-specific gene delivery systems. One is the adenoviral vector system with vascular-specific

promoter to regulate iNOS specific expression. Another is the development of vascular-specific iNOS inducible transgenic mice in which vascular-specfic promoter was employed. Our goal is to specifically target cardiac endothelial cells or smooth muscle cells. Therefore, we first identified a smooth muscle- or endothelial-specific promoter that can target cardiac vasculature well.

3.1.1 To identify smooth muscle- or endothelial cell-specific promoters *in vitro*

In the past decade, several endothelial- or smooth muscle cell-specific promoters have been identified. The endothelial cell-specific promoters include the murine TieSE (promoter + 1.6kb enhancer) (128), the murine Tie2LE (promoter + 10kb enhancer) (128), the human ICAM2 promoter (-292 ~ +44 bp) (129), the human vWF promoter (promoter + enhancer, -487 ~ +246 bp) (130), the human Flt-1 promoter (promoter, -748 ~ +284 bp) (137), the murine vascular endothelial cadherin promoter (-2486 ~ +24 bp) (131), the murine preproendothelin-1 promoter with small enhancer (5.9kb 5' flank region + first exon + first intron) (132), and the murine preproendothelin-1 promoter with large enhancer (9.2kb 5'flank region + first exon + first intron) (133). The smooth muscle cell-specific promoters include the rat SMMHCL promoter (promoter + large enhancer, -4229 ~ +11600 bp) (134), the rabbit SMMHCS promoter (promoter + enhancer, -2305 ~ -4 bp) (135) and the murine smooth muscle 22α promoter (SM22α, -441 ~ +41 bp) (136).

Though reports have suggested that the above promoters are capable of directing vascular-specific gene expression, conflicting results have also been reported. For example, the ICAM2 promoter was reported in several papers to drive endothelial-specific expression in transgenic mice (129, 161-165). However, Stuart *et al.* showed that this promoter also led to

leaky expression in human primary vascular smooth muscle cells, human primary foreskin fibroblasts, HeLa cells, and HepG2 cells when these cells were infected by an adenoviral vector driving the expression of *lacZ in vitro* (138). Moreover, these nominal endothelial- or smooth muscle cell-specific promoters were identified by different research groups, and direct comparison of these promoters' activity and specificity remains to be investigated. In our search for an effective endothelial- or smooth muscle cell-specific promoter for vascular-specific targeting, we tested five endothelial cell-specific promoters and two smooth muscle cell-specific promoters *in vitro*. The five endothelial cell-specific promoters include the murine TieSE promoter (128), the murine Tie2LE promoter (128), the human ICAM2 promoter (-292 ~ +44 bp) (129), the human vWF promoter (-487 ~ +246 bp) (130), and the human Flt-1 promoter (-748 ~ +284 bp) (137). The smooth muscle cell-specific promoters include the rat SMMHCL promoter (-4229 ~ +11600 bp) (134), and the rabbit SMMHCS promoter (-2305 ~ -4 bp) (135).

3.1.1.1 Characterization of the Tie2SE, Tie2LE, ICAM2, and Flt-1 promoters in endothelial cells *in vitro*

To compare the activity and specificity of three endothelial cell-specific promoters Tie2SE, ICAM2, and vWF, the DNA plasmids pTie2SE-FretMT, pICAM2-FretMT, and pvWF-FretMT were used to transfect endothelial cells (BAEC) and non-endothelial cells (primary rat smooth muscle cells and HEK293 cells). The DNA plasmid pCMV-FretMT was used as a positive control for the FretMT expression due to the promiscuous nature of the CMV promoter, and pCMV-lacZ served as a negative control. The expression of the reporter gene was represented by the percentage of cells exhibiting green fluorescence. Each transfection was performed in three wells of a 12-well plate. This experiment was repeated three times. The data shown represent the average from one experiment.

Table 2 Determination of endothelial cell-specific promoter.

	Rat SMC	BAEC	HEK293	Rat hepatocytes
pTie2-FretMT	0	3%	0.5%	/
pICAM2-FretMT	0.4%	5%	5%	/
pvWF-FretMT	0	0.5%	0.5%	/
pCMV-FretMT	10%	15%	60%	/
pTie2LE-lacZ	/	7%	0.3%	0.1%
pCMV-lacZ	/	30%	50%	10%

As shown in Table 2 and Figure 13, the Tie2SE promoter exhibited good gene expression and endothelial-specificity. The ICAM2 promoter also exhibited good gene expression and specificity in endothelial cells, although it also expressed some in HEK293 cells (approximately 5% of the cells exhibited green fluorescence). Compared to the CMV promoter which was associated with green fluorescence in 60% of HEK293 cells, the expression directed by the ICAM2 promoter was minor. The vWF promoter did not drive appreciable gene expression in any of the cells examined. The negative control pCMV-lacZ did not exhibit any green fluorescence.

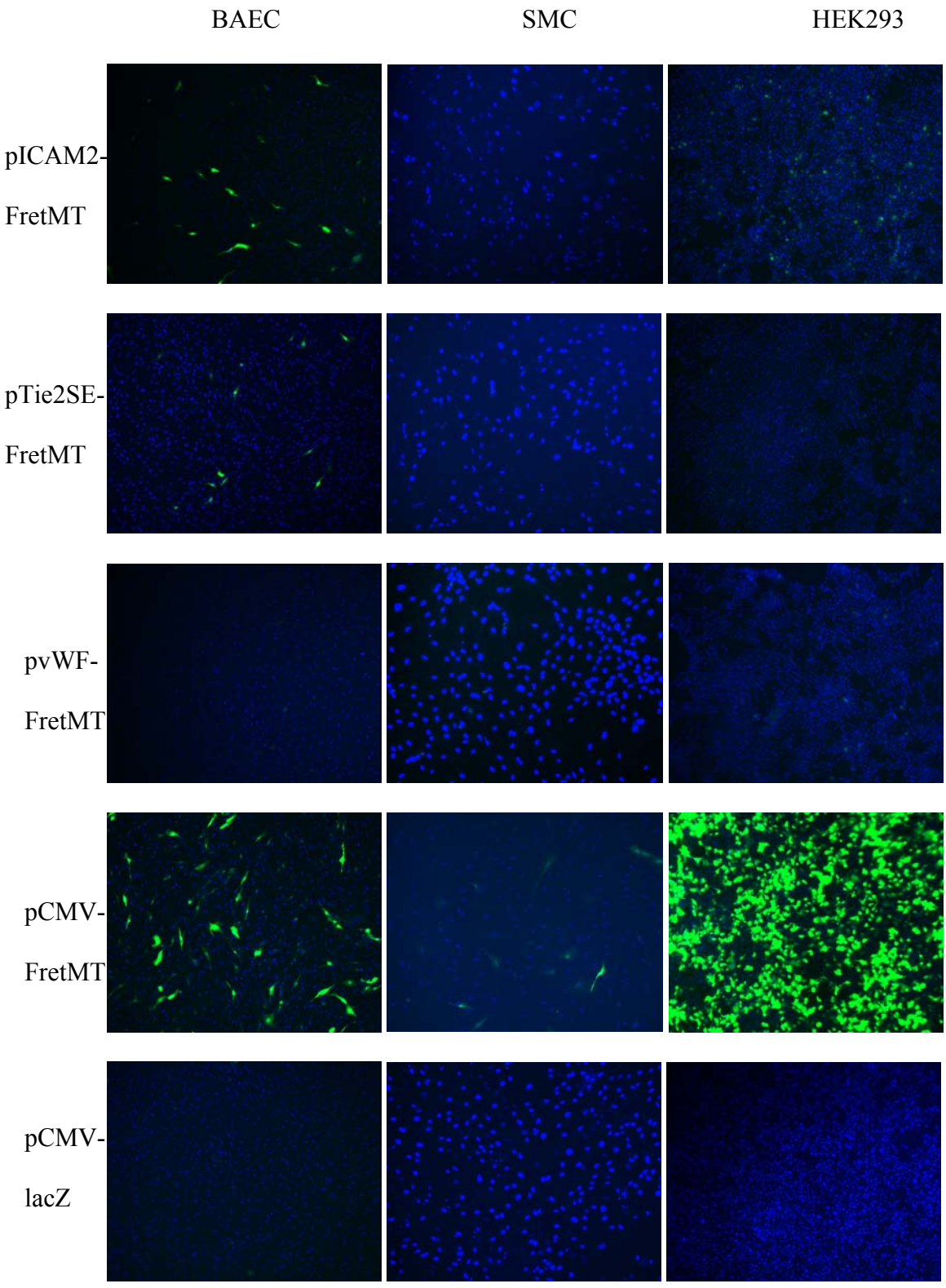

Figure 13 Green fluorescence of BAEC, rat smooth muscle cells, and HEK293 cells transfected by pICAM2-FretMT, pTie2SE-FretMT, pvWF-FretMT, pCMV-FretMT, or pCMV-lacZ.

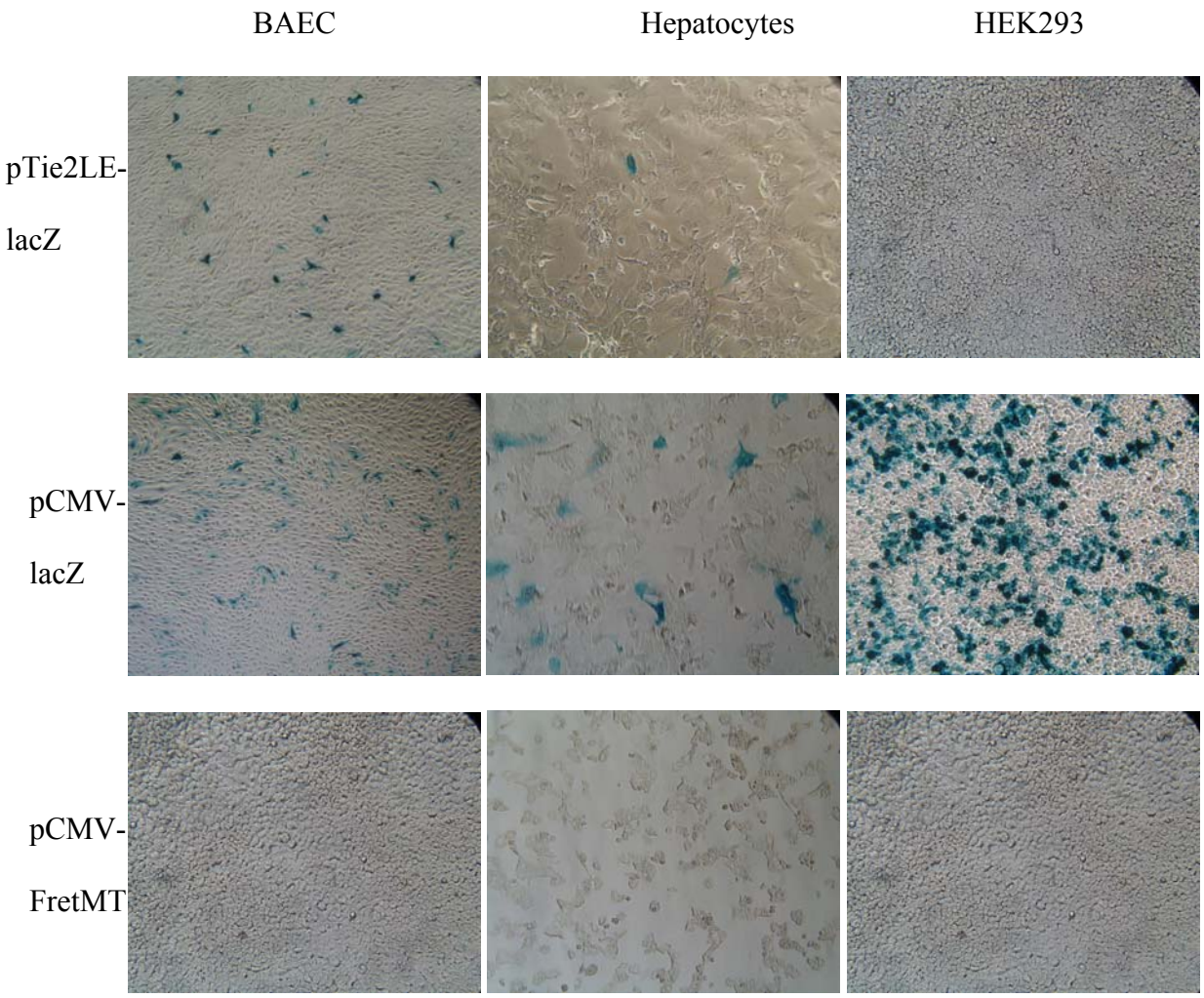

Figure 14 X-gal staining of BAEC, rat hepatocytes, and HEK293 cells transfected by pTie2LE-lacZ, pCMV-lacZ, or pCMV-FretMT.

To test the Tie2LE promoter, pTie2LE-lacZ, pCMV-lacZ and pCMV-FretMT were used to transfect BAEC, rat hepatocytes, and HEK293 cells. pCMV-lacZ and pCMV-FretMT served as positive and negative controls, respectively, for β-galactosidase expression. After transfection, X-gal staining was performed and the percentage of blue-stained cells was calculated. Each transfection was performed in three wells of a 12-well plate. This experiment was repeated three times. Table 2 and Figure 14 show that the Tie2LE promoter demonstrated good activity in

BAEC while exhibiting very low activity in rat hepatocytes and HEK293 cells. The negative control pCMV-FretMT did not exhibit any positive X-gal staining.

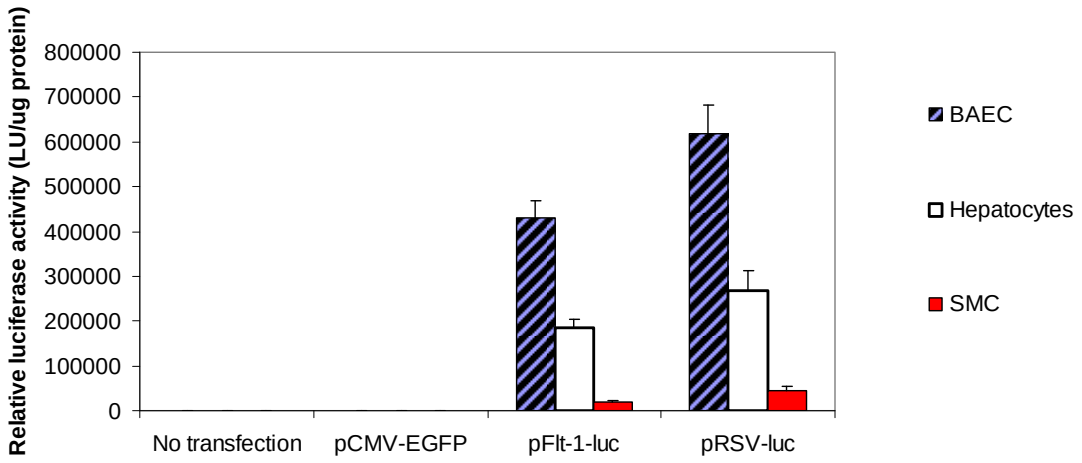

Figure 15 Relative luciferase activity of BAEC, rat smooth muscle cells, and HEK293 cells transfected by pFlt-1-luc, pRSV-luc and pCMV-EGFP.

To address the specificity and activity of the Flt-1 promoter, the DNA plasmids pFlt-1-luc, pRSV-luc, and pCMV-EGFP were transfected into BAEC, rat hepatocytes, and rat smooth muscle cells. pRSV-luc and pCMV-EGFP served as positive and negative controls, respectively. Forty-eight hours after transfection, the cells were lysed and the relative luciferase activity was compared. Each transfection was performed in three wells of a 12-well plate, which generates the mean and standard deviation of the relative luciferase activity. This experiment was repeated three times and the data shown in Figure 15 represents the result from one experiment. As shown in Figure 15, the Flt-1 promoter demonstrated good activity in BAEC, although it also exhibited some expression in rat hepatocytes.

3.1.1.2 Lack of SMC-specific activity of both the SMMHCL (-4229~ +11600bp) and the SMMHCS (-2305~ 4pb) promoters *in vitro*

We also tested two smooth muscle cell-specific promoters *in vitro*: rat SMMHCL (-4229 ~ +11600 bp) and rabbit SMMHCS (-2305~-4 bp). We compared their activity and specificity in both primary rat smooth muscle cells and other cell types (BAEC, rat hepatocytes, and HEK293 cells). The DNA plasmids pSMMHCL-luc, pSMMHCS-EGFP, pRSV-luc, and pCMV-EGFP were used to transfect cells. As shown in Figure 16 and Figure 17, the SMMHCL promoter was not effective at driving gene expression in either cultured smooth muscle cells or HEK293 cells. In contrast, the SMMHCL promoter drove some gene expression in BAEC and hepatocytes. The SMMHCS promoter did not lead to appreciable expression in either cultured smooth muscle cells (Figure 18), BAEC or HEK293 cells (data not shown).

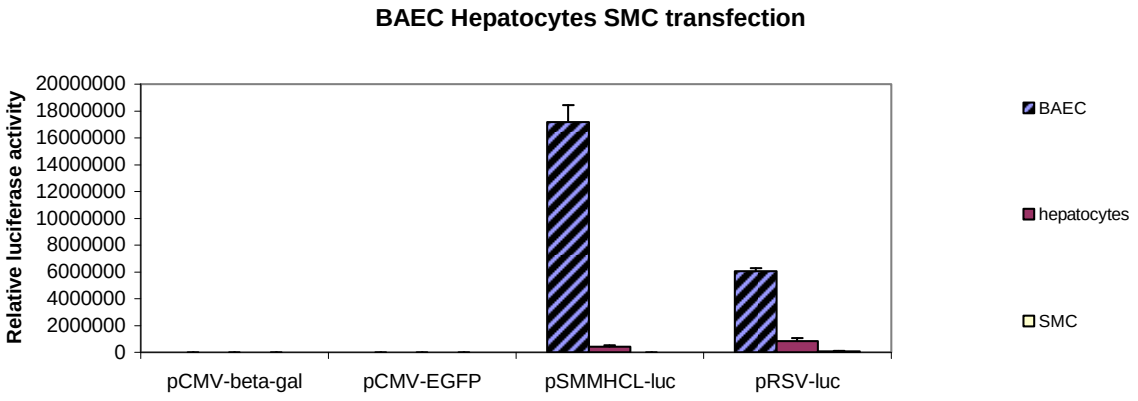

Figure 16 Relative luciferase activity when BAEC, hepatocytes and SMC cells were transfected by pSMMHCL-luc, pRSV-luc, pCMC-beta-gal and pCMV-EGFP.

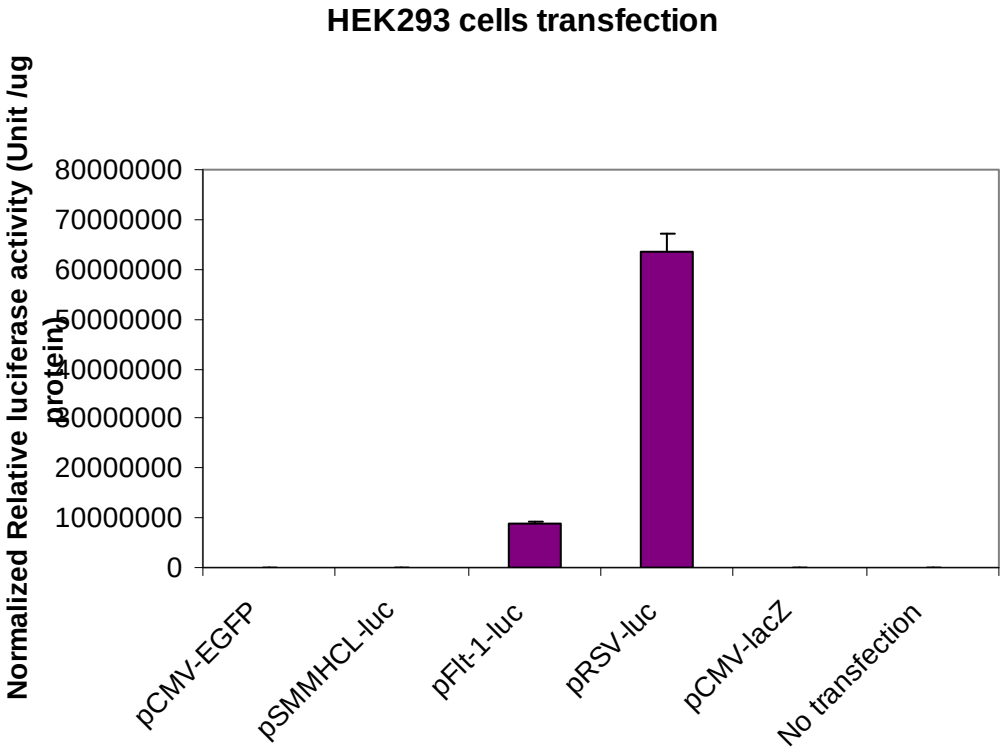

Figure 17 Relative luciferase activity when HEK293 cells were transfected by pSMMHCL-luc, pFlt-1-luc, pRSV-luc, pCMC-lacZ and pCMV-EGFP.

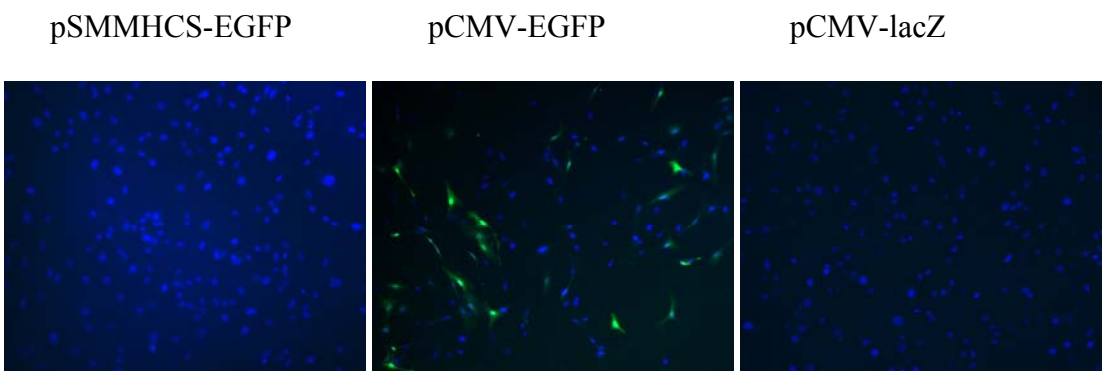

Figure 18 Green Fluorescence when SMC was tranfected by pSMMHCS-EGFP, pCMV-EGFP and pCMV-lacZ.

3.1.1.3 Conclusion

From the above study, we concluded that the Tie2SE, Tie2LE, ICAM2 and Flt-1 promoters demonstrated good endothelial activity and specificity *in vitro*. The vWF promoter did not exhibit endothelial-specific activity *in vitro*. The SMMHCS and SMMHCL promoters did not exhibit smooth muscle cell-specific activity *in vitro*.

3.1.2 Endothelial-specific activity of the Flt-1 and ICAM2 promoters i*n vitro* using AdFlt-1-lacZ and AdICAM2-lacZ to infect cells.

To further compare the endothelial activity and specificity of the Flt-1, ICAM2 and vWF promoters, we infected BAEC, rat SMC and hepatocytes in *vitro* at a MOI of 100 using adenovirus AdFlt-1-lacZ, AdICAM2-lacZ and AdvWF-lacZ. AdCMV-lacZ and AdCMV-EGFP were used as positive and negative controls, respectively. As shown in Table 3, both the Flt-1 and ICAM2 promoters exhibited good endothelial activity in BAEC while both of the promoters exhibited some activity in SMC and relatively high activity in hepatocytes. The vWF promoter did not exhibit any activity in any cell types.

Table 3 Endothelial activity of the Flt-1, ICAM2 and vWF promoters in SMC, BAEC and hepatocytes using adenovirus infection.

	SMC	BAEC	Hepatocytes
AdFlt-1-lacZ	5%	15%	30%
AdICAM2-lacZ	20%	25%	70%
AdvWF-lacZ	0	0	0
AdCMV-lacZ	30%	70%	95%
AdCVM-EGFP	0	0	0

3.1.3 Endothelial-specific activity of the Flt-1 and ICAM2 promoters in *ex vivo* transduced aorta

To further compare the specificity and activity of endothelial cell-specific promoters in intact tissues, rat aortae, cardiac muscle, and skeletal muscle were transduced using the adenoviral vectors AdFlt-1-lacZ, AdICAM2-lacZ, or AdvWF-lacZ at a dose of 2 x 10^9 PFU. In these studies, AdCMV-lacZ and AdCMV-EGFP served as positive and negative controls, respectively, for β-galactosidase expression. This experiment was repeated five times.

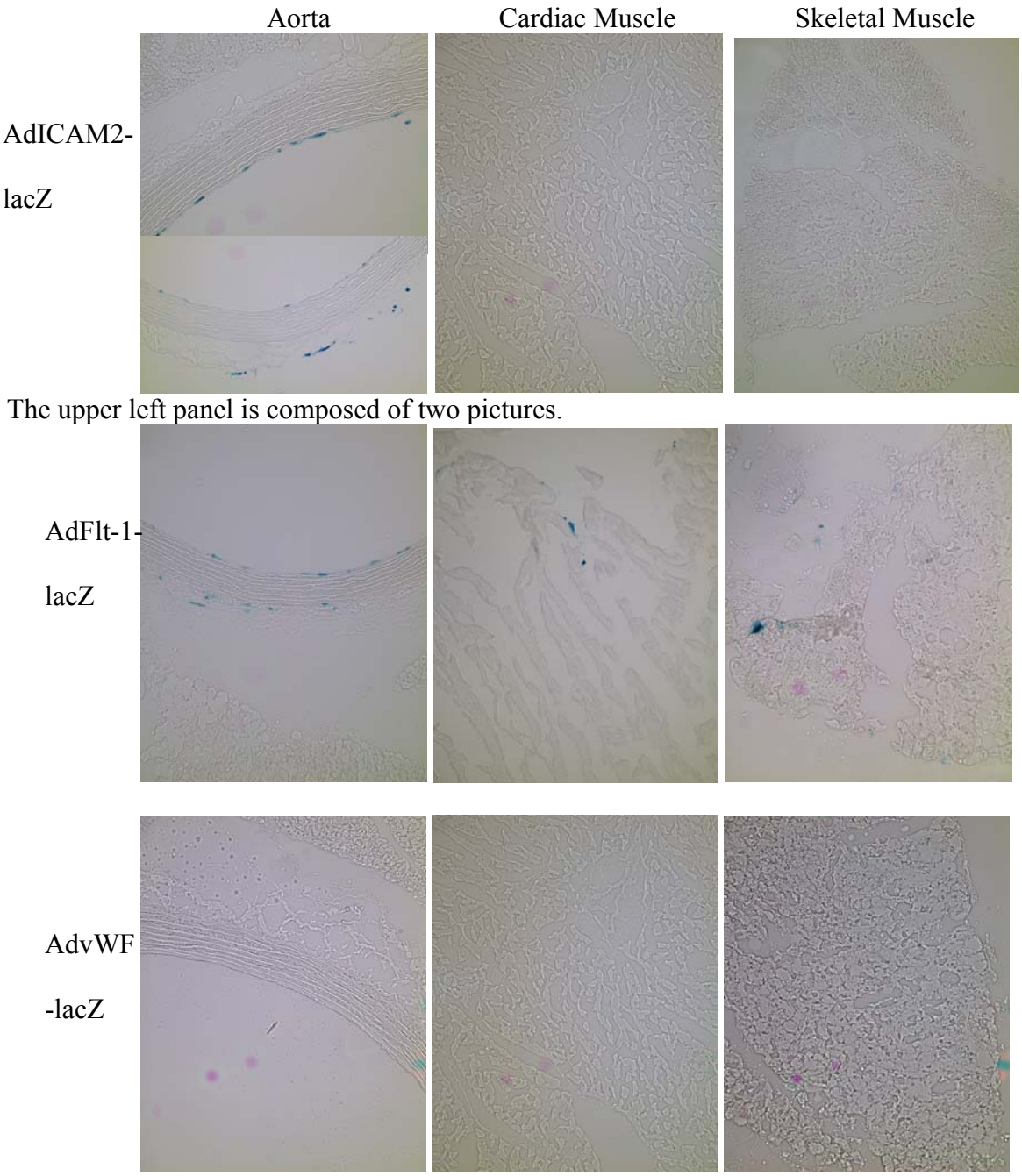

The upper left panel is composed of two pictures.

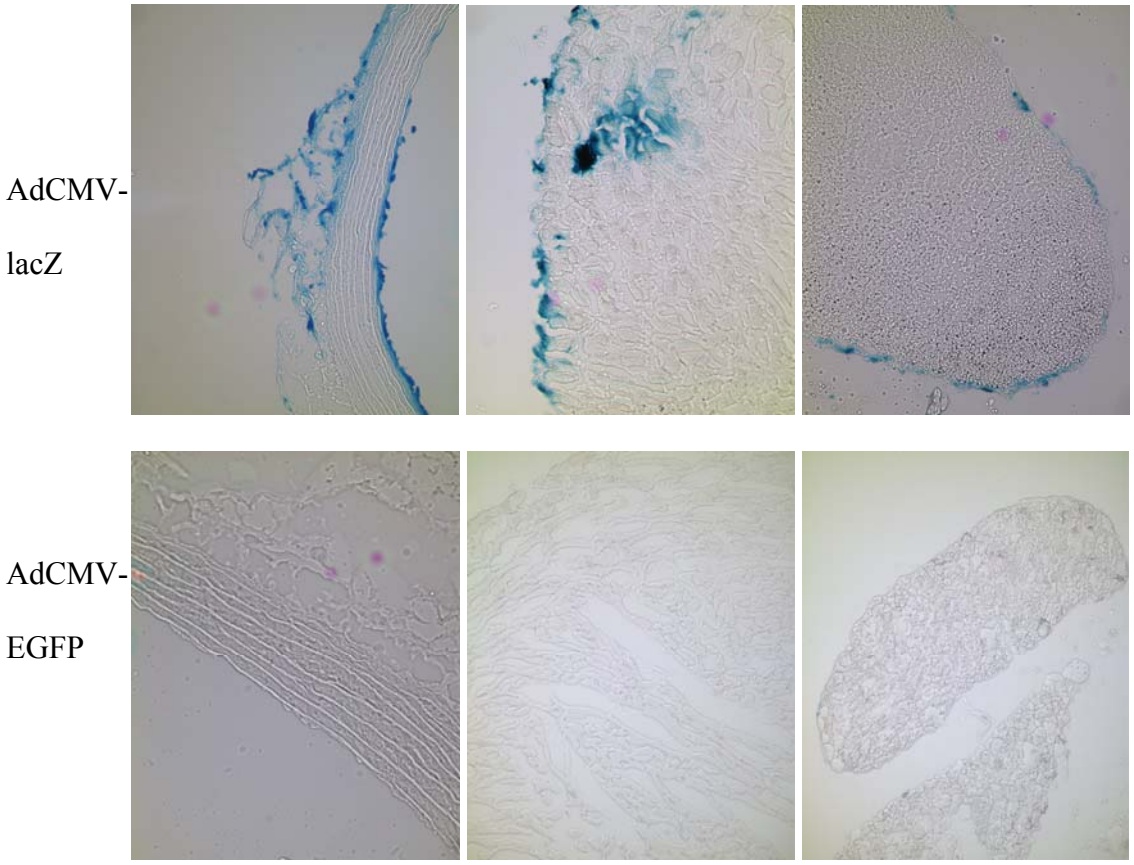

Figure 19 X-gal staining of rat aorta, cardiac muscle, and skeletal muscle transduced by AdICAM2-lacZ, AdFlt-1-lacZ, AdvWF-lacZ, AdCMV-lacZ, or AdCMV-EGFP.

As shown in Figure 19, approximately 10% of the endothelial cells and 8% of the adventitial cells exhibited X-gal staining in the AdFlt-1-lacZ-transduced aorta, but no staining was observed in smooth muscle cells. Transduction of cardiac muscle and skeletal muscle resulted in a low number of X-gal-positive muscle cells in both tissues. In the AdICAM2-lacZ transduced tissues, 7% of the endothelial cells and 2% of the adventitial cells exhibited X-gal staining, while few other cell types exhibited positive staining. In the AdvWF-lacZ-transduced tissues, few cells exhibited X-gal staining. The AdCMV-EGFP-transduced tissue was negative for *lacZ* expression. The vWF promoter did not lead to X-gal staining in any of the tissues examined. The negative control AdCMV-EGFP did not exhibit any positive X-gal staining.

3.1.4 Construction of adenovirus vectors AdFlt-1-iNOS, AdICAM2-iNOS and AdTie2SE-iNOS and test the endothelial specificity of the Flt-1, ICAM2, and Tie2SE promoters *in vitro*

Based on the *in vitro* and *ex vivo* test results, we can determine that the Flt-1, ICAM2, Tie2SE and Tie2LE promoters were possible candidates for endothelial-specific targeting. To achieve endothelial-specific expression of iNOS, we constructed three adenoviral vectors AdFlt-1-iNOS, AdICAM2-iNOS and AdTie2-iNOS and tested their specificity *in vitro*. These adenovirus are E1, E3 deleted adenovirus and can accommondate up to 7~8 kb of foreign genes. The Tie2LE promoter (>10kb) is too large to be inserted into the adenoviral vector.

The construction of the adenoviral vectors AdFlt-1-iNOS, AdICAM2-iNOS and AdTie2SE-iNOS was described in **2.5**.

Next, we wanted to determine if the Flt-1, ICAM2 and Tie2SE promoters lead to endothelial-specific expression of iNOS *in vitro* using AdFlt-1-iNOS, AdICAM2-iNOS and AdTie2SE-iNOS. BAEC and rat hepatocytes were infected by AdFlt-1-iNOS, AdICAM2-iNOS and AdTie2SE-iNOS with a MOI of 400 for 2 hours, then the infection media was replaced by the cell culture media. Twenty-four and 48 hours after infection, the culture media was collected and the nitrite level in the media was measured using the Greiss assay. Forty-eight hours after infection, RNA was extracted from cells. Cell lysates were harvested. RT-PCR and western blot were performed to determine iNOS expression.

As shown in Figure 20 and Figure 21, western blot results showed that the Flt-1, ICAM2 and Tie2SE promoters drove iNOS protein expression in BAEC, but not in hepatocytes. Figure 22 showed that the ICAM2 promoter led to significant increase of the nitrite level in the culture media at 48 hours after BAEC were infected by AdICAM2-iNOS, but no increase in that of

hepatocytes. The Flt-1 promoter did not lead to significant increase of the nitrite level in either BAEC or hepatocytes (Figure 23), and neither did the Tie2SE promoter (data not shown). The Flt-1 and Tie2SE promoters drove iNOS protein expression in BAEC that was detected by western blot, but the nitrite level could not be detected by Greiss assay. This controversy may be because that Greiss assay is less sensitive than western blot to detect iNOS expression. The RT-PCR results were shown in Figure 24. In AdFlt-1-iNOS and AdIACM2-iNOS infected rat hepatocytes, both the Flt-1 and ICAM2 promoter led the human iNOS gene to be transcribed. However, the iNOS protein expression could not be detected in the cells as shown in Figure 21. We have observed this when we used the DNA plasmid pTie2SE-iNOS to transfect hepatocytes, the human iNOS gene was transcribed in the hepatocytes (Figure 25). However, the iNOS protein was not detectable in hepatocytes by western blot (Figure 26).

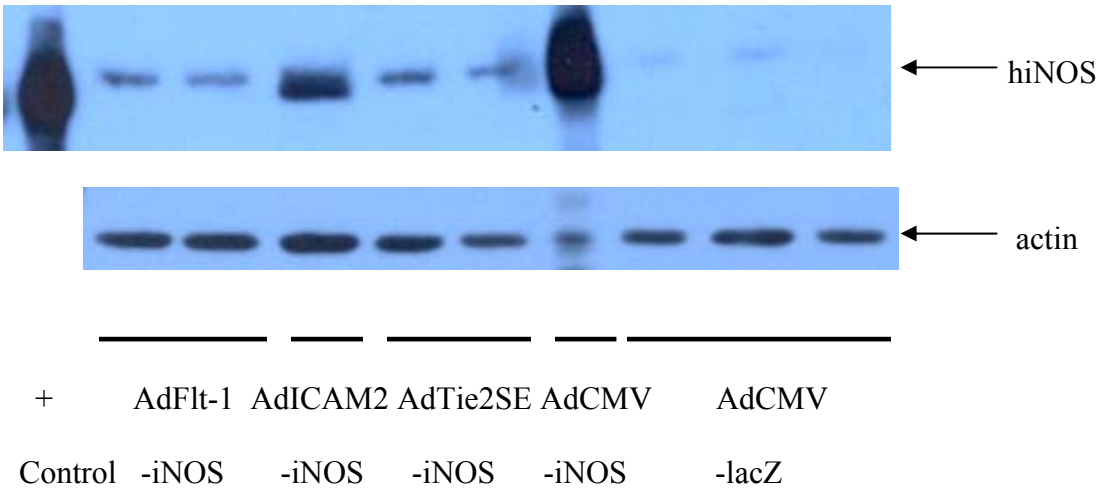

Figure 20 Western blot results show that the human iNOS protein was expressed in BAEC when BAEC were infected by AdFlt1-iNOS and AdICAM2-iNOS (400 MOI).

AdCMV-iNOS served as a positive control; AdCMV-lacZ was a negative control. From left to right, 1: hiNOS positive control; 2,3: AdFlt-1-iNOS; 4,5, 6: AdICAM2-iNOS; 7, AdCMV-iNOS; 8,9, 10: AdCMV-lacZ.

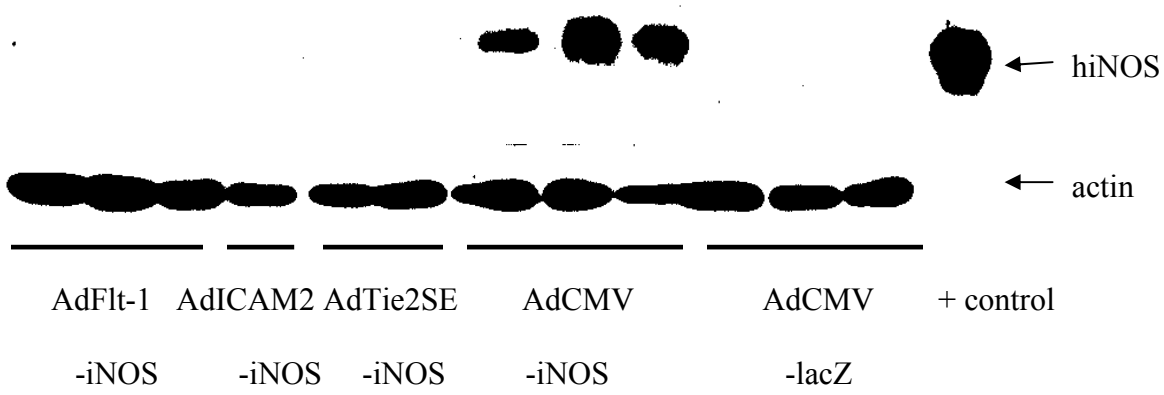

Figure 21 Western blot results show that the human iNOS protein was not detectable in rat hepatocytes when they were infected by AdFlt1-iNOS and AdICAM2-iNOS (400 MOI).

From left to right, 1, 2, 3: AdFlt-1-iNOS; 4, 5, 6: AdICAM2-iNOS; 7, 8.9: AdCMV-iNOS; 10, 11, 12: AdCMV-lacZ; 13: hiNOS positive control.

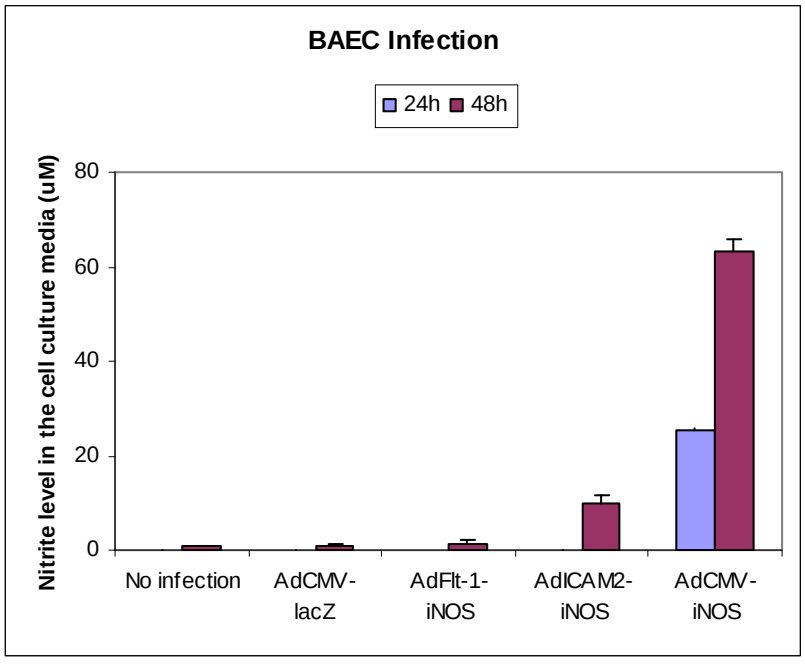

Figure 22 Nitrite levels in the cell culture meida when BAEC were infected by AdFlt-1-iNOS, AdICAM2-iNOS, AdCMV-iNOS and AdCMV-lacZ.

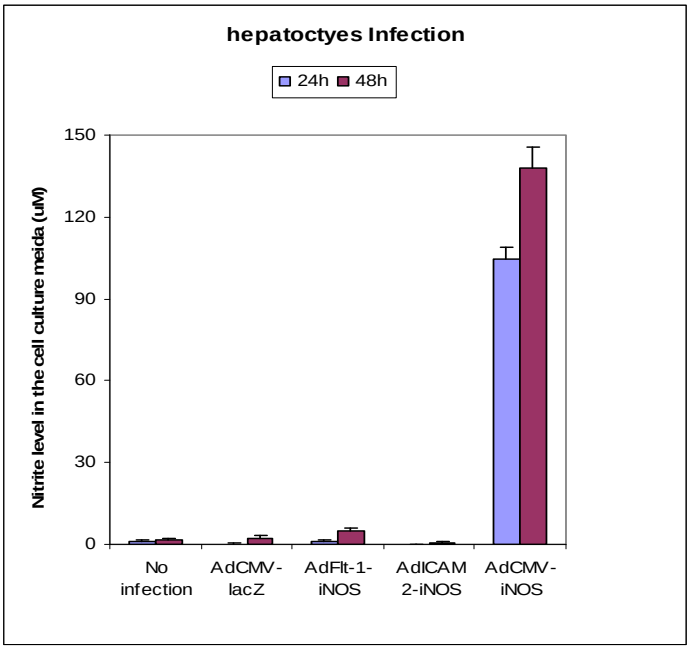

Figure 23 Nitrite levels in the cell culture meida when rat hepatocytes were infected by AdFlt-1-iNOS, AdICAM2-iNOS, AdCMV-iNOS and AdCMV-lacZ.

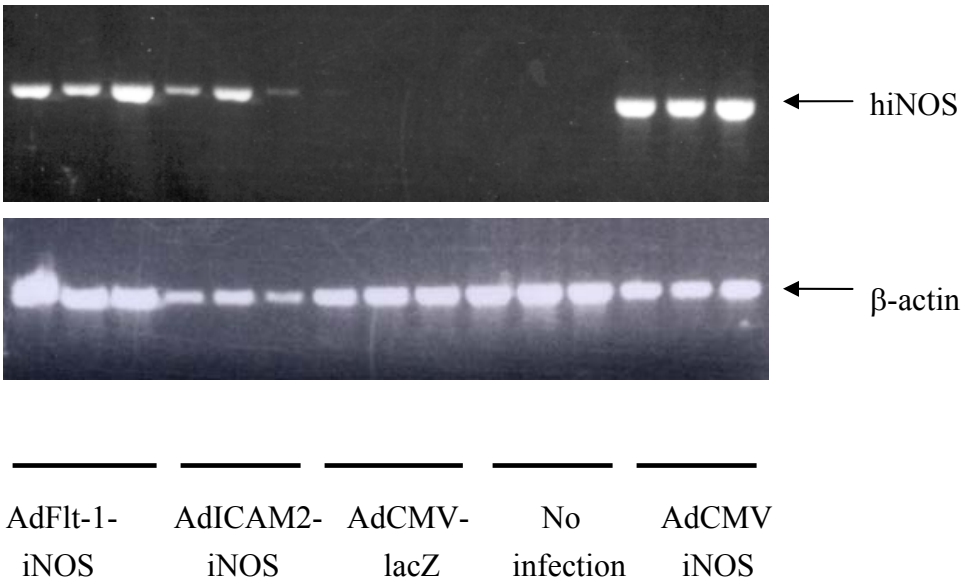

Figure 24 RT-PCR results show that human iNOS was transcribed in rat hepatocytes when they were infected by AdFlt-1-iNOS and AdICAM-iNOS (400MOI).

AdCMV-iNOS served as a positive control; AdCMV-lacZ and no infection were negative controls. From left to right, 1, 2,3: AdFlt-1-iNOS; 4,5, 6: AdICAM2-iNOS; 7, 8.9: AdCMV-lacZ; 10, 11, 12: AdCMV-lacZ; 13, 14, 15: AdCMV-iNOS

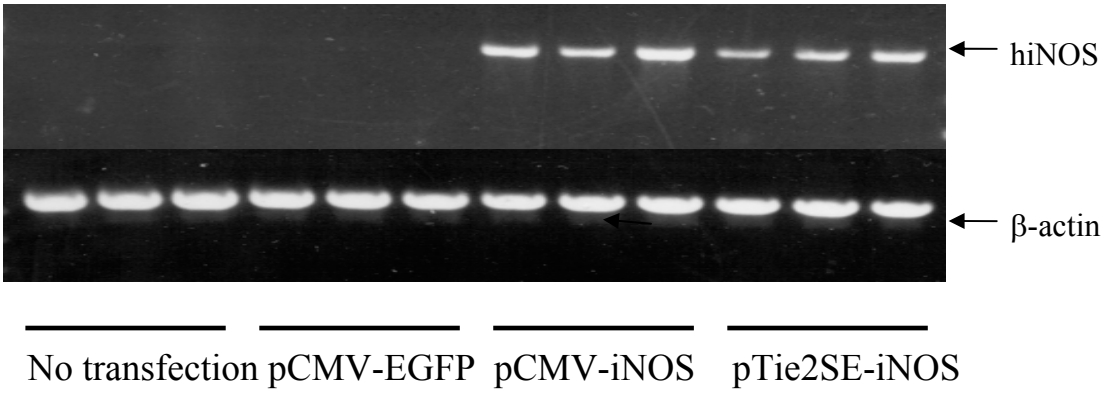

Figure 25 RT-PCR results show that human iNOS was transcribed in rat hepatocytes when they were transfected by pTieSE-iNOS.

pCMV-iNOS serves as a positive control; pCMV-EGFP and no infection were negative controls. From left to right, 1, 2,3: No infection; 4,5, 6: pCMV-EGFP; 7, 8.9: pCMV-iNOS; 10, 11, 12: pTieSE-iNOS.

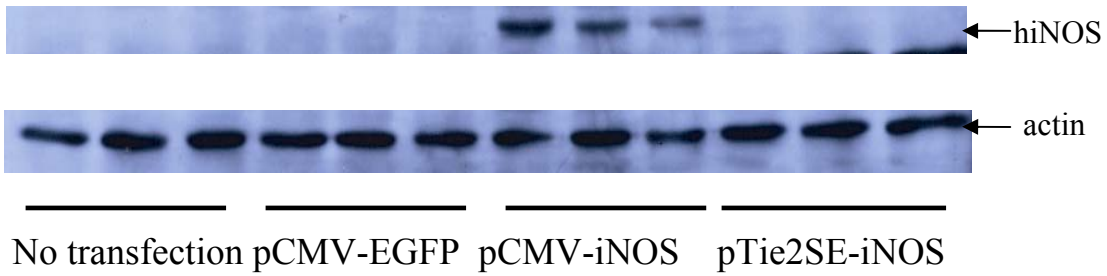

Figure 26 Western blot results show that the human iNOS protein was not detectable when rat hepatocytes were transfected by pTieSE-iNOS.

pCMV-iNOS served as a positive control. pCMV-EGFP and no transfection were negative controls. From left to right, 1, 2,3: No infection; 4,5, 6: pCMV-EGFP; 7, 8.9: pCMV-iNOS; 10, 11, 12: pTieSE-iNOS.

These data demonstrated that the Flt-1, ICAM2 and Tie2SE promoters led to endothelial-specific expression of the human iNOS in BAEC.

3.1.5 Endothelial-specific activity of the ICAM2 promoter in the endothelium of donor heart

Our goal is to identify an endothelial-specific promoter that will lead to iNOS specific expression in cardiac endothelium. We next determined if the Flt-1 and ICAM2 promoters drove gene expression in cardiac endothelium *in vivo* using AdFlt-1-lacZ and AdICAM2-lacZ.

To determine if the Flt-1 and ICAM2 promoters drove gene expression in cardiac endothelium *in vivo*, we employed a rat syngeneic heart transplantation model, in which we transduced donor hearts *ex vivo* using the adenoviral vector AdFlt-1-lacZ or AdICAM2-lacZ at a dose of 10^{10} PFU prior to transplantation. AdCMV-lacZ and AdCMV-EGFP were used as positive and negative controls, respectively. We adopted single injection of adenoviral vector into donor heart for transduction as described in **2.1.2**. Three days later, the donor heart was harvested and the expression of *LacZ* was determined by X-gal staining. As shown in Figure 27, good *lacZ* expression was observed in the endothelial cells of the coronary arteries and veins in 4 of 22 donor grafts that were transduced with AdICAM2-lacZ. In the 4 positive hearts, 22.2%, 33.3%, 50.9% and 56.7% of coronary vessels, respectively, exhibited positive X-gal staining, and the average positive staining spots per vessel is 0.96, 1.94, 1.53, 5.29, respectively. A small percentage of cardiomyocytes also showed positive staining (Figure 27). In other 18 AdICAM2-lacZ transduced grafts, <5% of the vessels were transduced and <0.2 staining spots were observed in each vessel. The Flt-1 promoter directed positive staining in a low number of endothelial cells (<5% of coronary vessels exhibited positive staining and <0.1 staining spots

were observed in each vessel) and a small percentage of cardiomyocytes. The CMV promoter drove extensive *lacZ* expression in cardiomyocytes while scattered and varied gene expression in endothelial cells. In one donor graft, 24.56% of coronary vessels exhibited positive staining and 0.474 staining spots was observed in each vessel. In another 5 grafts, <5% of the vessels were transduced and <0.16 staining spots was observed in each vessel. The negative control AdCMV-EGFP did not lead to positive staining in either endothelial cells or cardiomyocytes (data not shown).

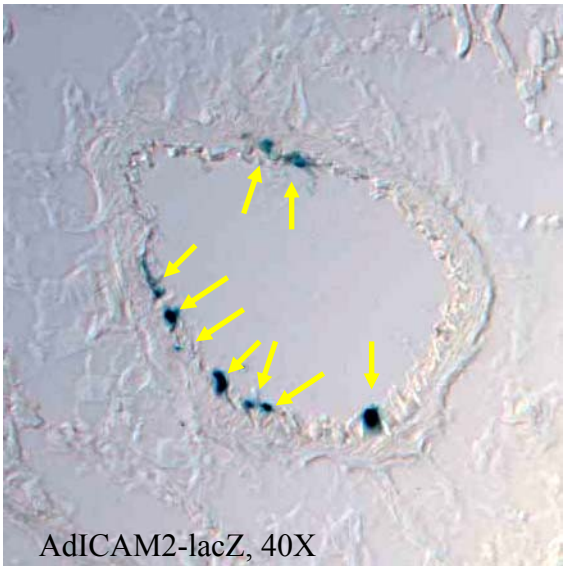
AdICAM2-lacZ, 40X

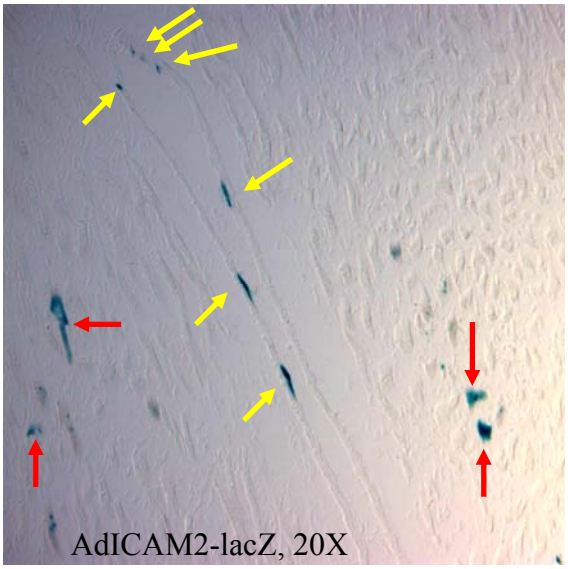
AdICAM2-lacZ, 20X

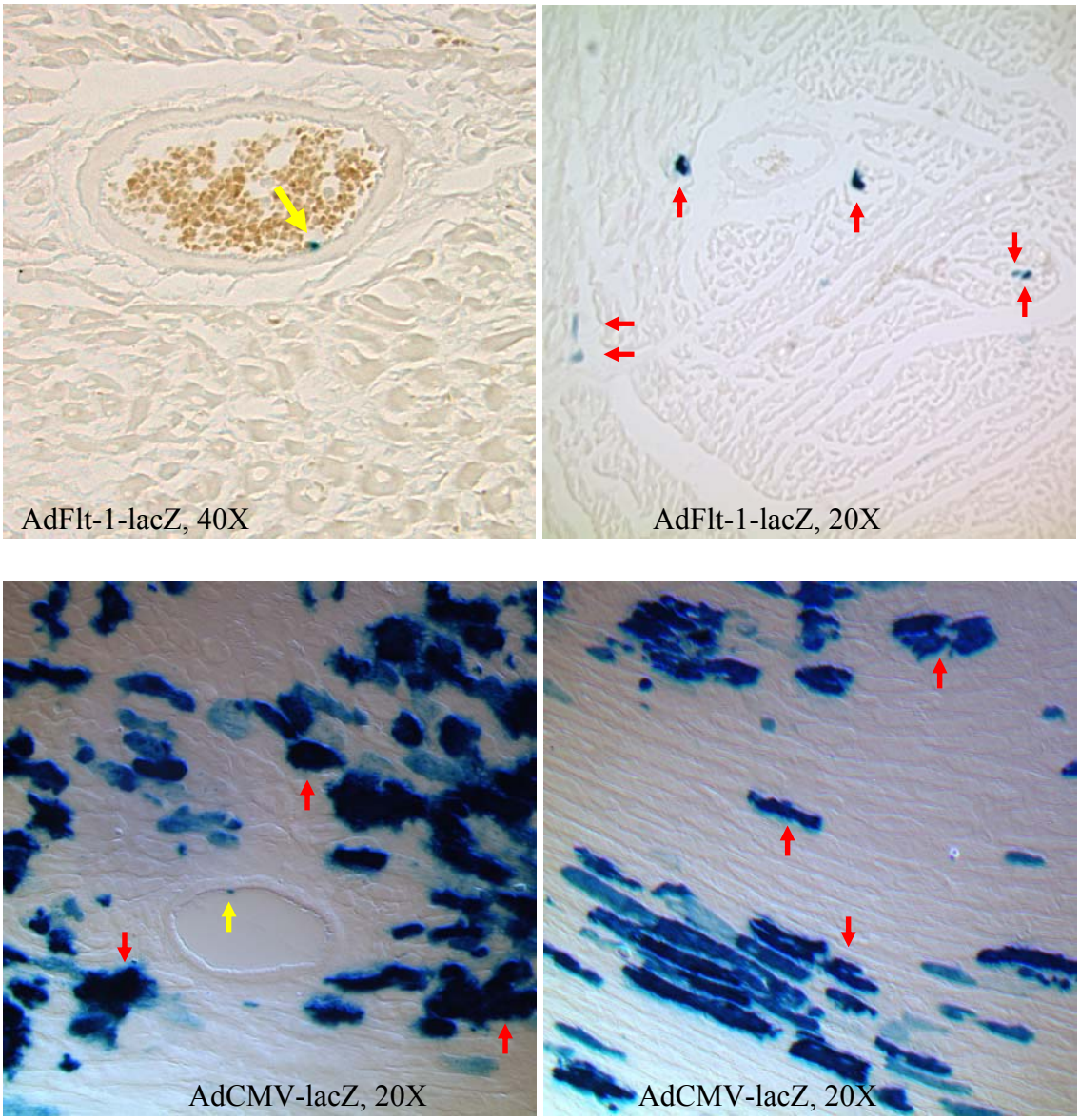

Figure 27 X-gal staining of donor heart that was transduced by AdFlt-1-lacZ, AdICAM2-lacZ and AdCMV-lacZ ex vivo.

Pictures were taken using a reflected light differential interference contrast microscope (Olympus Provis AX70, Tokyo, Japan). Magnification of the tissue sections was desribed in the picture.

3.1.6 Conclusion

The ICAM2, Flt-1, Tie2SE (with 1.6kb enhancer), and Tie2LE (with 10 kb enhancer) promoters demonstrated good specificity and activity in endothelial cells. These promoters may hold promise for endothelial-specific targeting in vascular gene therapy applications. The Tie2LE promoter exhibited better endothelial activity than the Tie2SE promoter. The Flt-1, ICAM2 and Tie2SE promoters not only drove the lacZ gene specifically expressed in endothelial cells, but demonstrated good endothelial-specificity when they directed the iNOS expression. The Flt-1 and ICAM2 promoter also exhibited good endothelial-specificity when they were tested in intact aorta, cardiac muscle and skeletal muscle. The ICAM2 promoter drove good lacZ gene expression in endothelium of the donor grafts although the transduction results varied a lot. The ICAM2 promoter may serve a candidate for cardiac endothelium-specific targeting. Due to the diversity of vasculature in different organs and tissues, additional *ex vivo* and *in vivo* tests are needed to determine the optimal promoters for specific applications. The human vWF, rat SMMHCL (-4229 ~ +11600 bp), and rabbit SMMHCS (-2305~-4 bp) promoters did not demonstrate vascular-specificity in this study, though additional studies may unmask specific applications for these promoters.

We have successfully constructed three adenoviral vectors with endothelial-specific promoters to drive the human iNOS expression: AdFlt-1-iNOS, AdICAM2-iNOS and AdTie2SE-iNOS. The three adenoviral vectors exhibited endothelial-specific activity *in vitro*.

3.1.7 Discusion

We compared five nominal endothelial cell-specific promoters and two putative smooth muscle cell-specific promoters *in vitro*. The activity and cell-type specificity of the Tie2LE, Tie2SE, ICAM2, Flt-1, and vWF promoters were tested in BAEC, rat smooth muscle cells, rat hepatocytes and HEK293 cells using DNA plasmid transfection. Moreover, the latter three promoters were also compared in intact tissues including rat aortas, cardiac muscle, and skeletal muscle using adenoviral transduction. We conclude that both the ICAM2 and Flt-1 promoters demonstrated good endothelial activity and specificity. However, the ICAM2 promoter drove a low degree of reporter gene expression in HEK293 cells and the Flt-1 promoter directed some expression in rat hepatocytes. Stuart *et al.* (138) and Renolds *et al.* (139) have also reported endothelial-specific activity of the Flt-1 promoter both *in vitro* and *in vivo*. The endothelial-specificity of the ICAM2 promoter has been demonstrated in several transgenic mice lines (128, 161-165), and our results are consistent with those findings. Stuart *et al.* reported that the ICAM2 promoter drove gene expression in several non-endothelial cell lines (human foreskin fibroblasts, human vascular smooth muscle cells, HepG2 cells, and Hela cells) when using the adenoviral vector AdICAM2-lacZ. We used AdFlt-1-lacZ and AdICAM2-lacZ to infect rat hepatocytes, smooth muscle cells and HEK293 cells and also found some non-specific expression in these cells (Table 3). The difference between the cell infection data and aorta transduction data may pertain to the difference between cells and tissues. Oh *et al.* demonstrated different expression of endogenous proteins between cultured lung endothelial cells and lung endothelium (167). This difference between cells and intact tissue may explain different transgene expression pattern between cells and tissues after gene delivery. Moreover, we constructed AdFlt-1-iNOS, AdICAM2-iNOS and AdTie2SE-iNOS and used the three adenoviral vectors to infect BAEC and

hepatocytes. All of the promoters led to iNOS protein expression in BAEC, but not in hepatocytes. These data further confirmed the endothelial-specificity of the Flt-1, ICAM2 and Tie2SE promoters. We observed that AdFlt-1-iNOS and AdICAM2-iNOS did not lead to iNOS protein expression in hepatocytes while AdFlt-1-lacZ and AdICAM2-lacZ drove lacZ expression in hepatocytes (Table 3). The difference could be due to the fact that AdFlt-1-iNOS and AdICAM2-iNOS are constructed in E1, E3 deleted adenovirus while AdFlt-1-lacZ and AdICAM2-lacZ are in E1 deleted adenoviral backbone. The adenoviral E3 gene may affect the activity of the Flt-1 and ICAM2 promoter. We also observed that the Flt-1, ICAM2 and Tie2SE promoter led the iNOS gene to be transcribed in rat hepatocytes, but iNOS protein was not translated. The reason for this result remains to be elucidated.

We also found that the vWF promoter was inactive in both cells and tissues. These findings are consistent with those of Stuart *et al.* (138), who showed that the vWF promoter was inactive in primary human endothelial cells, human vascular smooth muscle cells, human fibroblasts, HepG2 cells, and Hela cells. However, the vWF promoter has been reported to actively drive lacZ or amyloid-β gene expression in brain vascular endothelial cells of transgenic mice (130, 168). Takashi *et al*. also reported that this promoter directed specific β-galactosidase expression in endothelial cells of brain, heart, and skeletal muscle of transgenic mice, but not in other tissues (169). Whether this promoter is only active in endothelial cells from specific tissues--for example, brain, heart or skeletal muscles--remains to be determined. Takashi *et al.* suggested that the Flt-1 and vWF promoters are regulated by distinct transcriptional mechanisms, and this may explain our findings of different gene expression directed by the two promoters. This controversy also highlights the different expression patterns observed *in vitro* and *in vivo*. The Tie2SE and Tie2LE promoters also demonstrated good endothelial activity and specificity

when tested in cells. Because of their large sizes, we could not insert these promoters into adenoviral vectors to test their specificity in intact tissues.

To further determine if the Flt-1 and ICAM2 promoters would lead to good gene expression in cardiac endothelium *in vivo*, we tested the two promoters in a heterotopic heart transplantation model by *ex vivo* transduction of the donor heart using adenoviral vectors. We employed single injection of the adenoviral vector into donor heart and incubated the adenoviral vector in the heart since this resulted in better transduction efficiency in endothelial cells than that of recirculation of the adenoviral vector in the donor heart. For unknown reasons, the AdICAM2-lacZ transduction in endothelium of the donor grafts varied extensively. In four grafts, the ICAM2 promoter led to good gene expression in endothelial cells of the coronary arteries and veins, as along with low expression in cardiomyocytes. These results are consistent with those of others (161, 163, 165), who showed that the ICAM2 promoter directed good and specific *lacZ* or CD46 gene expression in cardiac endothelium of transgenic mice. However, in another 18 grafts, only a low number of endothelial cells exhibited positive staining. The Flt-1 promoter directed *lacZ* expression in only a low number of endothelial cells and a small percentage of cardiomyocytes. The CMV promoter drove low gene expression in endothelial cells while dramatic expression was observed in cardiomyocytes. This finding is consistent with previous reports showing that adenoviral gene expression driven by the CMV promoter transduced endothelial cells poorly in the donor heart (170-172). This finding also raises the possibility that our variable AdICAM2-lacZ transduction results may be due to the poor adenoviral transduction efficiency in vascular cells *in vivo*. This hypothesis awaits further testing using more efficient gene delivery vectors. Our data also indicate that the ICAM2 promoter may serve a candidate for cardiac endothelium-specific targeting. Because the great variety of

adenoviral transduction results, we did not use AdFlt-1-iNOS and AdICAM2-iNOS for further *in vivo* test.

In addition to the endothelial-specific promoters, we also tested two putative smooth muscle cell-specific promoters: SMMHCL and SMMHCS. These two promoters were tested in rat smooth muscle cells, BAEC, rat hepatocytes, and HEK293 cells. Neither of these promoters drove adequate gene expression in cultured smooth muscle cells. One possible explanation for these findings is that the transfection efficiency in cultured smooth muscle cells is very low when using DNA plasmids. This hypothesis awaits further testing using more efficient transduction vectors.

Moreover, we have sussessfully developed three endothelial cell-specific adenoviral vectors: AdFlt-1-iNOS, AdICAM2-iNOS and AdTie2SE-iNOS. All of the three adenoviral vectors exhibited endothelial-specific activity *in vitro*. The three adenoviral vectors drove iNOS protein expression in BAEC, but not in hepatocytes. Our original plan is to use the three vascular-specific adenoviral vectors to infect donor heart and test our hypothesis that endothelial-specific expression of iNOS inhibits cardiac allograft arteriosclerosis in a heart transplantation model. According to the data in **3.1.5**, since adenoviral transduction resulted in greatly variable results, we did not use the three vascular-specfic adenoviral vectors for *in vivo* test.

3.1.8 Liposome-AdCMV-EGFP or AdCMV-lacZ sequential injection did not lead to endothelial-specific gene expression in the heart

Another strategy to enhance endothelial delivery is to utilize liposomes to promote endothelial uptake of adenoviral vector. When a positively charged liposome is mixed with a negatively charged DNA plasmid, the liposome neutralizes the negatively charged plasma membrane of cell

and facilitateas the endocytosis of DNA plasmid into the cell. Similarly, Dr. Song Li's lab (U. Pittsburgh) showed that sequential injection of liposome and adenoviral vectors improved adenoviral infection efficiency in lung endothelial cells (237, 238). Specifically, 150 μl of liposome was quickly injected into mice via the tail veil. This injection developed hydrodynamic pressure in the inferior vena cava and drove liposomes into tissues, including the liver, lung, heart, and spleen. Five minutes later, 150 μl of AdCMV-EGFP was injected through the tail vein. This approach greatly enhanced the lacZ expression in pulmonary endothelial cells compared to the single AdCMV-lacZ injection alone. EGFP was mainly expressed in the capilliary endothelial cells (238). Ma *et al.* also found that coronary endothelial cells were well transduced (Figure 28, unpublished data). Based on their data, we tried sequential injection of liposome-AdCMV-lacZ and liposme-AdCMV-EGFP and determined transgene expression in the heart and lung.

Sequential injection of liposome-adenoviral vector was described in **2.19**. Four mice were injected with liposome-AdCMV-EGFP and another four mice were injected with liposome-AdCMV-lacZ. The control mice received single injection of AdCMV-lacZ or AdCMV-EGFP. Our results showed limited transgene expression (either EGFP or lacZ) in cardiomyoctes, endothelial cells or smooth muscle cells in the heart. In contrast, both EGFP and lacZ were expressed well in the lung, which is consistent with the Ma *et al.*' result. The results are shown in Figure 29 and 30. The Control mice that received a single injection of AdCMV-EGFP or AdCMV-lacZ expressed much less transgene in the lung compared to the liposome-AdCMV-EGFP or liposome-AdCMV-lacZ treatment (data not shown)

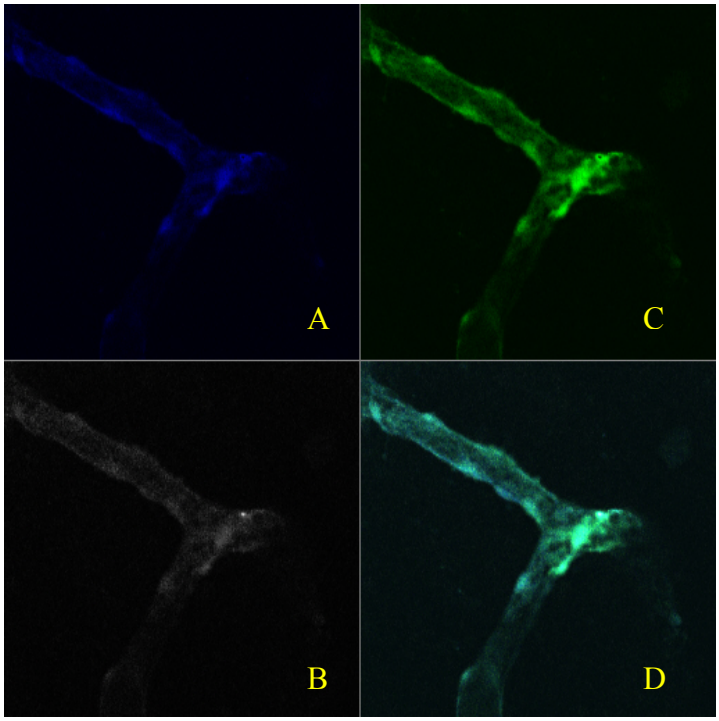

Figure 28 Sequential injection of liposome-AdCMV-EGFP led to EGFP expression in coronary endothelial cells.

A, B: Blue and while fluorescence represented autofluorescence of coronary vessel. C: Green fluorescence represented GFP expression in Coronary vessel. D. Merged fluorescence of blue and green represented EGFP expression in coronary vessels.

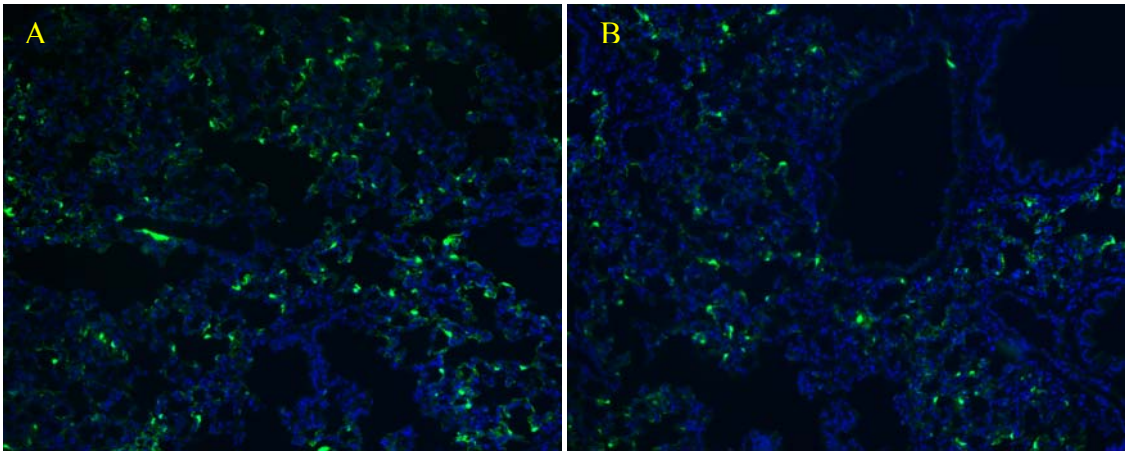

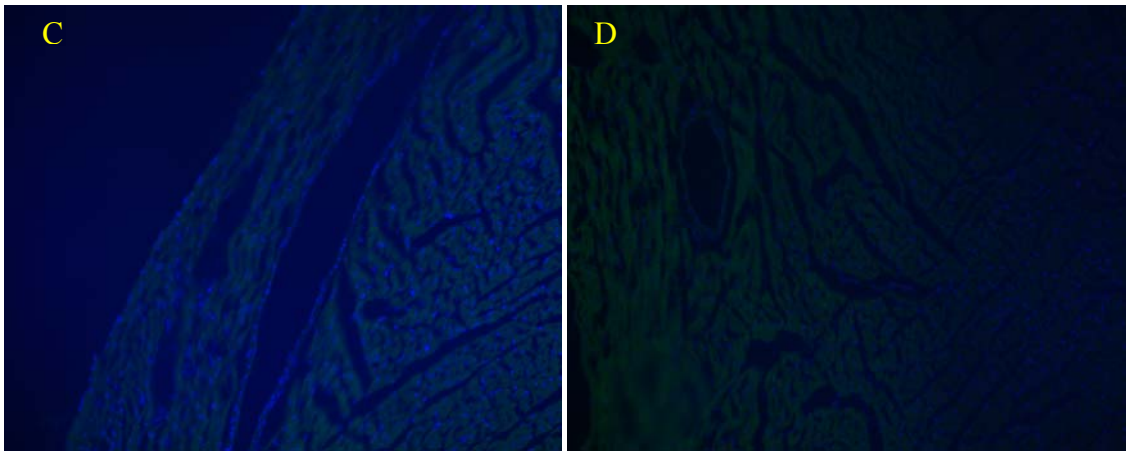

Figure 29 Sequenctial injection of liposome-AdCMV-EGFP drove EGFP expression in the lung, but not in the heart.

A and B: lung; C and D: heart.

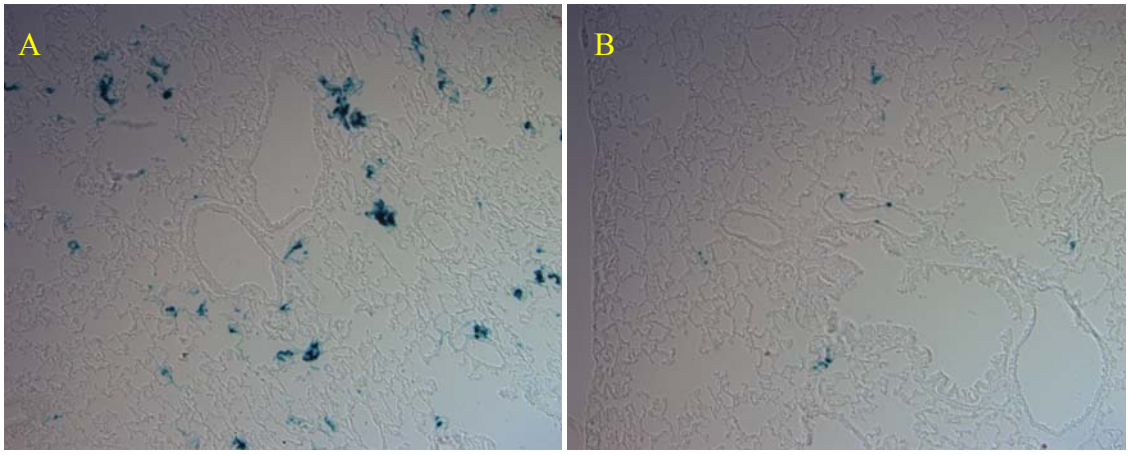

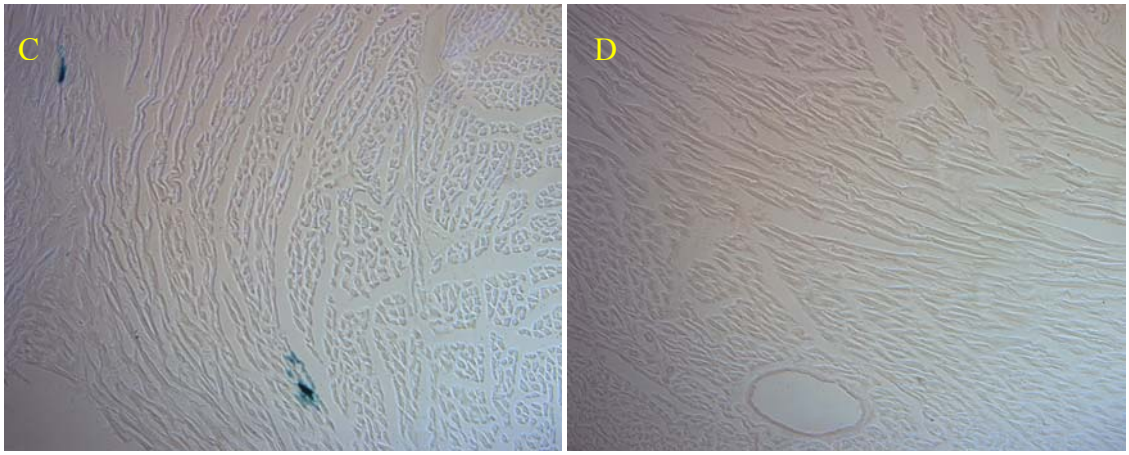

Figure 30 Sequential injection of liposome-AdCMV-lacZ led to lacZ expression in the lung, but not in the heart.

A: lacZ was expressed well in the lung; B: lacZ was expressed in large lung vessels; C: lacZ expression was exhibited in a few of cardiomyocytes; D: lacZ expression was barely detectable in the heart.

3.1.9 Discussion

In this section, we used adenoviral transduction approaches to achieve endothelial-specific expression in rat or mouse heart. The adenoviral vectors with endothelial-specific promoter AdFlt-1-lacZ or AdICAM2-lacZ or adenoviral vector with universal promoter CMV was used with the aid of positively charged liposomes. However, neither approach resulted in consistent and good endothelial-specific expression in rodent heart. To achieve consistent and good vascular-specific expression, we moved to establish vascular-specific iNOS inducible transgenic mice.

3.2 TO DEVELOP VASCULAR-SPECIFIC INOS INDUCIBLE TRANSGENIC MICE

3.2.1 GeneSwitch is an optimal choice to make vascular-specific iNOS inducible transgenic mice

In **3.1**, we invested considerable effort to test 5 endothelial-specific promoters and 2 smooth muscle cell-specific promoters *in vitro*, *ex vivo* and *in vivo*. Our goal was to identify a good endothelial- or smooth muscle cell-specific promoter that leads to iNOS vascular-specific expression in the heart. From our studies, we found that the ICAM2 promoter was a promising candidate for cardiac endothelium specifical targeting. For smooth muscle cell-specific targeting, we could not determine the activity and specificity of the two promoters, SMMHCL and SMMHCS, due to the poor transfection efficiency in cultured smooth muscle cells. Franz *et al.* have reported that the SMMHCS promoter led to the expression of lacZ or luciferase gene specifically in smooth muscle cells of coronary arteries in both transgenic mice and rabbits (135). Thus, the SMMHCS promoter may be a good candidate for smooth muscle cell-specific targeting. Since we have no information on whether endothelial cell- or smooth muscle cell-specific expression of iNOS will inhibit the development of cardiac allograft arteriosclerosis, we decided to develop both endothelial cell- and smooth muscle cell- specific expression of iNOS in vasculature at the same time. Therefore, we chose the ICAM2 and SMMHCS promoter for endothelial- and smooth muscle cell-specific targeting, respectively.

From **3.1.5**, we know that adenoviral transduction in donor grafts results in variable gene expression. To achieve consistent transgene expression, we chose to develop another gene delivery system: vascular-specific iNOS inducible transgenic mice. Until now, iNOS transgenic mice have not been successfully generated because transgenic mice with constitutively expressed

iNOS do not survive to the adult stage (117). Inducible iNOS transgenic mice could serve as a better model to determine the effect and function of iNOS. The GeneSwitch system (Invitrogen), which exhibits mild inducible ability and strict basal expression *in vitro* and *in vivo* (146-148), offers an opportunity to overcome these limitations. GeneSwitch is an optimal option for our cardiac allograft arteriosclerosis project for the following reasons: 1. NO is an intracellular signaling molecule and exogenous supply of NO may change vascular tone. In both of the eNOS transgenic mice developed by Crom *et al.* (159) and Channon *et al.* (173), consistent expression of eNOS results in hypotension. Moreover, substantial expression of NO in cardiomyocytes has a negative effect on cardiac function (111-115, 120, 121, 166, 236). Therefore, an appropriate approach would be to regulate both the timing and location of iNOS expression. iNOS expression should be regulated strictly. Here, GeneSwitch provided a lowest basal expression. 2. Since iNOS activity is 10^3 higher than that of eNOS, high level induction of iNOS may have adverse effects. GeneSwitch affords mild level induction of transgene, which matches our need of iNOS induction. 3. The ligand mifepristone in the GeneSwitch system does not inhibit the development of intimal hyperplasia (152-155). 4. Mifepristone does not affect cardiac function (156). 5. GeneSwitch is easily modified using vascular-specific promoter. Therefore, we employed GeneSwitch toward the goal of developing vascular-specific iNOS inducible transgenic mouse in which the SMMHCS or ICAM2 promoter regulates the Switch specific expression. We propose to take the transgenic mice heart as donor and test our hypothesis that specific induction of iNOS in smooth muscle or endothelial cells will inhibit the development of cardiac allograft arterioscleorsis without suppressing cardiac function.

3.2.2 GeneSwitch regulates *lacZ* expression strictly *in vitro*

To determine if GeneSwitch regulates transgene expression strictly, we transfected HEK293 cells using DNA plasmid pSwitch and pGenev5His-lacZ as described in **2.11**. Twenty-four and 48 hrs after transfection, X-gal staining was performed. Blue-stained cells were counted and the percentage of blue cells was calculated using Metamorph software as described in **2.11**. As shown in Figure 28 and 29, *lacZ* expression was tightly regulated by the ligand mifepristone. Without mifepristone, the basal expression of *lacZ* was mimimal which was represented that few cells showed blue staining. When cells were induced by mifepristone at doses of 10^{-10}~10^{-7} M, *lacZ* expression was induced and demonstrated a dose-dependent expression pattern. At doses ≤ 10^{-11}M, few cells expressed *lacZ*.

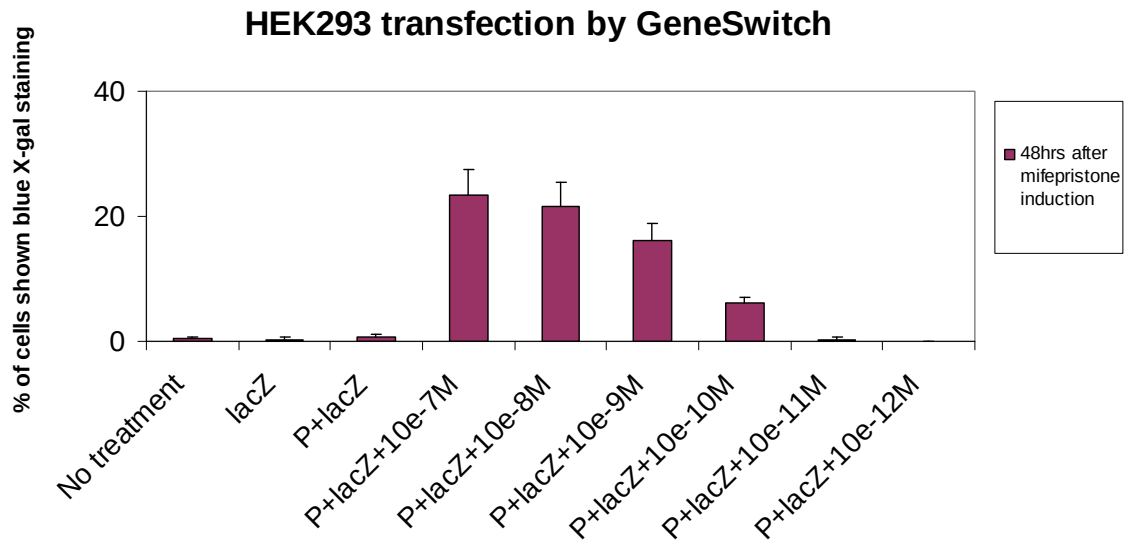

Figure 31 lacZ expression in HEK293 cells that were regulated by GeneSwitch.

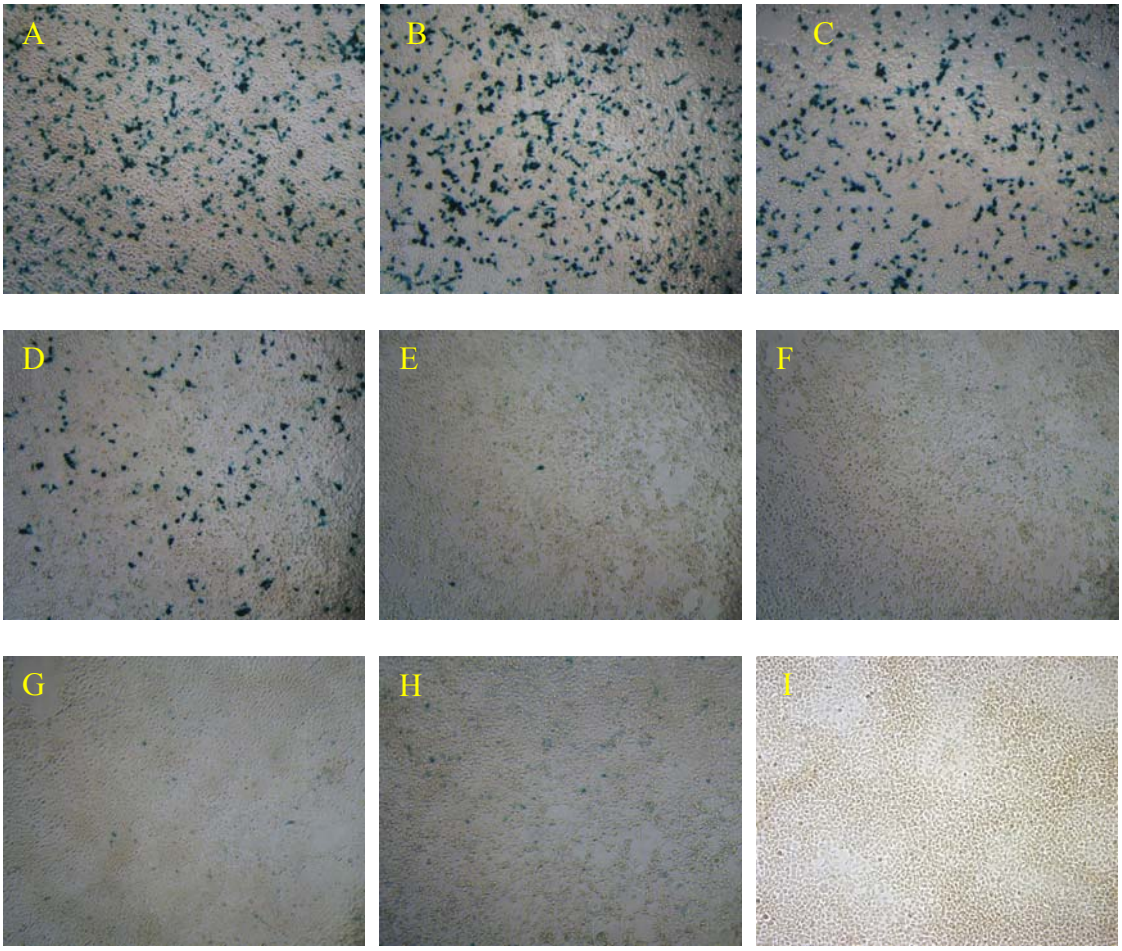

Figure 32 X-gal staining of HEK293 cells after cells were transfected by GeneSwitch (pSwitch + pGenev5His-lacZ) with or without mifepristone induction.

A-F: lacZ expression was induced by 10^{-7} ~ 10^{-12} M of mifepristone. G, H and I were used as negative controls. A: pSwitch + pGenev5His-lacZ + 10^{-7} M mifepristone; B: pSwitch + pGenev5His-lacZ + 10^{-8} M mifepristone; C: pSwitch + pGenev5His-lacZ + 10^{-9} M mifepristone; D: pSwitch + pGenev5His-lacZ + 10^{-10} M mifepristone; E: pSwitch + pGenev5His-lacZ + 10^{-11} M mifepristone; F: pSwitch + pGenev5His-lacZ + 10^{-12} M mifepristone; G: pGenev5His-lacZ; H: pSwitch + pGenev5His-lacZ; I: No transfection..

3.2.3 GeneSwitch regulates iNOS expression tightly *in vitro*.

After confirmation that GeneSwitch regulates *lacZ* expression tightly *in vitro*, we modified GeneSwitch and made three DNA plasmids in order to make vascular-specific iNOS inducible

transgenic mice. The ICAM2 and SMMHCS promoters are employed to replace the universal promoter herpes simplex virus thymidine kinase mini-promoter to regulate the Switch expression. The three DNA plasmids are: pICAM2-Switch, pSMMHCS-Switch and pGeneA-iNOS. The construction procedure is described in **2.16**.

To determine how GeneSwitch regulates iNOS expression, we transfected HEK293 cells using DNA plasmids pSwitch and pGeneA-iNOS. Subsequently, we induced the iNOS expression using a concentration gradient of mifepristone from 10^{-14} to 10^{-7}M. Twenty-four, 48 or 72 hrs later, we measured the nitrite level in the culture media by Greiss assay and detected iNOS expression by western blot. As shown in Figure 33 and 34, iNOS expression was well-regulated by GeneSwitch. Without mifepristone induction, the basal level of nitrite in the culture media was mimimal. When cells were induced by mifepristone at doses of 10^{-10}~10^{-7} M, iNOS expression was significantly induced, which was represented by the nitrite level in the culture media (Figure 33) and the protein band shown by western blot (Figure 34). At doses $\leq 10^{-11}$ M, iNOS expression went back the basal minimal level. From the time course of iNOS induction, we can see that iNOS expression was induced as early as 6 hrs after addition of mifepristone (Figure 35), reached the peak level at 24 hrs and maintained this peak level until 48 hrs after mifepristone induction (Figure 36). At 72 hrs after mifepristone induction, iNOS expression decreased considerably, which was demonstrated by western blot. As we know, HEK293 cells are rapidly proliferating cells and need to be split every two or three days. At the time point of 72 hrs after addition of mifepristone, the cells had been seeded into the plate for at least 106 hrs and the cell viability decreased greatly. This loss of viability may be associated with the decrease of iNOS expression.

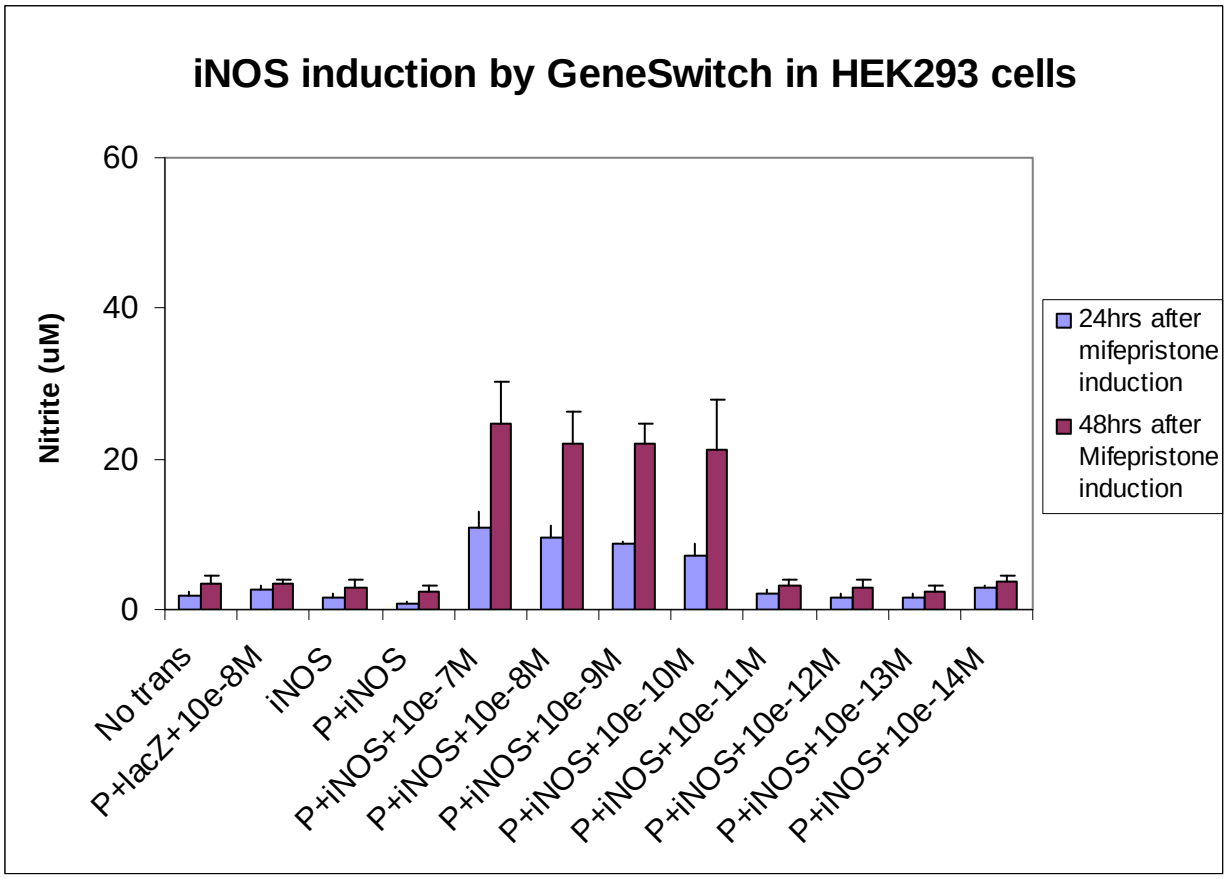

Figure 33 Nitrite induction in the culture media after HEK293 cells were co-transfected by pSwitch and pGeneA-iNOS and induced by 10^{-14} ~ 10^{-7}M of mifepristone.

Cells that were tranfected by pGeneA-iNOS, pSwitch + pGeneA-iNOS, pSwitch + pGenev5His-lacZ + 10^{-8}M mifepristone, or without transfection, were used as negative controls.

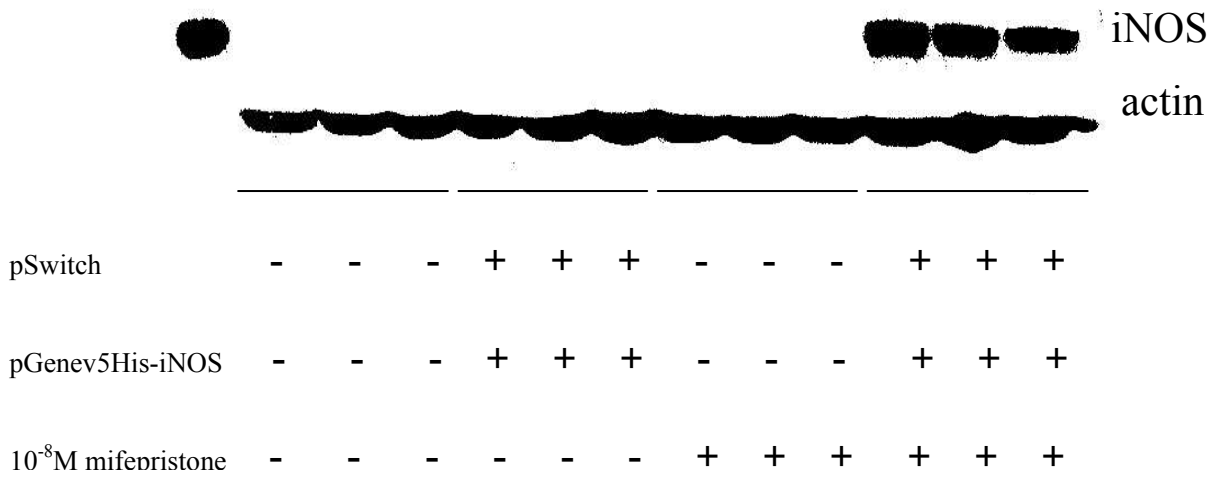

Figure 34 iNOS induction by GeneSwitch in HEK293 cells. The human iNOS protein was induced when cells were co-transfected by pSwitch and pGenev5-iNOS and induced by 10^{-8}M mifepristone for 24hrs.

In control cells, or the cells that were co-transfected by pSwitch and pGenev5-iNOS but without mifepristone induction, or cells that were treated by 10^{-8}M mifepristone only, the human iNOS protein was not detectable.

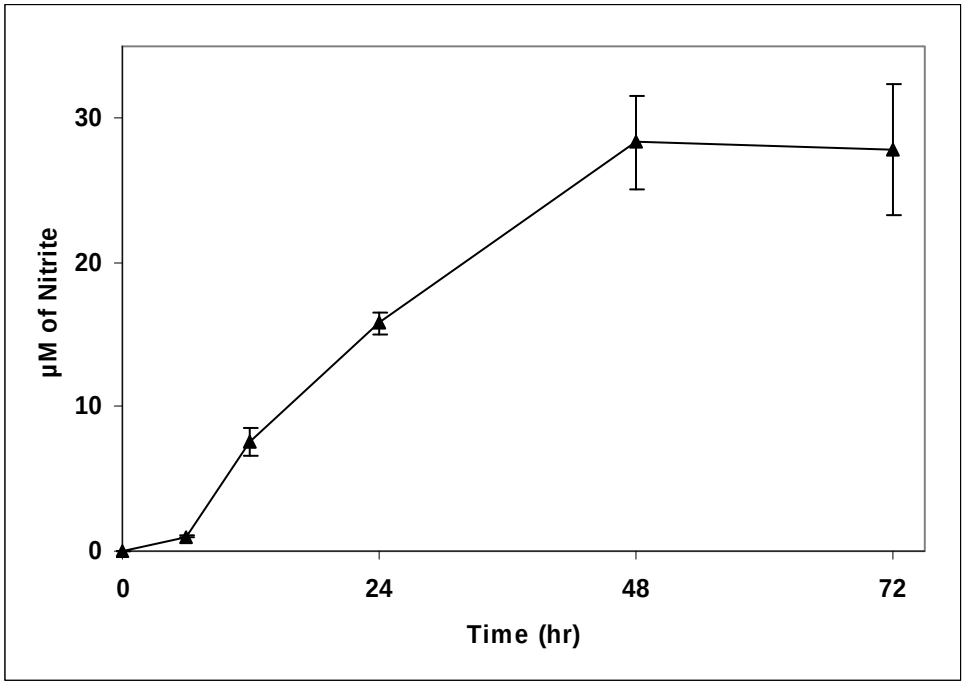

Figure 35 Time course of nitrite induction after HEK293 cells were co-transfected by pSwitch and pGeneA-iNOS and induced by 10^{-8} M mifepristone.

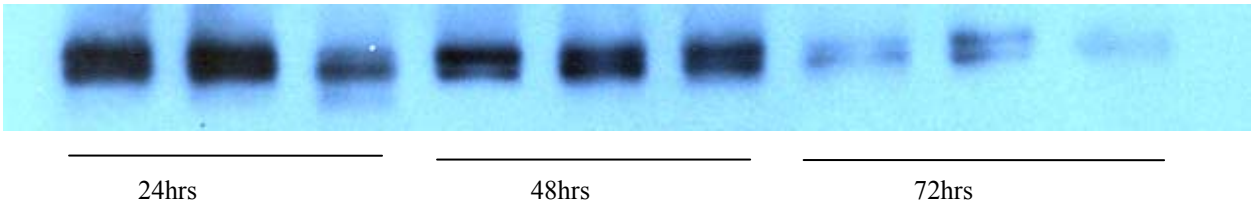

Figure 36 Western blot results showed the time course of iNOS induction after HEK293 cells were transfected by pSwitch and pGeneA-iNOS and induced by 10^{-8}M mifepristone.

At 24 hrs after mifepristone induction, iNOS expression reached the peark and this expression level was maintained until 48 hrs after mifepristone. At 72 hrs after mifepristone induction, iNOS was not induced but degraded.

3.2.4 Generation of vascular-specific iNOS inducible transgenic mice

After we confirmed that GeneSwitch regulates iNOS expression strictly *in vitro*, starting February 2006, we began a collaboration with Revivicor Inc. (Blacksburgh, VA) to make the vascular-specific iNOS inducible transgenic mice. Three DNA plasmids were constructed to make the vascular-specific iNOS inducible transgenic mice: pICAM2-Switch, pSMMHCS-Switch and pGeneA-iNOS (Figure 11). Preparation of vascular-specific iNOS inducible mice requires two steps. The first step is to linearize the three DNA plasmids and microject the DNA fragment into oocytes to make three transgenic mice lines: TgICAM2-Switch, TgSMMHCS-Switch and TgGeneA-iNOS. In the first two lines, the regulatory protein Switch is specifically expressed in smooth muscle or endothelial cells. TgGeneA-iNOS is an iNOS basal expression line. The second step is to cross TgICAM2-Switch or TgSMMHCS-Switch with TgGeneA-iNOS and get the vascular-specific iNOS inducible transgenic mice TgICAM2-Switch-iNOS and TgSMMHCS-Switch-iNOS.

Revivicor Inc. first microinjected pGeneA-iNOS DNA fragment into C3B6F1 mice oocytes and got 117 pups. By extracting genomic DNA from mouse tails and performing PCR, they identified 12 founders of TgGeneA-iNOS, in which the human iNOS gene is integrated into mice genome. Theoretically, in the transgenic mice line TgGeneA-iNOS, iNOS should not be expressed but is inducible when provided by the regulatory protein Switch and the ligand mifepristone. However, since the DNA fragment is randomly integrated into mice genome, iNOS could be inducible, constitutively expressed, or silent due to different integration sites. Therefore, we needed to screen in which line iNOS is inducible.

The 12 founders of TgGeneA-iNOS mice (C3B6F1 strain) were housed in the animal facility of University of Virginia. Unfortunately, the importation of these mice into our quarantine facility was denied due to an infection in the Revivicor colony. To access the inducibility of iNOS, Revivicor Inc. harvested fibroblasts from tails of the 12 founders and shipped them to us for screening. The 12 founders are numbered as #24, 36, 43, 56, 63, 64, 88, 100, 109, 110, 111 and 115, respectively. The cell number from each line was very limited, only 1.2×10^5 to 6×10^5. These numbers of cells were not adequate for the Greiss assay used to measure nitrite levels or for western blot of iNOS protein. Therefore, these cells were cultured and allowed to proliferate. For the lines 24, 109 and 111, many of the cells died after seeding and the study could not be performed. The remaining 9 lines were tested.

3.2.4.1 Optimization of the transfection condition in adult C3B6F1 mice tail fibroblasts using liposome-DNA plasmid complex or by electroporation

As described in **1.9.2**, to determine in which line of cells iNOS was inducible, we need to provide cells with the regulatory protein, Switch and the ligand mifepristone. In order to provide cells with the Switch protein, we first transfected the cells using a DNA plasmid pSwitch-

liposome mixture. As we know, the transfection effiency using DNA plasmids in adult mouse tail fibroblast is very poor. To guanrantee that there was enough Switch protein produced in cells to induce the iNOS expression, we compared the transfection efficiency of DNA-liposome in wild-type C3B6F1 mice tail fibroblasts using different transfection reagents, including lipofectamine LTX with Plus (Invitrogen), lipofectamine 2000 with Plus (Invitrogen), GenePORTER (Genelantis, San Diego, CA), TransIT express (Mirus Bio) and Fugene 6 (Roche Diagnostics). We also tranfected cells by electroporation. **2.12** describes how the tail fibroblasts from wild-type mice C3B6F1 were harvested and **2.13** describes the transfection methods. The DNA plasmid pCMV-lacZ was used to test the transfection efficiency. Table 4 shows the transfection results.

Table 4 Optimization of transfection efficieny in C3B6F1 tail fibroblasts by different transfection reagents.

Transfection reagents	Lipofectamine LTX + Plus	Lipofectamine 2000 + Plus	Gene-PORTER	TransIT express	Fugene 6	Electro-poration
% of cells with blue staining	20%	5~10%	0.2%	0.2%	0.125%	<0.1%

Using lipofectamine LTX with Plus, 20% of tail fibroblasts were transfected and exhibited blue staining. Lipofectamine LTX is a new transfection reagent and transfection effiency of 20% in adult mouse tail fibroblasts has not been previously reported in the literature.

3.2.4.2 Identification of iNOS inducible transgenic mice using pSwitch-lipofectamine LTX transfection

As mentioned in the introduction of **3.2.4**, we had obtained 9 lines of cells from TgGeneA-iNOS founders for testing: 36, 43, 56, 63, 64, 88, 100, 110 and 115. We transfected these cells using lipofectamine LTX with Plus mixed with pSwtich and determined which line of cells was inducible for iNOS expression. According to the cell number, these cells were seeded in 6-well plates at a density of 1×10^5 cells/well or 2×10^5 cells/well. Each line of cells was seeded in 3 wells of a 6-well plate. One well of cells was transfected by pSwitch, but not induced by mifepristone as a negative control, the other two wells of cells were transfected by pSwitch and induced by mifepristone to determine the iNOS induction. The transfection and induction conditions were described in **2.14**.

The transfection results showed that none of the cell lines demonstrated production of nitrite (data not shown). This could be due to the possibility that the cell line is inducible but with only 20% transfection efficiency the cells still did not generate enough Switch protein to induce the iNOS expression, or it could be that these cell lines were not inducible for iNOS expression. To increase the transfection efficiency, we aquired an adenoviral vector that expresses the Switch protein. The GeneSwitch system has been placed in adenoviral vectors as AdSwitch and Ad5xGal4-luc in Dr. Ramesh A Bhat's laboratory (Weyth Research). AdSwitch is the regulatory vector that expresses the Switch protein and Ad5xGal4-luc is the responsive vector that regulates the induction of luciferease gene. We obtained the adenoviral vectors AdSwitch and Ad5xGal4-luc from Dr. Ramesh A Bhat. We then used AdSwitch to infect founder tail fibroblasts, established a condition under which >95% of cells could be infected and determined if any of the cell line was inducible for iNOS.

3.2.4.3 Optimization of infection condition in adult mice tail fibroblasts using AdSwitch

We first tried to find a condition under which >95% of the adult mouse tail fibroblasts were infected and produced transgene when infected by the adenoviral vector.

We infected adult mouse tail fibroblasts from wild-type C3B6F1 mice using AdCMV-lacZ for 6 or 18 hrs with different MOI: 100, 200, 300, 400 and 500. The cells were then incubated in fresh cell culture media for 48 hrs. Next, X-gal staining was performed to determine the infection efficiency. There was no cell toxicity observed in any of the above infection conditions. As shown in Table 5, when infected for 6 hrs, with the MOI of 500, 95% of the cells exhibited blue staining; when infected for 18 hrs, with the MOI of 300, 400 or 500, at least 95% of the fibroblasts exhibited blue staining. However, with different MOI and infection duration, the amount of lacZ produced by the cells varied, which was represented by the intensity of blue color. The higher MOI, the longer infection duration, the more intense the blue staining was. Finally, we chose the MOI of 500 and infection for 18 hrs as our infection condition.

Table 5 Determine transfection efficiency in adult mouse tail fibroblasts using AdCMV-lacZ.

	MOI 100	MOI 200	MOI 300	MOI 400	MOI 500
% of blue cells when infected for 6 hrs	50%	60%	80%	90%	95%
% of blue cells when infected for 18 hrs	80%	90%	95%	>95%	>95%

Next, we determined if AdSwitch and Ad5xGal4-luc infection led to functional protein in the cells. We first determined if AdSwitch made the Switch protein. We infected wild-type C3B6F1 tail fibroblasts using AdSwitch at a MOI of 500 for 18 hours, and then incubated the

cells in fresh culture media for 48 hours. Subsequently, we harvested the cell lysate for western blot. The uninfected cells were used as a negative control. A stem cell line, B6G-2 (Riken BioResource center, Ibaraki, Japan), was also infected by AdSwitch, as a positive control, and non-infected cells as a negative control. A rabbit anti-Gal4 (DBD) (N-19) polyclonal antibody (Santa Cruz Biotechnology, Santa Cruz, CA) was used to detect the Switch protein (147). As shown in Figure 37, AdSwitch infected fibroblasts and B6G-2 cells produced the Switch protein, but this is not seen in non-infected cells.

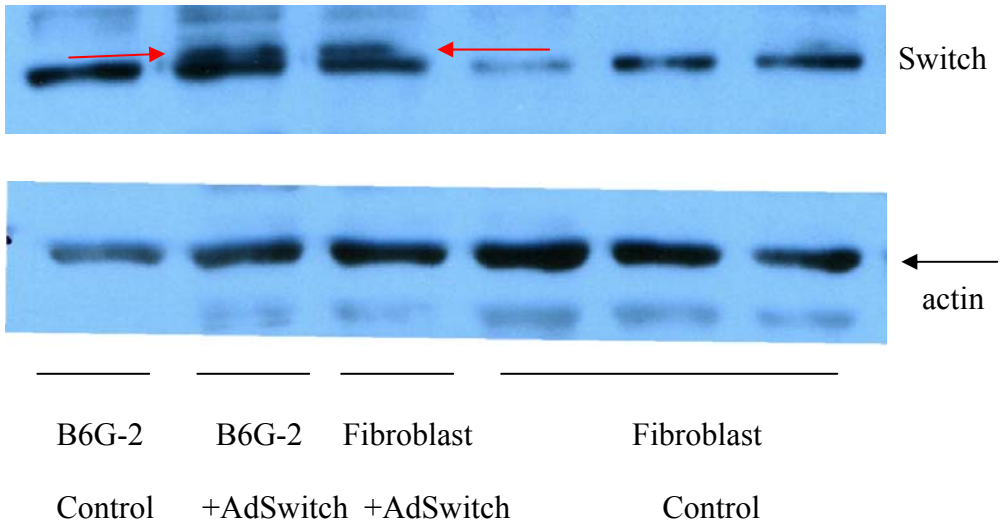

Figure 37 AdSwitch made the Switch protein in mouse tail fibroblasts.

To determine if AdSwitch was a functional protein, we also infected wild-type C3B6F1 tail fibroblasts using AdSwitch and Ad5xGal4-luc at a MOI of 500, respectively, and determined if luciferase activity could be induced by the ligand mifepristone. As shown in Figure 38, mifepristone induced luciferase activity at least five times greater than the control without mifepristone induction.

After we confirmed that AdSwitch made the Switch protein in wild-type C3B6F1 mouse tail fibroblasts and this protein is functional to induce luciferase activity, we determined which line of cells from our TgGeneA-iNOS founders were inducible for iNOS expression.

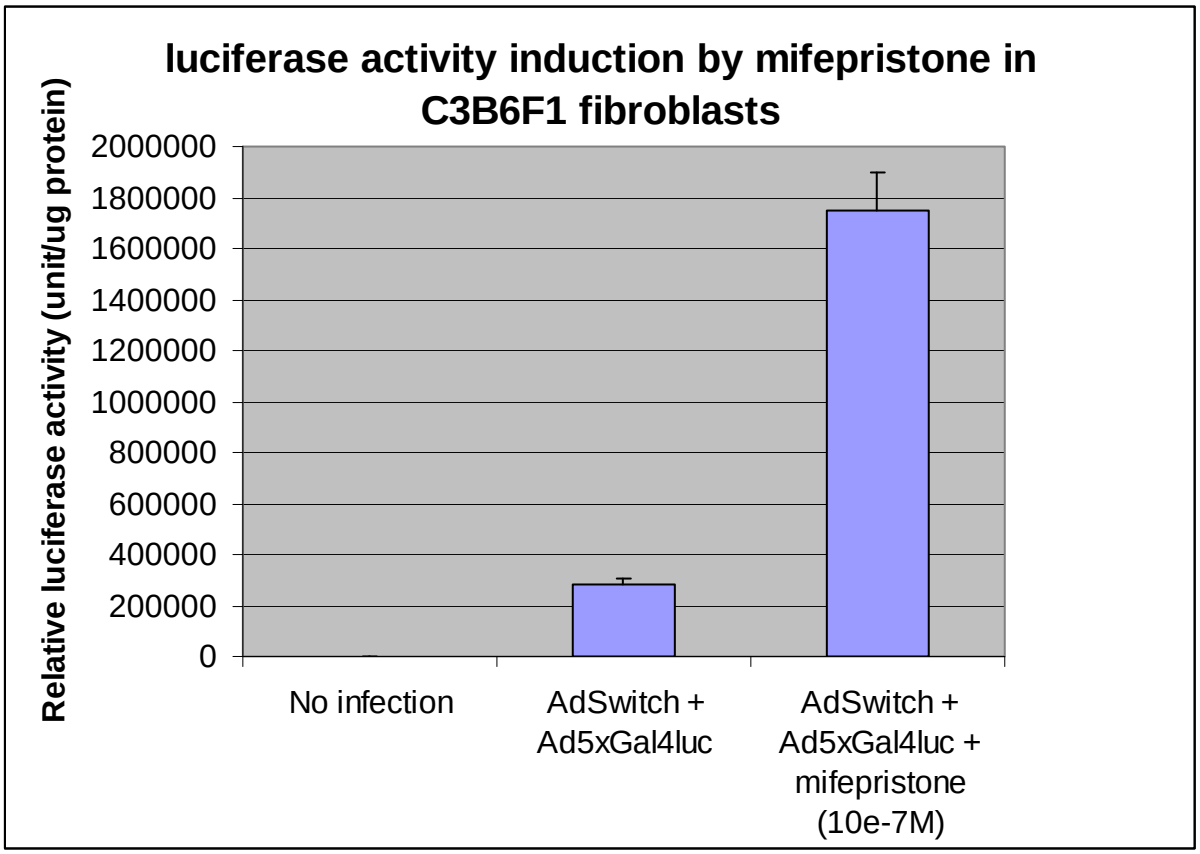

Figure 38 Induction of luciferase activity with 10^{-7}M mifepristone in wild-type C3B6F1 tail fibroblasts after cells were co-infected by AdSwitch and Ad5xGal5luc with a MOI of 500.

3.2.4.4 Identification of iNOS inducible transgenic mice TgGeneA-iNOS using AdSwitch

As mentioned before, we had 9 lines of cells from TgGeneA-iNOS founders for testing: 36, 43, 56, 63, 64, 88, 100, 110 and 115. According to the cell number, these cells were seeded in 6-well plates at a density of 1×10^5 cells/well or 2×10^5 cells/well. Each line of cells was seeded in 3 wells of a 6-well plate. One well of cells was infected by AdSwitch, but not induced by mifepristone as a negative control, the other two wells of cells were infected by AdSwitch and

induced by mifepristone to determine iNOS induction. Theoretically, we should have more wells without AdSwitch infection as negative control. However, we were limited by cell number and this is the best experimental design under these circumstances. The infection and induction conditions are shown in Figure 39.

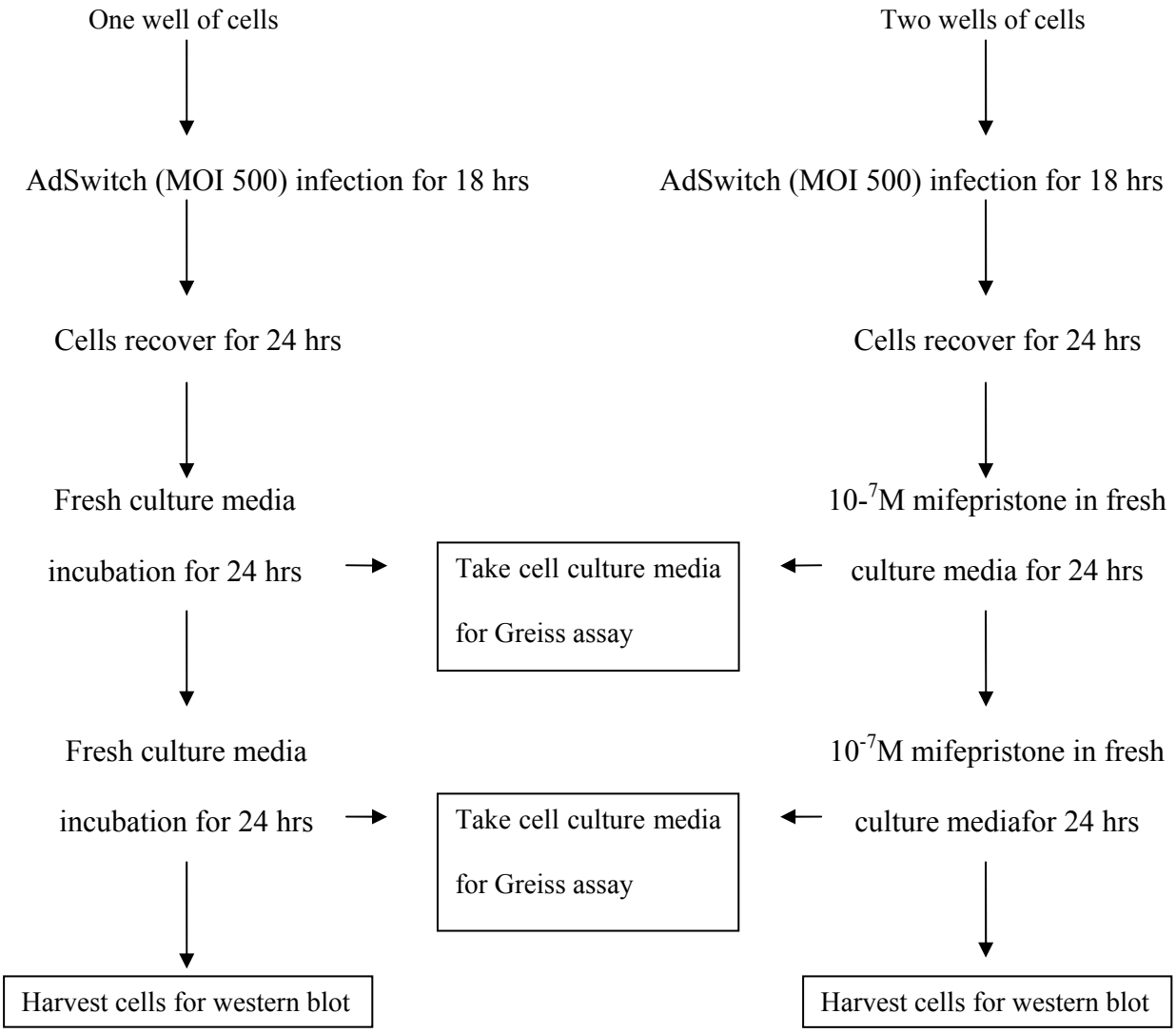

Figure 39 Experimental design for induction of iNOS.

As shown in Figure 39, cells were first infected by AdSwitch for 18 hrs, then allowed to recover for 24 hrs in fresh culture media. Next, cells were induced by 10^{-7}M mifepristone for 24

hrs and the culture media was taken to measure the nitrite level using Greiss assay. Subsequently, the cells were induced by fresh mifepristone (10^{-7}M) again for another 24 hrs. The culture media was collected to measure the nitrite level and cells were harvested for western blot.

The nitrite levels in culture media were measured using Greiss assay. Table 6 and 7 show the reading of absorbance at 550 nm using Greiss assay. There was no significant induction of nitrite in any of cell lines at either 24 or 48 hrs after mifepristone induction

Table 6 Absorbance at 550 nm in cell culture media 24 hrs after mifepristone induction.

Mouse line	Wild-type	36	43	56	63
- Mifepristone	0.005	0.000	-0.004	-0.001	0.000
+ Mifepristone	0.010	-0.001	0.002	0.000	0.010
+ Mifepristone	0.015	-0.001	-0.004	0.000	0.000
Mouse line	64	88	100	110	115
-Mifepristone	-0.006	-0.004	-0.002	0.001	-0.002
+ Mifepristone	0.002	-0.005	0.002	0.001	-0.002
+ Mifepristone	-0.004	-0.004	N/A	0.002	-0.002
Nitrite Standards	0 μM	1 μM	2 μM	4 μM	8 μM
Absorbance (550 nm)	0.000	0.006	0.010	0.014	0.052

Table 7 Absorbance at 550 nm in cell culture media 48 hrs after mifepristone induction.

Mouse line	Wild-type	36	43	56	63
-Mifepristone	0.005	0.001	0.004	0.002	0.000
+ Mifepristone	0.010	0.006	0.009	0.007	0.008
+ Mifepristone	0.015	0.007	0.013	0.008	0.000
Mouse line	64	88	100	110	115
-Mifepristone	0.003	-0.001	0.000	0.001	0.004
+ Mifepristone	0.007	0.001	0.002	0.003	0.005
+ Mifepristone	0.011	0.000	N/A	0.002	0.010
Nitrite Standards	0 μM	2 μM	4 μM	8 μM	16 μM
Absorbance (550 nm)	0.000	0.008	0.014	0.052	0.111

In Table 6 and 7, the absorbance at 550 nm is shown but not the nitrite level. To get the nitrite concentration, we needed to make a standard curve according the standard nitrite concentration and absorbance at 550 nm. These absorbance values are at the basal level and it would not be accurate to convert to nitrite concentration using the standard curve because they are at the bottom of the standard curve.

Next, we performed western blot analysis to detect iNOS protein expression. To distinguish exogenous human iNOS expression from endogenous mouse iNOS expression, a rabbit anti-human iNOS antibody (Biodesign international, Saco, Maine) was used for western blot. We have proven that this antibody specifically binds to human iNOS, but not mouse iNOS.

As shown in Figure 40, in line 88 and 110, human iNOS was induced when given mifepristone, but was not expressed in non-induced cells; in line 43, 56 and 63, human iNOS

was expressed constitutively, with or without mifepristone induction; in line 36, 64, 100 and 115, human iNOS was neither expressed, nor inducible by mifepristone; in wild-type C3B6F1 tail fibroblasts (negative control), human iNOS was not expressed nor inducible by mifepristone.

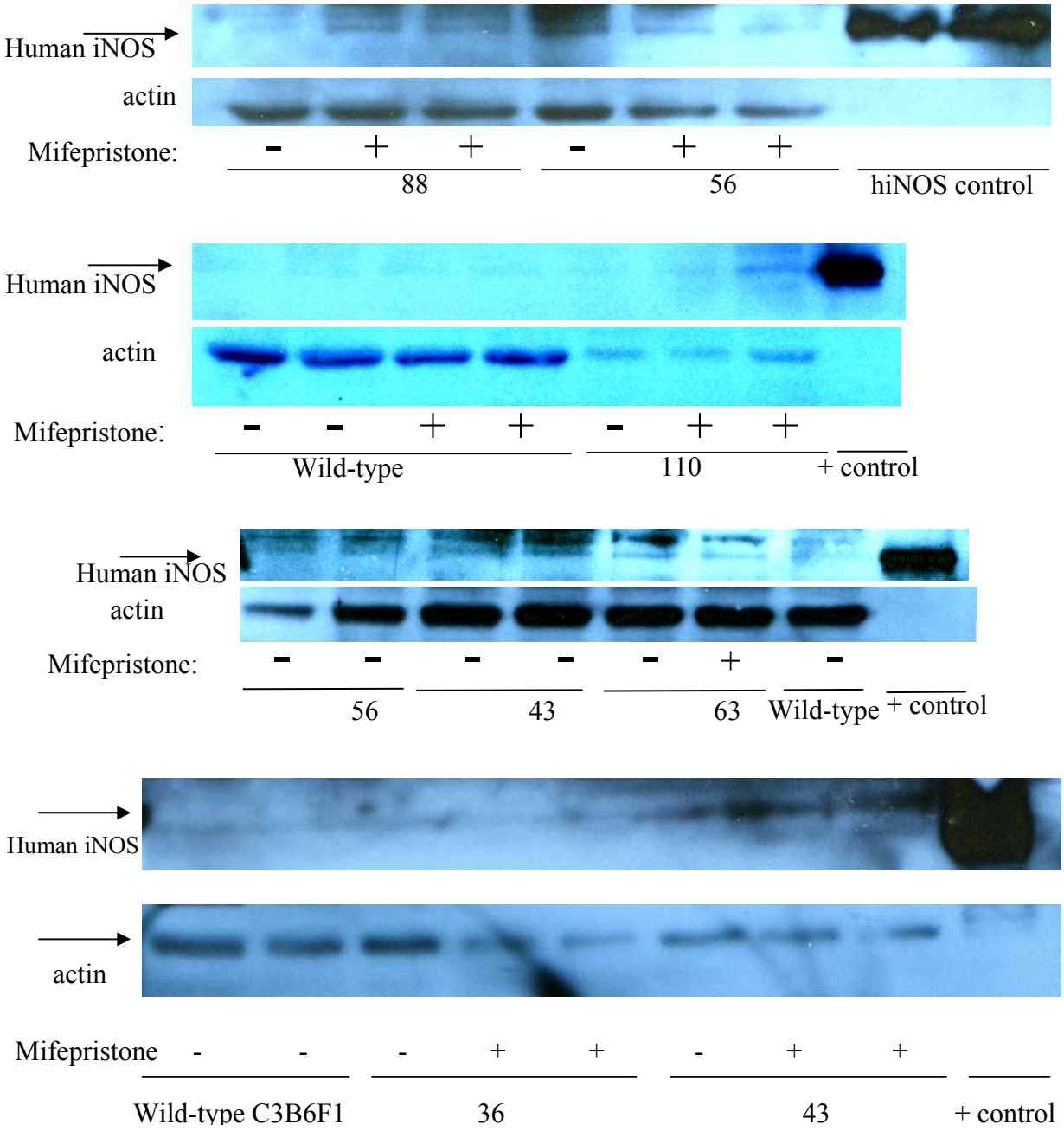

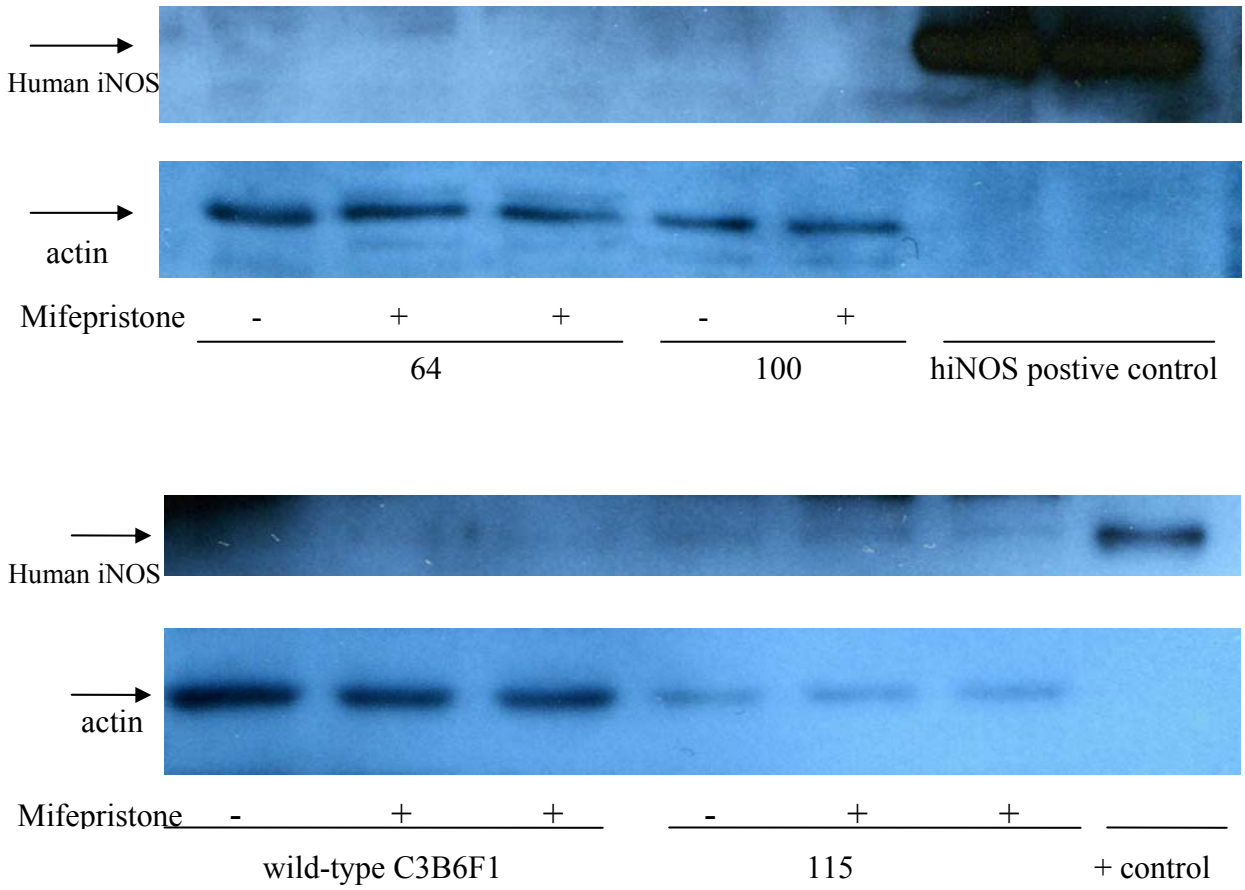

Figure 40 Induction of human iNOS by mifepristone in tail fibroblasts from 9 TgGeneA-iNOS founder lines.

Wild-type C3B6F1 mice tail fibroblast were used as a negative control.

3.2.5 Conclusion

We indentified a good inducible system (GeneSwitch), in which the transgene lacZ or iNOS exhibited strict basal expression and inducibility dependent on the concentration of the ligand mifepritien when tested *in vitro*. We modified this system to develop our vascular-specific iNOS inducible mice. We have successfully generated two iNOS inducible mice lines: TgGeneA-iNOS 88 and TgGeneA-iNOS 110, in which human iNOS is not expressed at the basal condition but inducible when given mifepristone. These two lines are now undergoing rederivation for future

characterization. The other three lines TgGeneA-iNOS, 43, 56 and 63 constitutively express iNOS. Another four lines TgGeneA-iNOS 36, 64, 100 and 115 neither express iNOS nor inducible. The last three lines TgGeneA-iNOS 24, 109 and 111 could not be tested due to poor cell growth.

We also successfully established a methodology by which to identify the iNOS inducible transgenice mice, which has not been previously reported in the literature.

3.2.6 Discussion

Because adenoviral vector transduction resulted in great variability in our heterotopic heart transplantation model, we abondoned the adenoviral vector transduction strategy. Nonetheless, we have successfully characterized three endothelial-specific adenoviral vectors and these vectors showed promise for endothelial-specific targeting *in vitro*. As an alternative approach, we made considerable progress in the development of vascular-specific iNOS inducible transgenic mice. We modified the GeneSwitch system to develop vascular-specific iNOS inducible mice. To generate vascular-specific iNOS inducible transgenic mice, two transgenic mice lines are required. One is TgSMMHCS-Switch or TgICAM2-Switch, in which the Switch protein will be regulated by the vascular-specific promoter SMMHCS or ICAM2 and will be constitutively expressed in smooth muscle or endothelial cells. Another is the iNOS basal expression transgenic mice line TgGeneA-iNOS, in which human iNOS gene is not expressed in normal conditions, but inducible when given the Switch protein and the inducer mifepristone. The DNA plasmids used to generate the three transgenic mice lines have been constructed as shown in Figure 11 as described in **2.16**. By collaborating with Revivicor Inc., we sussessfully generated two iNOS basal transgenic mice lines: TgGeneA-iNOS 88 and TgGeneA-iNOS 110.

The next step is to make transgenic mice TgICAM2-Switch and TgSMMHCS-Switch and cross them with TgGeneA-iNOS, respectively. Finally, we will get vascular-specific iNOS inducible transgenic mice TgICAM2-Switch-iNOS and TgSMMHCS-Switch-iNOS.

4.0 EFFICACY OF ENDOTHELIAL-SPECIFIC ENOS OVEREXPRESSION ON INHIBITION OF CARDIAC ALLOGRAFT ARTERIOSCLEROSIS

In **Chapter 3**, we developed two gene delivery systems: adenoviral vector and vascular-specific iNOS inducible transgenic mice. The adenoviral vectors did not lead to consistent transduction results when they were used to transduce donor heart *ex vivo*. The iNOS inducible transgenic mice are still under development and it will take a while before they are ready to be used to test our hypothesis. To test our hypothesis that specific expression of NOS (eNOS or iNOS) in smooth muscle or endothelial cells will inhibit cardiac allograft arteriosclerosis, we imported eNOS transgenic mice from Dr. Rini De Crom (Netherland). In this transgenic mice line, the human eNOS promoter regulates the human eNOS endothelial-specific expression. Crossing this transgenic mice line with apo E knockout mice has been shown to result in regression of atherosclerotic lesions (159). In our project, we used this transgenic mice line as donor and tested if endothelial-specific overexpression of eNOS will inhibit cardiac allograft arteriosclerosis.

4.1 DEVELOPING A CHRONIC REJECTION MODEL USING C57BL/6 MICE AS DONOR

In our preliminary data, we employed a rat chronic rejection model in which PVG and ACI rats were used as donor and recipient, respectively. Now we shifted to use the eNOS transgenic mice

as donor. We needed to develop an appropriate chronic rejection model in which the wild-type C57BL/6 mice should be used as donor since the eNOS transgenic mice are generated from the C57BL/6 mice strain. We started a collaboration with Dr. Noriko Murase and Dr. Atsunori Nakao for the development of chronic rejection model.

4.1.1 Combination of C57BL/6 (H-2^b) and C3H/HeOuJ (H-2^k) resulted in severe inflammation

We first employed an MHC class I mismatched model in which male C57BL/6 (H-2^b) and C3H/HeOuJ (H-2^k) mice were used as donor and recipient, respectively. Three forms of FK506, oral, intramuscular (IM) and intravenous (IV), were administrated to the recipients individually or in combination. Five methods of immunosuppression were compared, including oral, IM, IV, IM + oral, and IM + IV. The dose and timing for each immunosuppression are listed in Table 8.

Table 8 Five modes of FK506 Administration to recipients.

FK506 form	IM	IV	Oral	IM + oral	IM + IV
Dose (mg/kg/day)	2.0	1.0	1.0	IM: 2.0 Oral: 1.0	IM: 2.0 IV: 1.0
timing (days)	14	14	14	IM: the first 14 days Oral: the first 7 days	IM: the first 14 days IV: the first 7 days
Graft survival (days)	>30	19, 21	>30	>30	>30

When the IV form of FK506 was given to recipients, the grafts survived less than 30 days. Therefore, this immunosuppressive protocol was excluded. For the other four approaches

of immunosuppression, we compared the inflammation that developed in the donor grafts. The grafts were palpated daily and harvested when they stopped beating. The grafts without FK506 treatment were used as positive controls; the isografts (both donor and recipients were C57BL/6 mice) and native heart served as negative controls. The method that was used to determine the inflammation grade is described in **2.17**. Briefly, each graft was cut into 2 to 4 sections from apex to base, numbered as 1, 2, 3 and 4, respectively. The heart tissue was embedded into paraffin and H&E staining slides were made for each section. Inflammation was graded according to the 1990 IHLTS grading system.

As shown in Table 9 and Figure 41, with the four methods of immunosuppression (IM, oral, IM + oral, IM + IV of FK506), the donor grafts survived from 34 to 93 days except for a few grafts that failed before 12 days due to technical failure. In the surviving wild-type donor grafts, all developed active inflammation with grades of 3A, 3B or 4. Extensive infiltrates accumulated in myocardium and vasculature. The coronary vessels developed endothelialitis and the middle layer exhibited vasculitis. However, mild inflammation appeared in the wild-type grafts HB14 and HB31, which failed at 6 and 12 days after transplantation due to technical failure. Compared to HB28 and HB29 (without FK506 treatment) that generated myocardial infarction and necrosis, modest inflammation developed in the grafts HB14 and HB31 (with FK506) indicating that FK506 actually suppressed the immune reaction well during the first two weeks after transplantation. Active inflammation is normally observed during the acute rejection stage after heart transplantation when there is no immunosuppression or immunosuppression is weak, but not in the chronic stage. In our heart transplantation model, FK506 suppressed acute rejection. However, severe inflammation persisted in the graft at 60 or even 93 days after transplantation. Therefore, the long-term inflammation generated in the allografts very likely

came from the MHC haplotype mismatch between donor and recipient. The transgenic donors HB32 and HB33 also demonstrated similar extensive inflammation, which was not significantly different from the wild-type donors. One exception is that the transgenic donor HB35 exhibited mild inflammation (inflammation grade is 1A/1B). However, since more than 50% of the graft tissue was necrotic, this graft should not be taken as representative.

Table 9 Inflammation grade in allografts with four modes of FK506 administration.

Donor # (genotype)		Days post transplant-tation	FK506 administration	Inflammation grade
HB11 (WT)		70	IM	3A
HB13 (WT)	section 1	93	IM	3B
	section 2	93	IM	3B
HB24 (WT)	section 1	34	Oral	4
	section 2	34	Oral	4
HB23 (WT)	section 1	63	Oral	4
	section 2	63	Oral	4, no myocytes
HB25 (WT)	section 1	90	Oral	4
	section 2	90	Oral	4
HB 16 (WT)		34	IM--Oral	3B, no significant change in the vessel
HB 17 (WT)		35	IM--Oral	3A/3B, vasculitis and endothelialitis
HB 15 (WT)		36	IM--IV	3B
HB 18 (WT)		68	IM--IV	3A
HB 29 (WT)		11	No treatment	Myocardial infarction
HB 28 (WT)		13	No treatment	Difficult to judge, infarction, 70% necrosis
HB 32 (Tg)	section 1	45	IM--Oral	3A, focal transmusal + vascularitis
	section 2	45	IM--Oral	3B, focal transmusal + vascularitis
	section 3	45	IM--Oral	3A, endothelialitis
HB 33	section 1	34	IM--Oral	4, multifocal and severe vasculitis

(Tg)	section 2	34	IM--Oral	4, multifocal and severe vasculitis
HB 34 (WT)	section 1	45	IM--Oral	3B, multifocal vasculitis
	section 2	45	IM--Oral	3A, multifocal vasculitis
	section 3	45	IM--Oral	3A, multifocal vasculitis
HB 35 (Tg)	section 1	38	IM--Oral	1A/1B, myocardial infarction, 50% is necrotic, no vasculitis, no endothelialitis
	section 2	38	IM--Oral	1A/1B, myocardial infarction, 70% is necrotic, no vasculitis, no endothelialitis
HB 36 (WT)	section 1	44	IM--Oral	1B, endothelialitis
	section 2	44	IM--Oral	3A, endothelialitis + mild vasculitis+ multifocal transmusal
	section 3	44	IM--Oral	3A, endothelialitis + mild vasculitis+ multifocal transmusal
HB 14 (WT)		6	IM	1A
HB 31 (WT)	section 1	12	IM--Oral	1A/1B, no vasculitis
	section 2	12	IM--Oral	1A/1B, no vasculitis
HB 37 (Tg)	section 1	2	IM--Oral	1A
	section 2	2	IM--Oral	1A
	section 3	2	IM--Oral	1A

Figure 41 demonstrates the inflammation grade for each allograft according to Table 9.

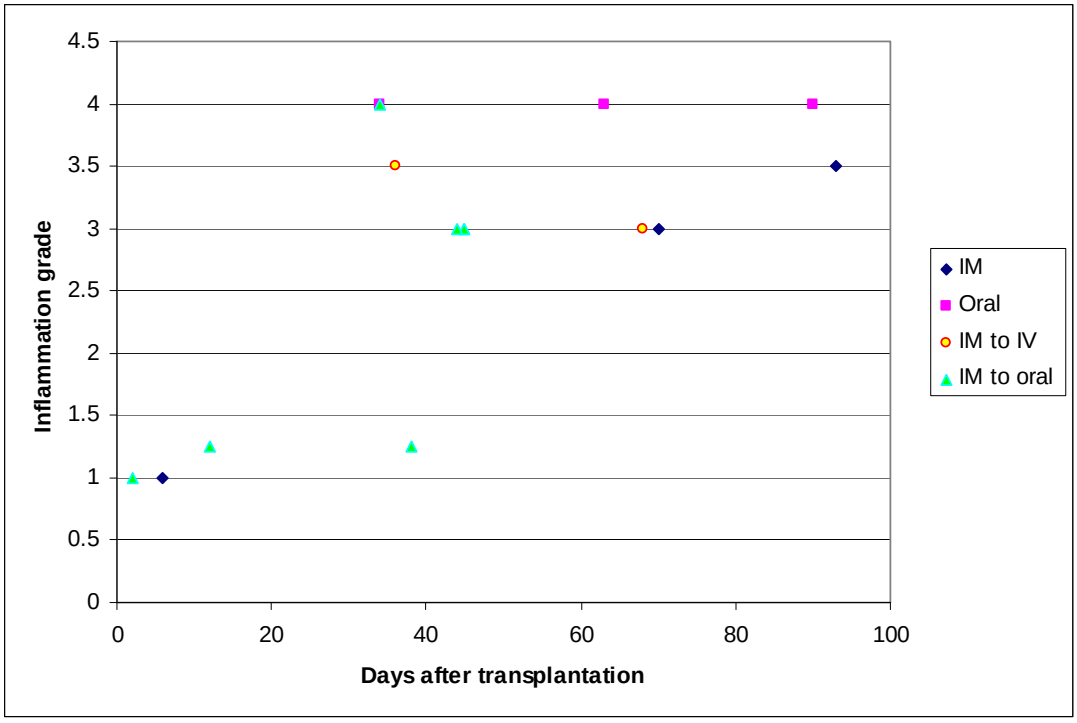

Figure 41 Inflammation grade in the donor graft with different modes of FK506 administration.

H&E staining further confirmed that severe inflammation generated in the donor grafts, as shown in Figure 42.

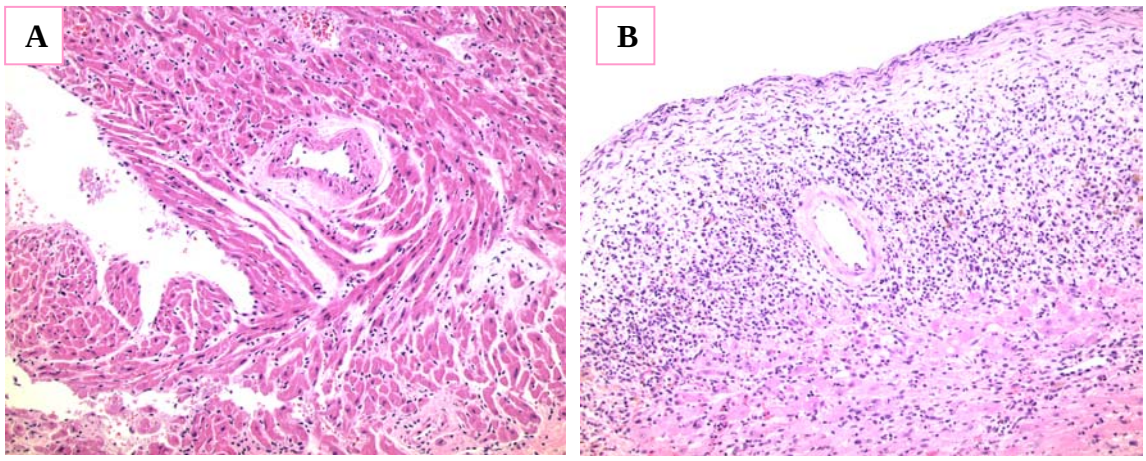

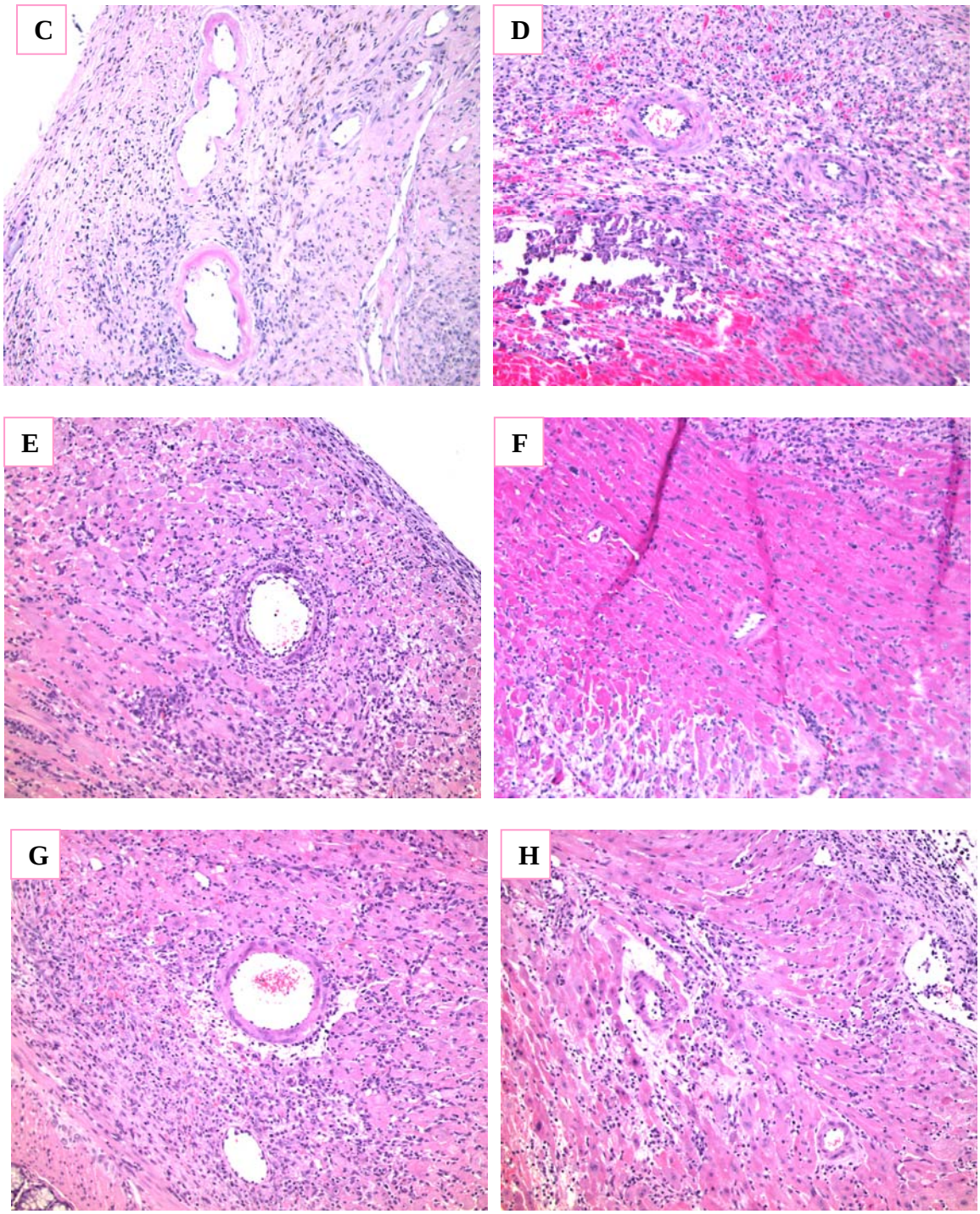
C
D
E
F
G
H

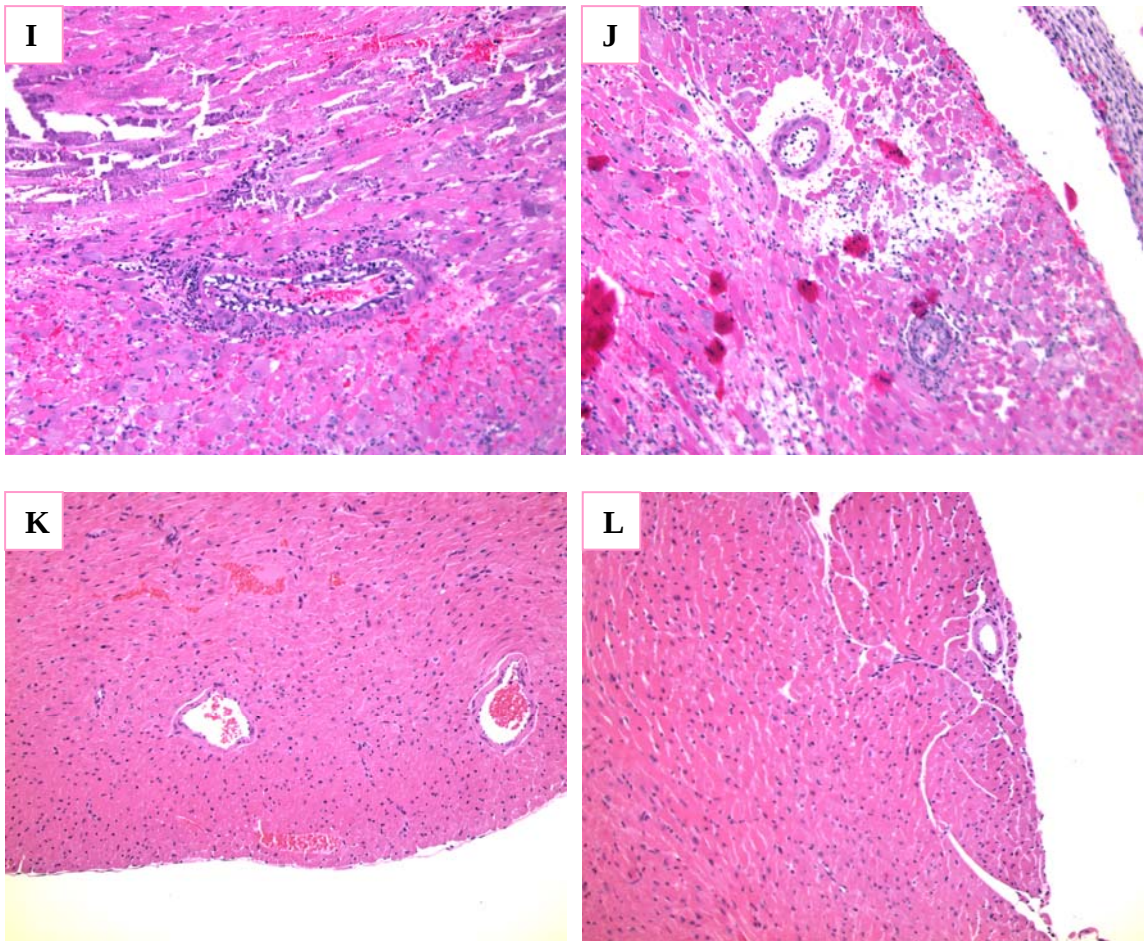

Figure 42 H&E staining of donor grafts with different modes of FK506 administration.

The grafts were palpated daily and harvested when they stopped beating. A: IM, 70 days after transplantation (HB11), inflammation grade 3A; B: IM, 93 days after transplantation (HB13), inflammation grade 3B; C: Oral, 34 days after transplantation (HB23), inflammation grade 4; D: Oral, 63 days after transplantation (HB24), inflammation grade 4; E: IM+IV, 36 days after transplantation (HB15), inflammation grade 3B; F: IM+IV, 68 days after transplantation (HB18), inflammation grade 3A; G: IM+Oral, 34 days after transplantation (HB16), inflammation grade 3B; H: IM+Oral, 35 days after transplantation (HB17), inflammation grade 3A/3B; I: No FK506 treatment, 13 days after transplantation (HB28); J: No FK506 treatment, 11 days after transplantation (HB29); K: C57BL/6 isografts, 60 days after transplantation; L: Native heart. I and J (without FK506 treatment) were used as positive controls; K (isografts) and L (native heart) were used as negative controls.

4.1.2 Combination of C57BL/6 (H-2^b) and C3H/HeOuJ (H-2^k) did not develop significant cardiac allograft arteriosclerosis

To characterize the development of cardiac allograft arteriosclerosis, donor hearts from wild-type C57BL/6 mice and eNOS transgenic mice were transplanted into wild-type C3H/HeOuJ mice. Three donors were used for each group. The transgenic donors were named HB32, HB33 and HB35; the wild-type donors were named HB31, HB 34 and HB36. The combination of IM and oral forms of FK506 is thought to be more effective because the two routes have different kenetics. The oral form results in hight levels for a short period while the IM form results in sustained but lower levels. Thus, adequate FK506 levels are assured when both routes are used simultaneously. Therefore, our immunosuppression protocol evolved to the administration of the IM form of FK506 to recipients for the first 14 days after transplantation at a dose of 2.0 mg/kg/day, combined with the oral form of FK506 for the first 7 days at a dose of 1.0 mg/kg/day. Donor grafts were harvested at 45 days after transplantation. At this time point, only three donor grafts survived, including one transgenic (HB32) and two wild-type grafts (HB34 and HB36). For the other three grafts, HB31 was lost at 12 days after transplantation because of technical failure. HB33 and HB35 were harvested at 34 and 38 days after transplantation, respectively, when the grafts stopped beating.

As described in **2.18**, to evaluate the degree of cardiac allograft arteriosclerosis, HB32, 34 and 36 were cut into 2 to 4 sections, respectively, and each section was embedded into paraffin. For each section, cross sections were cut at two levels, which were 40 μm apart. Tissue sections were stained using verhoeff's Van Geison (vVG) stain and vessel occlusion was evaluated. As shown in Figure 43, “bubbling” occlusion developed in coronary vessels with

foam cells and leukocytes infiltrated and accumulated in the lumen. Both transgenic and wild-type donor grafts developed “bubbling” occlusion.

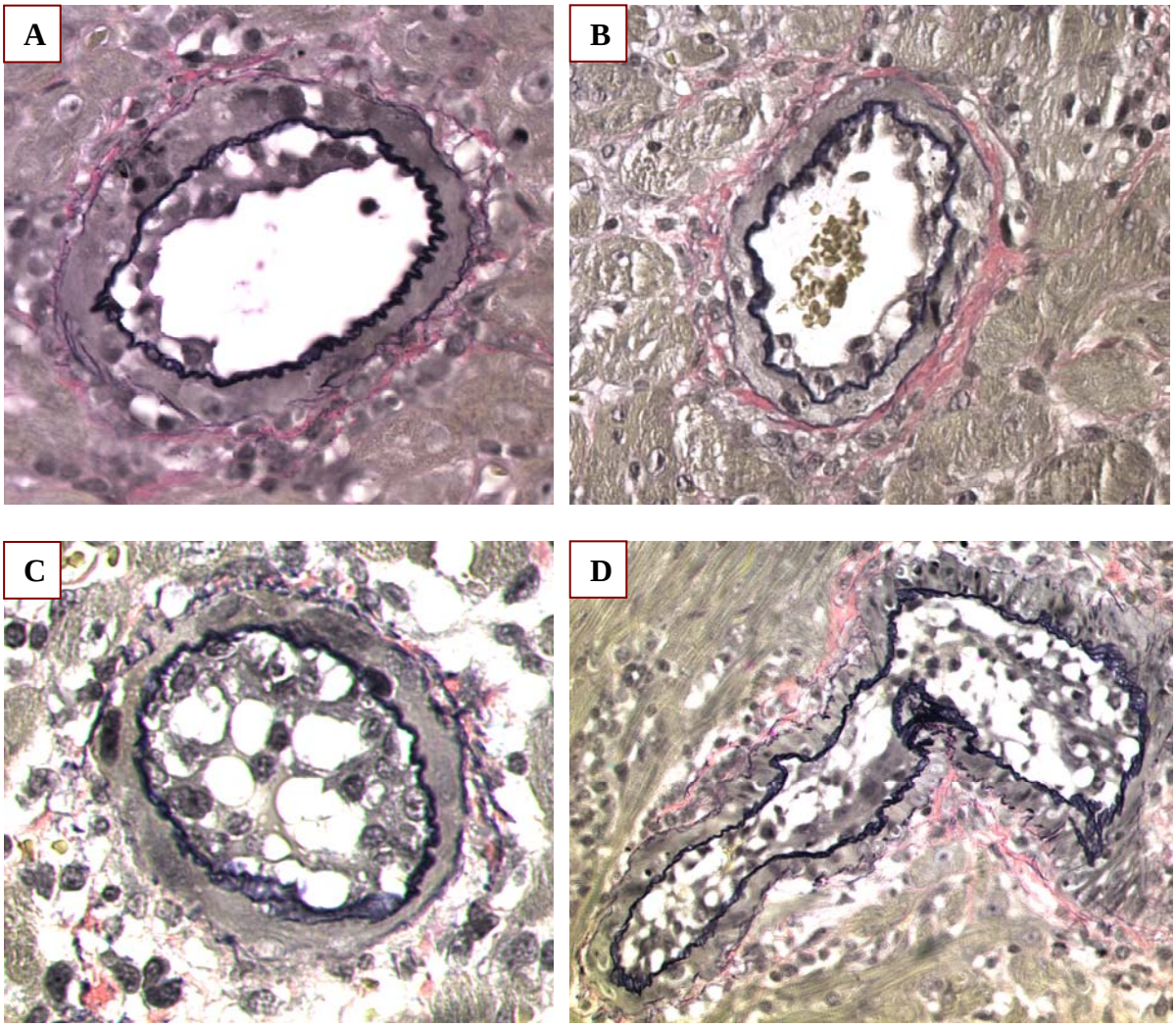

Figure 43 “Bubbling” occlusion developed in coronary vessels of both transgenic and wild-type grafts.

The grafts were harvested at 45 days after transplantation. A and B: HB32, eNOS transgenic donor; C: HB34; wild-type donor; D: HB36, wild-type donor.

As shown in Figure 44, H&E staining demonstrated that severe inflammation developed in both transgenic and wild-type donor grafts. The inflammation grades in these grafts were 3 or 4 except for HB35, which exhibited extensive necrosis.

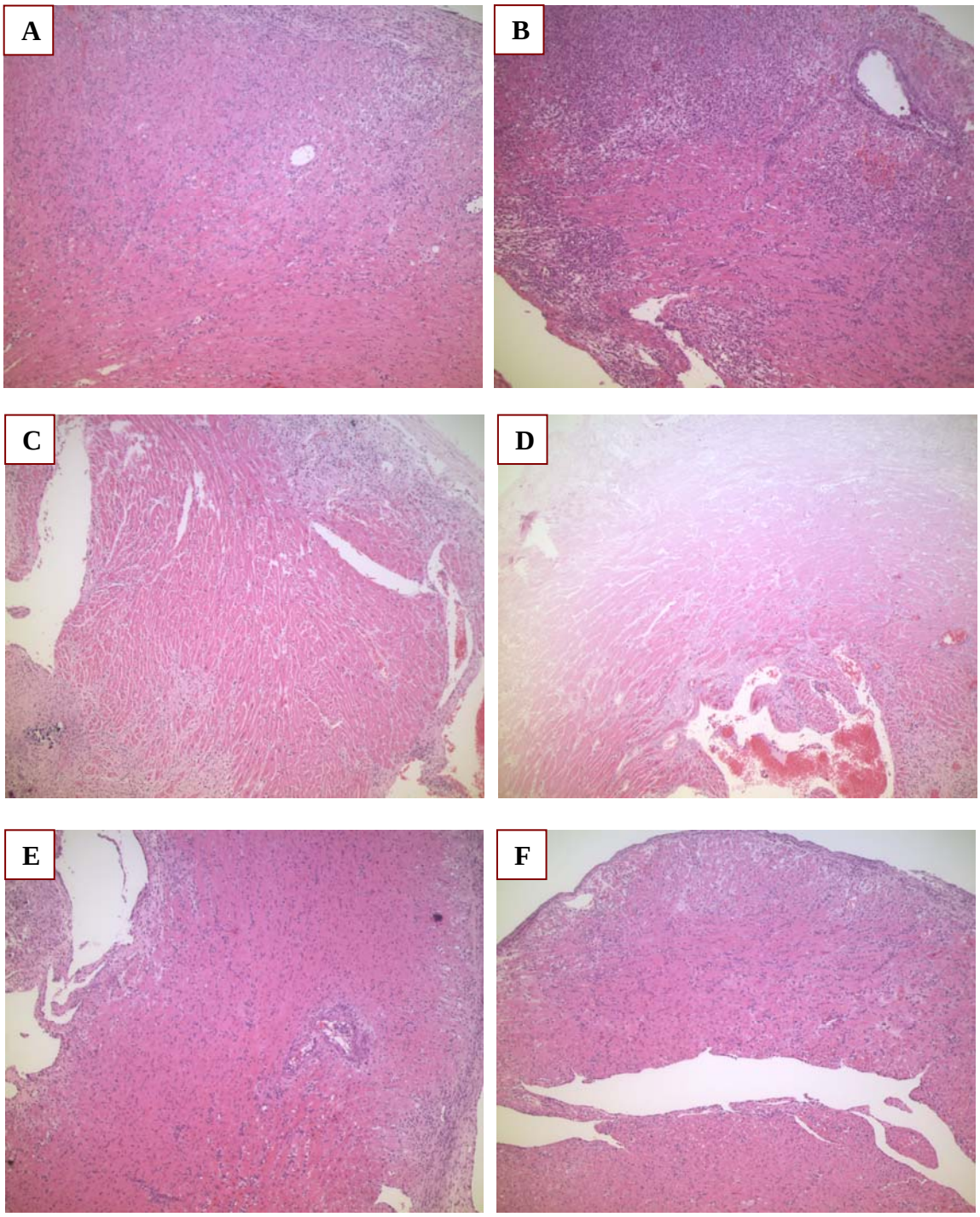

Figure 44 Severe inflammation developed in both transgenic and wild-type donor grafts.

A: HB32, eNOS transgenic donor, 45 days after transplantation, inflammation grade 3A/3B; B: HB33, eNOS transgenic donor, 34 days after transplantation, inflammation grade 4; C: HB35, eNOS transgenic donor, 38 days after transplantation, inflammation grade 1A/1B, necrotic; D: HB35, eNOS transgenic donor, 38 days after

transplantation, inflammation grade 1A/1B, necrotic; E: HB34, wild-type donor, 45 days after transplantation, inflammation grade 3A/3B; E: HB36, wild-type donor, 45 days after transplantation, inflammation grade 3A.

This chronic rejection model did not lead to the development of cardiac allograft arteriosclerosis. The presence of "bubbling occlusion" suggested that intimal hyperplasia in the coronary vessels may have occured at the early stage of development. However, mature cardiac allograft arteriosclerosis should exhibit fibrotic, collagen-rich and smooth muscle cell-dominated intimal thickening with monocyte and lymphocyte infiltration. Figure 45 left (182) represents a cross section of left anterior descending coronary artery from a 52-year old woman with severe cardiac allograft arteriosclerosis. The right picture in Figure 45 represents another example of mature cardiac allograft arteriosclerosis from a patient (239). Moreover, in this chronic rejection model, severe inflammation (grade 3 or 4) developed in donor grafts with endothelialitis and vascularitis (as shown in Table 9, Figure 42 and Figure 44) even with immunosuppression with FK506. During the natural development of cardiac allograft arteriosclerosis in human heart, only mild-inflammation (grade 1A or 1B) is observed (Figure 46, 182). Therefore, this chronic rejection model did not mimic the natural development of this disease well. Furthermore, in this chronic rejection model, the graft survival rate was low. We performed eight transplantations in total and five grafts (HB31, HB33, HB35, HB39 and HB40) did not survive with the required 45 days. Due to the reasons given above, we chose another chronic rejection model.

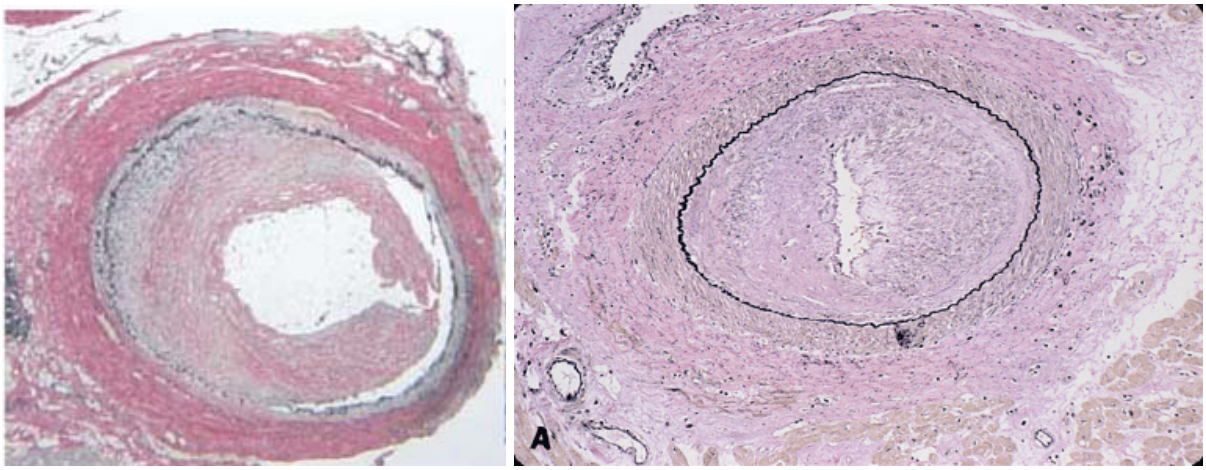

Figure 45 Cardiac allograft arteriosclerosis developed in human biopsy.

Left: from literatue 182; Right: from literature 239.

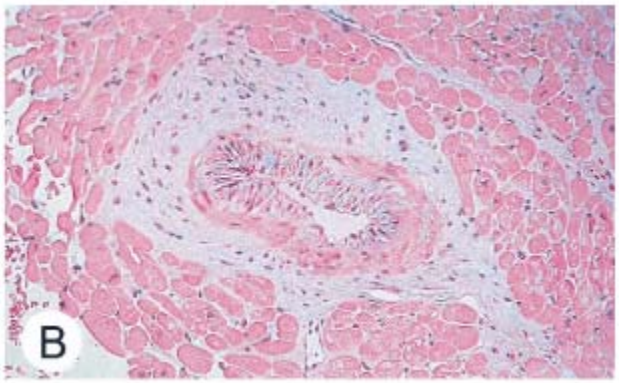

Figure 46 Mild inflammation developed in human biopsy with cardiac allograft arteriosclerosis (189).

4.1.3 Combination of male and female C57BL/6 mice resulted in mild inflammation and modest cardiac allograft arteriosclerosis

The first chronic rejection model did not lead to cardiac allograft arteriosclerosis. Next, we chose another MHC class II mismatched model in which male and female C57BL/6 mice were used as donor and recipient, respectively, and no immunosuppressive was given. This model was

developed by Uehara *et al*., who showed that 56 days after transplantation, intimal hyperplasia developed in the donor cardiac grafts (174).

To determine if cardiac allograft arteriosclerosis developed in the wild-type donor graft and the effect of eNOS overexpression on cardiac allograft arteriosclerosis, donor hearts from male wild-type C57BL/6 mice or eNOS transgenic mice were transplanted into female wild-type C57BL/6 mice. The donor grafts were harvested at 60 days after transplantation. The transgenic donors were named HB45, HB53 and HB54, and the wild-type donors were named HB44, HB62, HB63, HB64, HB65 and HB66. As represented in Figure 47, mild inflammation developed in both wild-type and transgenic donor grafts and the inflammation grade for these grafts is 1A/1B. There was no significant difference between wild-type and transgnenic donors. Compared to the first chronic rejection model that developed severe inflammation (grade is 3 or 4), the inflammation that developed in the second chronic rejection model better mimicked the human condition.

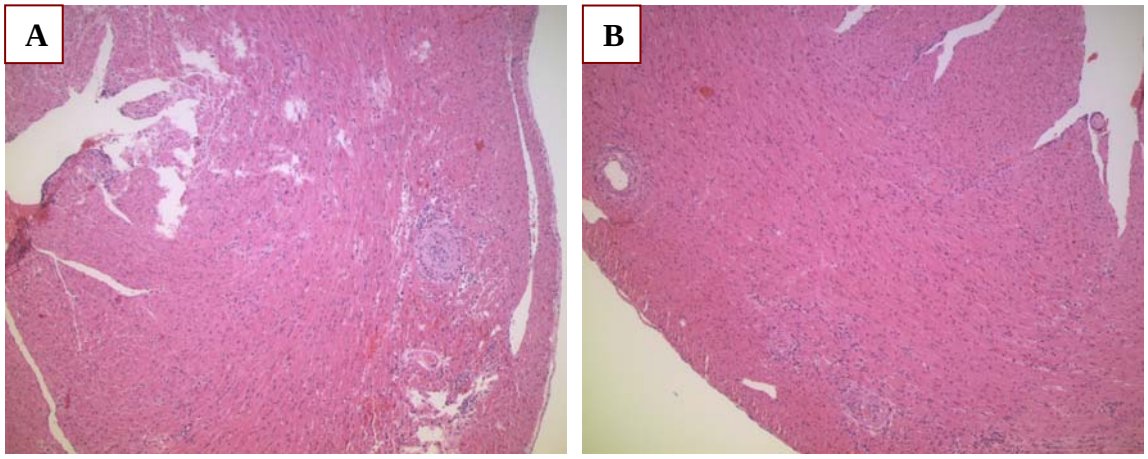

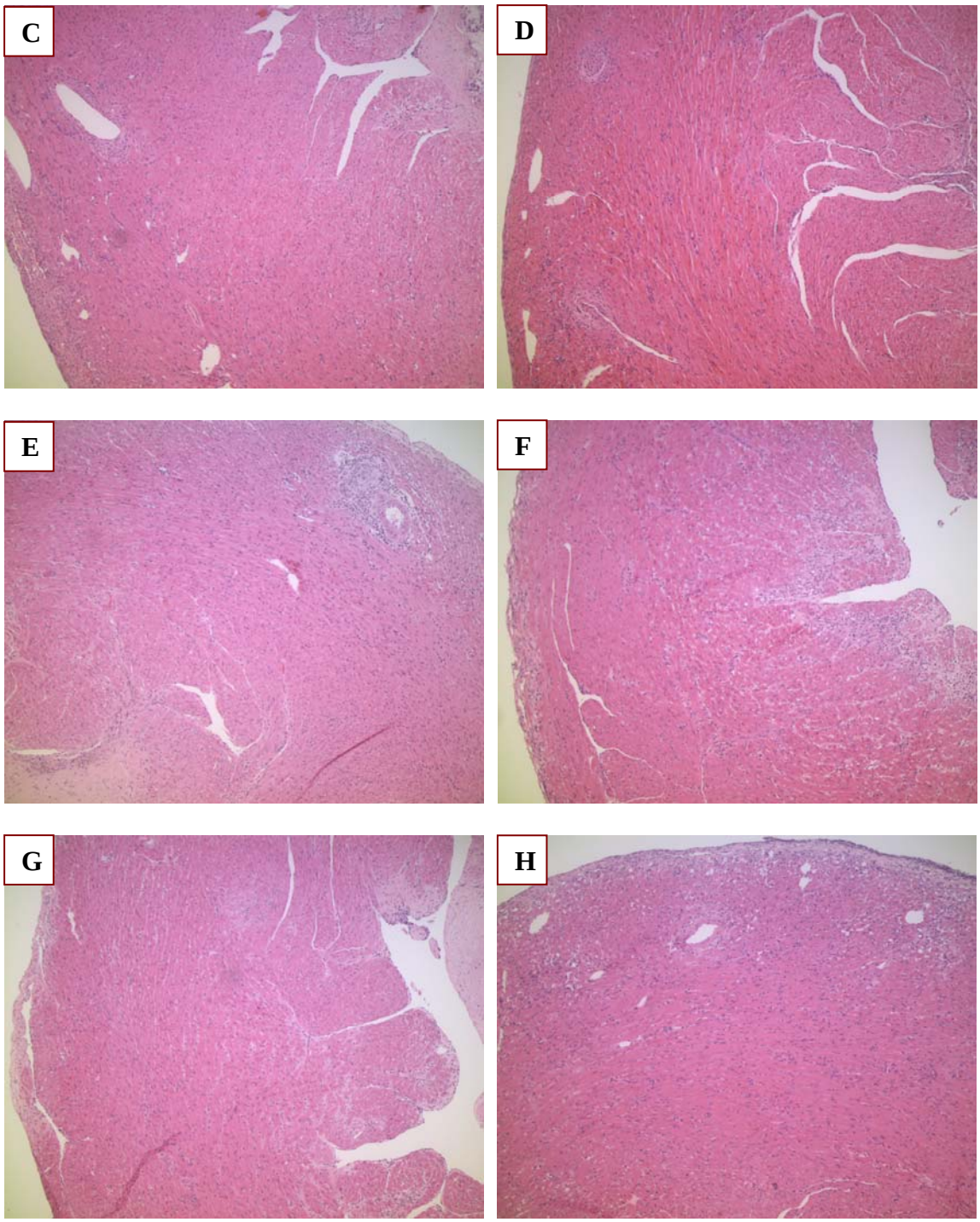

Figure 47 Mild-inflammation developed in both transgenic and wild-type donor.

All of the grafts were harvested at 60 days after transplantation and the grafts were functional well. A, B: HB45, eNOS transgenic donor; C: HB53, eNOS transgenic donor; D: HB54, eNOS transgenic donor; E: HB62, wild-type

donor; F: HB63, wild-type donor; G: HB64, wild-type donor; H: HB66, wild-type donor. The inflammation grades in the seven grafts are 1A/1B.

Moreover, in the second chronic rejection model, mature intimal thickening was observed in the coronary vessels of wild-type donor grafts, especially in large- and middle-sized vessels (Figure 48). In these vessels, the neointima layer exhibited fibrotic and smooth muscle cell-rich occlusions with some infiltrates. At the same time, some of the vessels developed bubbling occlusion and some vessels are intact. Furthermore, except for the grafts that failed due to technical reasons, the graft survival rate (percentage of the grafts that beated well until harvest at 60 days after transplantation) was high (73.8%). Therefore, this chronic rejection model gave better results.

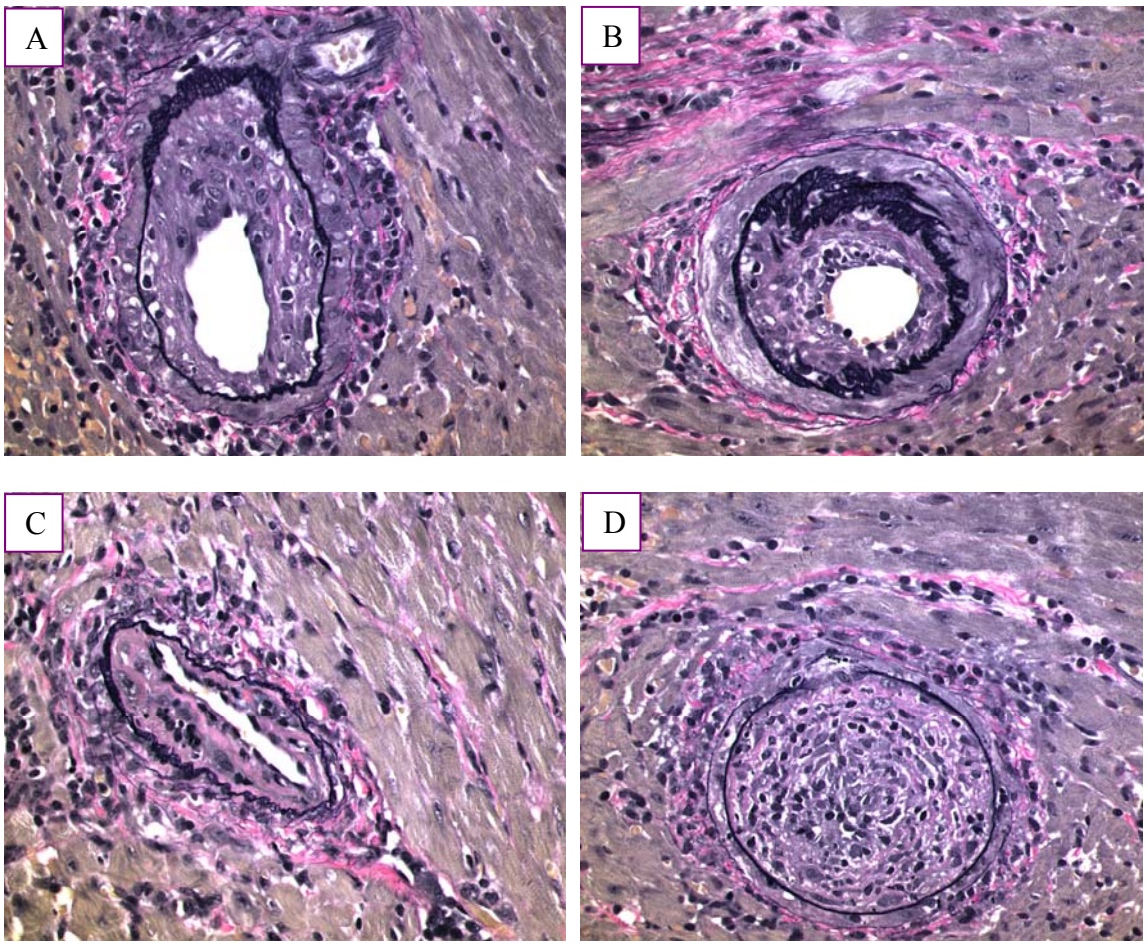

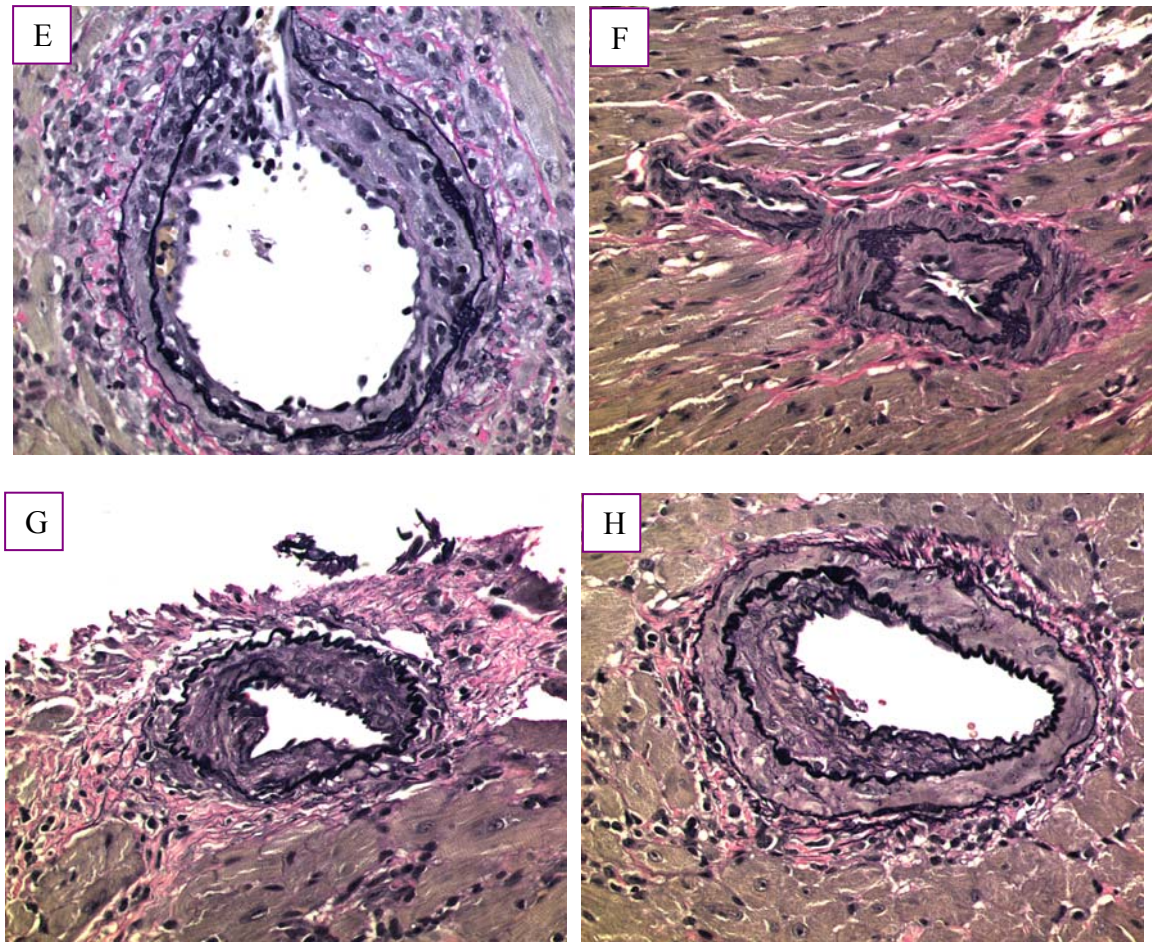

Figure 48 Mature cardiac allograft arteriosclerosis developed in both transgenic and wild-type donor grafts.

A and B: HB53, transgenic donor; C and D: HB54, transgenic donor; E: HB44, wild-type donor; F: HB62, wild-type donor; G: HB63; wild-type donor; H: HB64; wild-type donor.

To determine the effect of endothelial-specific eNOS overexpression on cardiac allograft arteriosclerosis, we compared vessel occlusion between wild-type and transgenic grafts. The genotype of both donor and recipient mice was confirmed by PCR using the human specific eNOS primer as suggested by Dr. Crom (159). Figure 49 shows that HB45, HB53 and HB54 donors are transgenic by PCR. We also confirmed that the human eNOS protein was overexpressed in transgenic donors by immunohistochemistry, as represented in Figure 50.

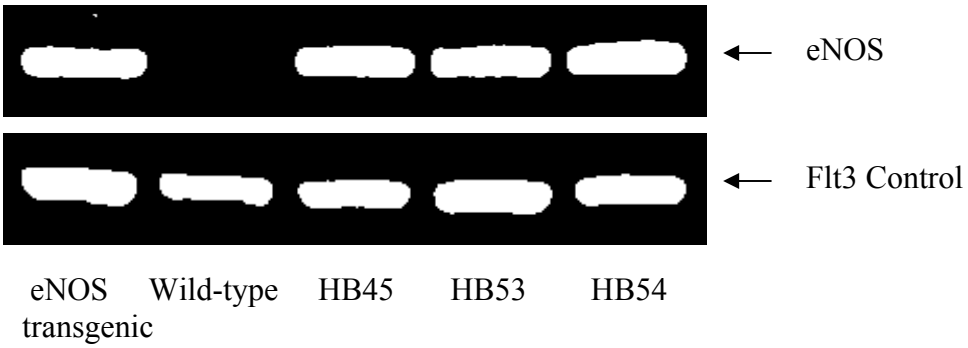

Figure 49 PCR results show that HB45, HB53 and HB54 donors were eNOS transgenic.

From left to right, 1: eNOS transgenic control; 2: wild-type control; 3: HB45 donor; 4: HB53 donor; 5: HB54 donor.

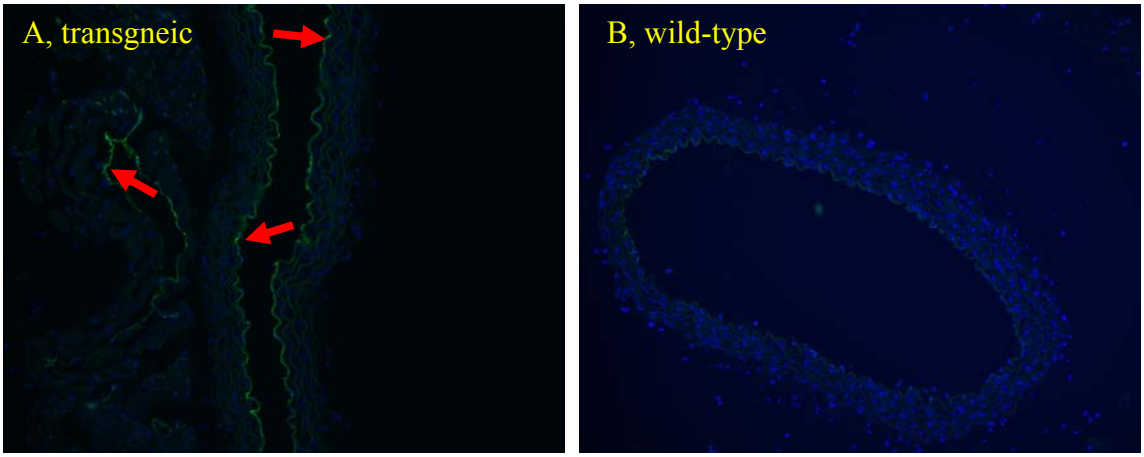

Figure 50 Immunohistochemistry confirmed that eNOS protein was overexpressed in transgenic donor mouse aorta.

A: HB45 donor aorta, eNOS trasnsgenic; B: HB44 donor aorta, wild-type C57BL/6 mouse.

The functional grafts were harvested at 60 days after transplantation. The method to evaluate vessel occlusion was described in **2.18**. Figure 51 shows percentage of vessel occlusion of three transgenic donor grafts, including HB45, HB53 and HB54, and six wild-type donor grafts, including HB44, HB62, HB63, HB64, HB65 and HB66. Figure 52 shows the mean and standard deviation of the mean of the six wild-type and three transgenic grafts. Vessel occlusion

in the transgenic grafts was not significantly different from that of wild-type grafts. We also graded the vessel occlusion according to the method described by Dr. Anthony J. Demetris (175) on **2.18**. As shown in Figure 53, the grade of vessel occlusion correlated very well with the percentage of vessel occlusion. The grade of vessel occlusion was not significantly different between transgenic and wild-type grafts.

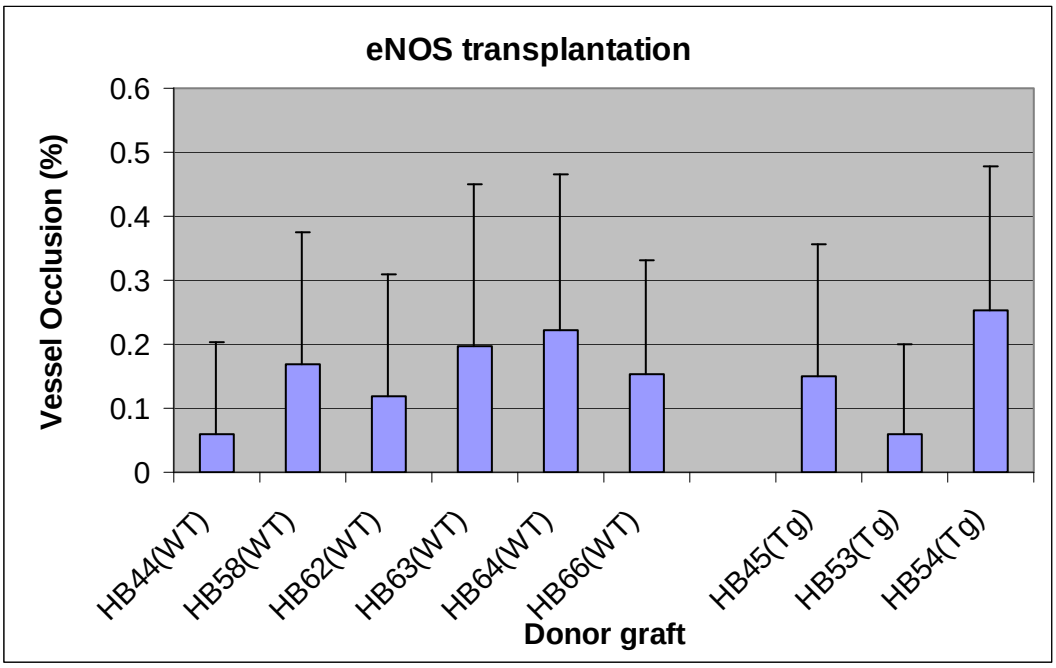

Figure 51 Vessel occlusion developed in transgenic and wild-type donor grafts.

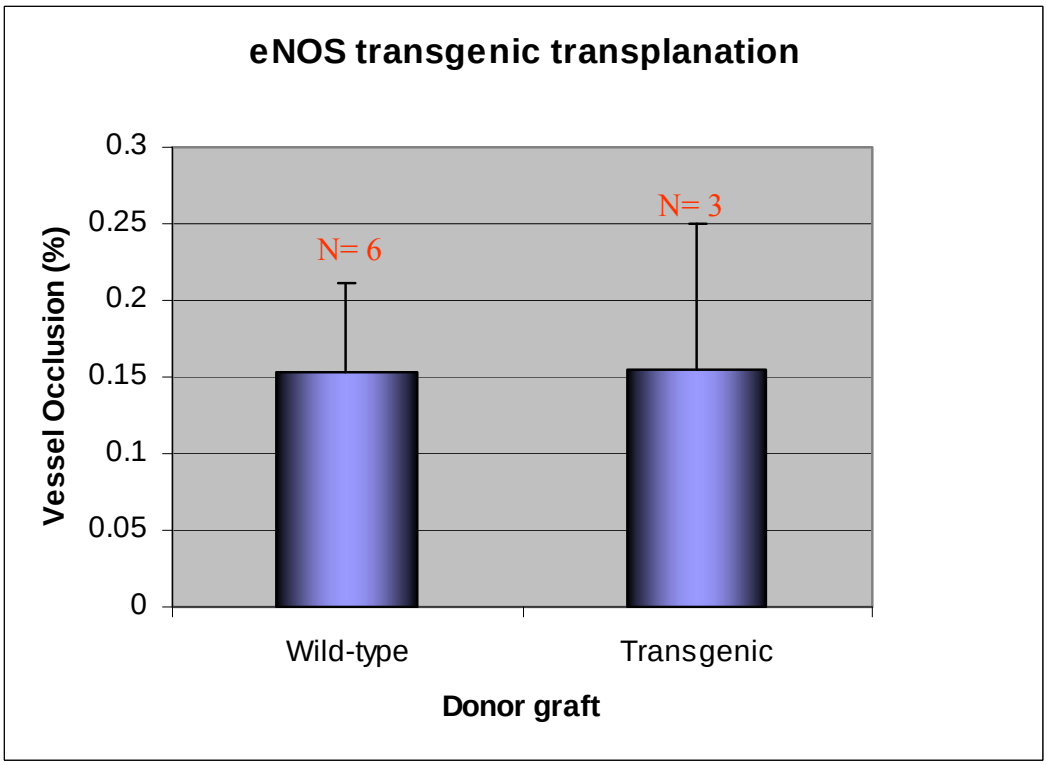

Figure 52 Vessel occlusion in wild-type and eNOS transgenic donor grafts did not show significant difference.

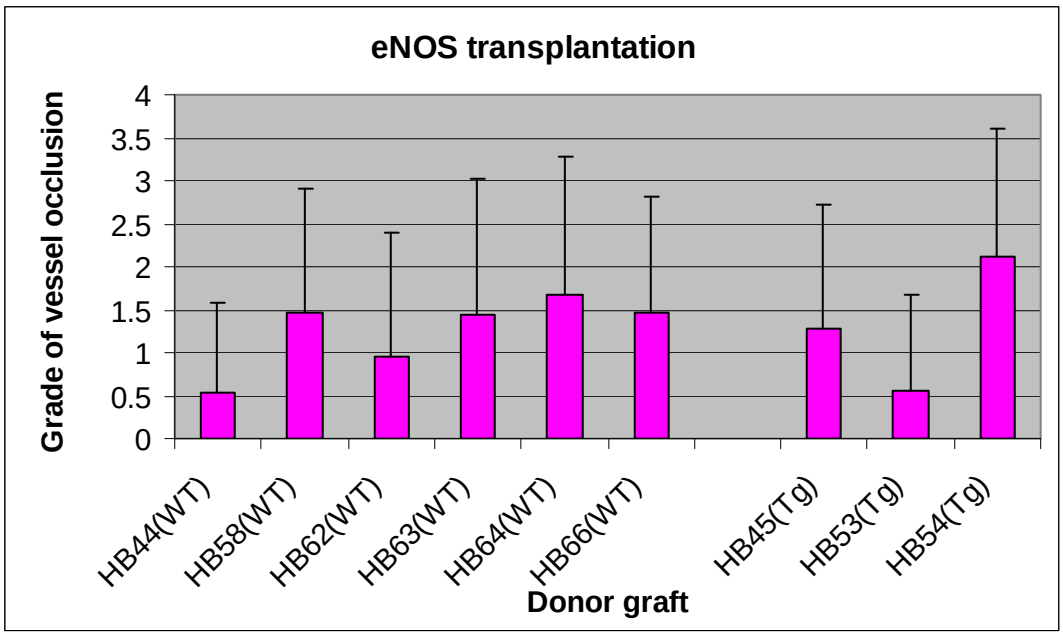

Figure 53 Grade of vessel occlusion in transgenic and wild-type donor grafts.

4.1.4 Conclusion

We successfully developed a mouse chronic rejection model, in which male and female C57BL/6 mice were used as donor and recipient, respectively. In this chronic rejection model, modest cardiac allograft arteriosclerosis developed at 60 days after transplantation and mild inflammation was seen in the graft tissues. This model mimics the natural development of cardiac allograft arteriosclerosis. Another chronic rejection model we tried involved the use of male C57BL/6 and male C3H/HeOuJ mice as donor and recipient, respectively. Immature cardiac allograft arteriosclerosis and severe inflammation developed in the recipients. The severe inflammation persisted up to 60 and 93 days after transplantation even with FK506. This model did not mimic the natural disease well.

Endothelial-specific overexpression of human eNOS driven by the human eNOS promoter in eNOS transgenic mice did not exhibit significant suppression of cardiac allograft arteriosclerosis.

4.1.5 Discussion

Endothelial overexpression of eNOS in eNOS transgenic/apo E knockout mice has been shown to suppress atherosclerotic lesion by van Haperen *et al.* (159). Paradoxically, in another eNOS transgenic mice line in which the murine preproendothelin-1 promoter regulated the bovine eNOS overexpression, Ozaki *et al.* showed that eNOS overexpression accelerated the atherosclerotic lesion in eNOS/apo E knockout transgenic mice (176). This controversy led to the question: what happens when eNOS is overexpressed in transgenic mice? NO levels in the aorta of eNOS transgenic mice have been shown to be much higher than that of wild-type mice (177).

Meanwhile, superoxide levels in eNOS transgenic mice was significantly upregulated and the amount of (6*R*)-5,6,7,8-tetrahydrobiopterin (BH_4) in the aorta, an essential cofactor of eNOS, significantly decreased, compared to that of wild-type mice (178). The increased superoxide level is likely due to "eNOS uncoupling", when the availability of BH_4 becomes rate-limited. The concept of "eNOS uncoupling" has been studied extensively, which is characterized by a stoichiometric discordance between eNOS protein levels and NO production.

BH_4 plays an important role in the catalytic process of L-arginine oxidation and NO synthesis by eNOS (180). There is one BH_4 binding site in the oxygenase domain of each monomer, so 2 molecules of BH_4 are incorporated into each functional eNOS dimmer (Figure 54, 181). *In vitro* experiments with electron paramagnetic resonance spectroscopy demonstrated that BH_4 stabilizes the dimeric form of the enzyme and donates electrons to the ferrous-dioxygen complex in the oxygenase domain, as the initiating step of L-arginine oxidation. BH_4 forms the protonated trihydrobiopterin cation radical $BH_3^{\cdot}H+$, which is subsequently reduced by electron transfer from eNOS flavins (Figure 55, 177). When BH_4 is limiting, electron transfer from eNOS flavins becomes uncoupled from L-arginine oxidation, the ferrous-dioxygen complex dissociates, and superoxide is produced from the oxygenase domain.

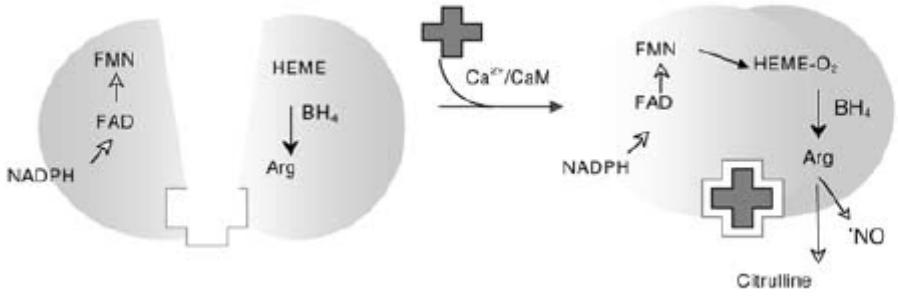

Figure 54 Subunit composition of eNOS. Left panel shows the enzyme in the resting state.

Right panel shows the enzyme in an active form where electrons flow from reductase to oxygenase domain enabling the conversion of L-arginine to †NO and L-citrulline.

To overcome this, Channon et al. developed an eNOS/GTPCH double transgenic mice in which the murine preproendothelin-1 promoter regulates the bovine eNOS overexpression and the murine Tie2LE promoter drives the expression of GTP cyclohydrolyse (GTPCH) (179). The schematic structure of this double transgenic line is shown in Figure 56. GTPCH is a rate-limiting enzyme for the generation of BH_4. Overexpression of GTPCH led to increased level of BH_4 and decreased level of superoxide in eNOS/GTPCH double transgenic mice compared to the eNOS single transgenic mice (177). To evaluate the role of BH_4 on eNOS transgenic mice, the eNOS/GTPCH double transgenic mice were crossed with apo E knockout mice. Overexpression of eNOS in eNOS/GTPCH double transgenic/apo E knockout mice reduced the atherosclerotic lesion compared to that of eNOS transgenic/apo E knockout mice (179). This study supports the notion that BH_4 plays an important role on NO production in eNOS transgenic mice. If BH_4 is deficient, there is no guarantee that the increased eNOS protein will be functional.

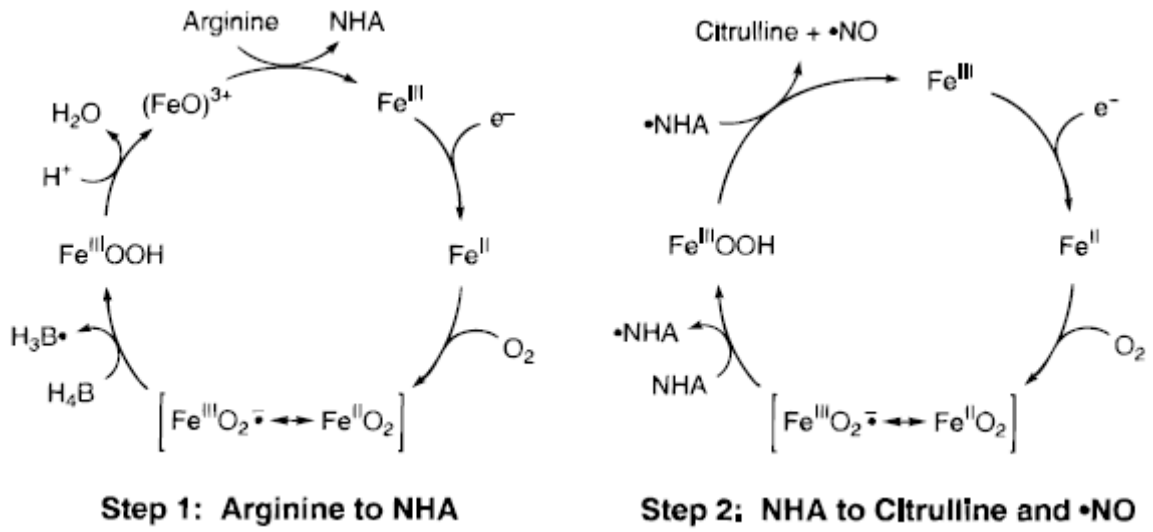

Figure 55 Schematic model for oxidation of L-arginine or NHA by NOS.

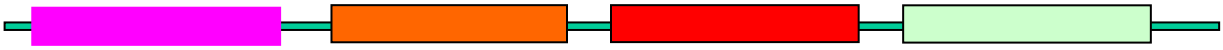

Murine Preproendothelin 1 promoter | Bovine eNOS | Murine Tie2 promoter | Human GTPCH

Figure 56 Schematic structure of eNOS/GTPCH double transgenic mice.

4.2 FUTURE DIRECTIONS

We have imported the eNOS/GTPCH double transgenic mice from Dr. Keith M Channon (Figure 56). We plan to use this transgenic mice as donor and test our hypothesis that **overexpression of eNOS in endothelial cells plays an inhibitory role on the development of cardiac allograft arteriosclerosis.**

Meanwile, we are still developing vascular-specific iNOS inducible transgenic mice. We have obtained two lines of iNOS basal expression transgenic mice, named as TgGeneA-iNOS 88 and TgGeneA-iNOS 110. We will make two more transgenic mice lines TgSMMHC-Switch and TgICAM2-Switch. TgGeneA-iNOS 88 and 110 will be crossed with the vascular-specific Switch transgenic mice with the goal of producing vascular inducible iNOS transgenic mice. If these two lines of mice are successfully generated, we will be able to test if induction of iNOS in endothelial cells or smooth muscle cells will play the dominant role on the development of cardiac allograft arteriosclerosis.

BIBLIOGRAPHY

1. Meiser B. Reichart B. Graft vessel disease: the impact of immunosuppression and possible treatment strategies. Immunology Review 1993; 134: 99-116

2. Sebastian Kerber, Axel Rahmel, Olaf Heinemann-Vechtel, Thomas Budde, Mario Deng, Hans Heinrich Scheld and Günter Breithardt. Angiographic, intravascular ultrasound and functional findings early after orthotopic heart transplantation. International Journal of Cardiology. 1995; 49(2):119-129.

3. Mehra MR. Ventura HO. Smart FW. Stapleton DD. Collins TJ. Ramee SR. Murgo JP. White CJ. New developments in the diagnosis and management of cardiac allograft vasculopathy. Texas Heart Institute Journal 1995; 22(2):138-144.

4. Ardehali A. Heart transplantation: accelerated graft atherosclerosis. Adv. Card. Surg. 1995; 6:195-205.

5. Ventura HO. Smart FW. Stapleton DD. Toups T. Price HL. Cardiac allograft vasculopathy: current concepts. Journal of the Louisiana State Medical Society 1993; 145(5):195-198, 200-202

6. Ventura HO. Mehra MR. Smart FW. Stapleton DD. Cardiac allograft vasculopathy: current concepts. American Heart Journal 1995; 129(4):791-799

7. Kriett JM, Kaye MP. The Registry of the International Society for Heart and Lung Transplantation: eighth official report--1991. J Heart Lung Transplant 1991; 10: 491

8. Turek PL: In Support and Replacement of the Failing Heart Frazier OH (ed): Philadelphia, Penn: Lippincott-Raven; 1996, p 261

9. Tanaka H. Swanson SJ. Sukhova G. Schoen FJ. Libby P. Early proliferation of medial smooth muscle cells in coronary arteries of rabbit cardiac allografts during immunosuppression with cyclosporine A. Transplantation Proceedings. 1995; 27(3): 2062-2065

10. P. Häyry. Common Pathways in Allograft Arteriosclerosis and Experimental Vascular Injury: New Potential Sites of Inhibition. Transplantation proceedings 1998; 30 (3): 685-686

11. Wagner CR, Morris TE, Shipley GD, et al. Regulation of human aortic endothelial cell-derived mesenchymal growth factors by allogeneic lymphocytes in vitro. J. Clin Invest 1993; 92: 1269-1277

12. Zhao, Xiao-Ming. Yeoh, Tiong-Keat. Frist, William H.. Porterfield, Diane L. Miller, Geraldine G. Molecular and Cellular Responses: Induction of Acidic Fibroblast Growth Factor and Full-Length Platelet-Derived Growth Factor Expression in Human Cardiac Allografts: Analysis by PCR, In Situ Hybridization, and Immunohistochemistry. Circulation 1994; 90 (2): 677-685.

13. Hosenpud, Jeffrey D. 2,3,4. Morris, Tony E. 2. Shipley, Gary D. 2,5. Mauck, Kimberly A. 3. Wagner, Cynthia R. CARDIAC ALLOGRAFT VASCULOPATHY: Preferential Regulation of Endothelial Cell-Derived Mesenchymal Growth Factors in Response to a Donor-Specific Cell-Mediated Allogeneic Response. Transplantation 1996; 61(6): 939-948
14. Torry RJ, Labarrere CA, Torry DS, Holt VJ, Faulk WP. Vascular endothelial growth factor expression in transplanted human hearts. Transplantation 1995 Dec 27;60(12):1451-7
15. Suzuki J. Aikawa M, Isobe M, et al. Altered expression of smooth muscle and non-muscle myosin heavy chain isoforms in rejected hearts: a sensitive marker for acute rejection and graft conornary arteriosclerosis. Transplantation proceedings. 1995; 27: 578.
16. Anne Raisaner-Sokolowski and Pekka Hayry. Chronic allograft arteriosclerosis: contributing factors and molecular mechanisms in the light of experimental studies. Transplant immunology 1996; 4: 91-98.
17. Motomura No, Lou H, Maurice P, Foegh ML. Acceleration of arteriosclerosis of the rat aorta allograft by insulin growth factor-1. Transplantation 1997; 63: 932
18. Lin H, Wilson JE, Roberts CR, Horley KJ, Winters GL, Costanzo MR, McManus BM. Biglycan, decorin, and versican protein expression patterns in coronary arteriopathy of human cardiac allograft: distinctness as compared to native atherosclerosis. J Heart Lung Transplant. 1996 Dec;15(12):1233-47.
19. Ignoltz R, Massague J. Transforming growth factor-beta stimulates the expression of fibronectin and collagen and their incorporation into the extracellular matrix. J. Biol Chem 1986; 261; 4337-4345
20. Thyberg J, Blomgren K, Roy J, Tran PK, Hedin U. Phenotypic modulation of smooth muscle cells after arterial injury is associated with changes in the distribution of laminin and fibronectin. J Histochem Cytochem. 1997 Jun;45(6):837-46.
21. Bredt DS, Snyder SH. Nitric oxide, a physiological messenger molecule. Annu Rev Biochem. 1994;63:175-195.
22. Nathan C. Nitric oxide as a secretory product of mammalian cells. FASEB J. 1992;6:3051-3064.
23. Nathan C. Natural resistance and nitric oxide. Cell. 1995;82: 873-876.
24. Moncada S, Higgs A. Mechanisms of Diseases: The L-arginine- nitric oxide pathway. N Engl J Med. 1993;329:2002-2012
25.Georg Kojda, Karin Kottenberg. Regulation of basal myocardial function by NO. Cardiovascular research 1999; 41: 514-523
26. Nathan C, Xie :QW. Nitric oxide synthase: roles, tolls, and controls. [Review] Cell 1994; 78: 915
27. Geller DA, Nussler AK, Di Silvio M, Lowenstein CJ, Shapiro RA, Wang SC, Simmons RL, Billiar TR. Cytokines, endotoxin, and glucocorticoids regulate the expression of inducible nitric oxide synthase in hepatocytes. Proc. Natl. ACAd. Sci. (USA). 1993; 90: 522
28. S. M. Morris, Jr and T. R. Billiar. New insights into the regulation of inducible nitric oxide synthesis. Am J Physiol Endocrinol Metab 1994; 266: E829-E839.
29. Nussler AK, Billiar TR. Inflammation, immunoregulation, and inducible nitric oxide synthase. J. Leukoc. Biol. 1993; 171: 54

30. de Vera ME, Shapiro RA, Nussler AK, Mudgett JS, Simmons RL, Morris SM, Jr., Billiar TR, Geller DA. Transcriptional regulation of human inducible nitric oxide synthase (NOS2) gene by cytokines: initial analysis of the human NOS2 promoter. . Proc. Natl. ACAd. Sci. (USA). 1996; 93: 1054
31. HM Abu-Soud and DJ Stuehr. Nitric Oxide Synthases Reveal a Role for Calmodulin in Controlling Electron Transfer. PNAS 1993; 90: 10769-10772.
32. J Wang, DJ Stuehr, M Ikeda-Saito, and DL Rousseau. Heme coordination and structure of the catalytic site in nitric oxide synthase. J. Biol. Chem., Oct 1993; 268: 22255 - 22258.
33. Garg UC, Hassid A. Nitric oxide-generating vasodilators and 8-bromo-cyclic guanosine monophosphate inhibit mitogenesis and proliferation of cultured rat vascular smooth muscle cells. J Clin Invest. 1989; 83: 1774-1777.
34. Cornwell TL, Arnold E, Boerth NJ, Lincoln TM. Inhibition of smooth muscle cell growth by nitric oxide and activation of cAMP-dependent protein kinase by cGMP. Am J Physiol. 1994; 267: C1405-C1413.
35. Guo J, Panday M, Counsigny P, Lefer A. Mechanisms of vascular preservation by a novel NO donor following rat carotid artery intimal injury. Am J Physiol. 1995; H1122-31
36. Dubey RK, Jackson EK, Luscher TF. Nitric oxide inhibits angiotensin II-induced migration of rat aortic smooth muscle cell. Role of cyclic-nucleotides and angiotensin-1 receptors. J Clin Invest 1995;96:141–149.
37. Sarkar R, Meinberg EG, Stanley JC, Gordon D, Webb RC. Nitric oxide reversibly inhibits the migration of cultured vascular smooth muscle cells. Circ Res. 1996; 78: 225-230.
38. Mellion BT, Ignarro LJ, Myers CB, Ohlstein EH, Ballot BA, Hyman AL, Kadowitz PJ. Inhibition of human platelet aggregation by S-nitrosothiols. Heme-dependent activation of soluble guanylate cyclase and stimulation of cyclic GMP accumulation. Mol Pharmacol. 1983 May;23(3):653-64.
39. McCall TB, Boughton-Smith NK, Palmer RM, Whittle BJ, Moncada S. Synthesis of nitric oxide from L-arginine by neutrophils. Release and interaction with superoxide anion. Biochem J. 1989 Jul 1;261(1):293-6.
40. Radomski MW, Palmer RM, Moncada S. Endogenous nitric oxide inhibits human platelet adhesion to vascular endothelium. Lancet. 1987 Nov 7;2(8567):1057-8.
41. Yan ZQ, Yokota T, Zhang W, Hansson GK. Expression of inducible nitric oxide synthase inhibits platelet adhesion and restores blood flow in the injured artery. Circ Res. 1996 Jul;79(1):38-44.
42. Kubes P, Suzuki M, Granger DN. Nitric oxide: an endogenous modulator of leukocyte adhesion. Proc Natl Acad Sci USA 1991; 88:4651.
43. Suzuki M, Inauen W, Kvietys PR, Grisham MB, Meininger C, Schelling ME, Granger HJ, Granger DN. Superoxide mediates reperfusion-induced leukocyte-endothelial cell interactions. Am J Physiol. 1989 Nov;257(5 Pt 2):H1740-5
44. M.J. Hickey, K.A. Sharkey, E.G. Sihota *et al.*, Inducible nitric oxide synthase-deficient mice have enhanced leukocyte–endothelium interactions in endotoxemia. FASEB J 11 (1997), pp. 955–964.
45. Peng HB, Spiecker M, Liao JK. Inducible Nitric Oxide: An Autoregulatory Feedback Inhibitor of Vascular Inflammation. J Immunol. 1998 Aug 15;161(4):1970-6.

46. Fingerle J, Johnson R, Clowes AW, Majesky MW, Reidy MA. Role of platelets in smooth muscle cell proliferation and migration after vascular injury in rat carotid artery. Proc Natl Acad Sci U S A. 1989 Nov;86(21):8412-6.
47. McEver RP, Cummings RD. Perspectives series: cell adhesion in vascular biology. Role of PSGL-1 binding to selectins in leukocyte recruitment. J Clin Invest. 1997 Aug 1;100(3):485-91.
48. Diacovo TG, deFougerolles AR, Bainton DF, Springer TA. A functional integrin ligand on the surface of platelets: intercellular adhesion molecule-2. J Clin Invest. 1994 Sep;94(3):1243-51
49. Diacovo TG, Roth SJ, Buccola JM, Bainton DF, Springer TA. Neutrophil rolling, arrest, and transmigration across activated, surface-adherent platelets via sequential action of P-selectin and the beta 2-integrin CD11b/CD18. Blood. 1996 Jul 1;88(1):146-57.
50. Ross R, Glomset J, Kariya B, Harker L. A platelet-dependent serum factor that stimulates the proliferation of arterial smooth muscle cells in vitro. Proc Natl Acad Sci U S A. 1974 Apr;71(4):1207-10.
51. Ross R. George Lyman Duff Memorial Lecture. Atherosclerosis: a problem of the biology of arterial wall cells and their interactions with blood components. Arteriosclerosis. 1981 Sep-Oct;1(5):293-311.
52. Mitra AK, Del Core MG, Agrawal DK. Cells, cytokines and cellular immunity in the pathogenesis of fibroproliferative vasculopathies. Can J Physiol Pharmacol. 2005 Aug-Sep;83(8-9):701-15.
53. Suzuki J, Aikawa M, Isobe M, Sekiguchi M, Yazaki Y, Nagai R. Altered expression of smooth muscle and non-muscle myosin heavy chain isoforms in rejected hearts: a sensitive marker for acute rejection and graft coronary arteriosclerosis. Transplant Proc. 1995 Feb;27(1):578.
54. Suzuki J, Isobe M, Aikawa M, Kawauchi M, Shiojima I, Kobayashi N, Tojo A, Suzuki T, Kimura K, Nishikawa T, Sakai T, Sekiguchi M, Yazaki Y, Nagai R. Nonmuscle and smooth muscle myosin heavy chain expression in rejected cardiac allografts. A study in rat and monkey models. Circulation. 1996 Sep 1;94(5):1118-24.
55. Davies MG, Hagen PO. Pathobiology of intimal hyperplasia. Br J Surg. 1994 Sep;81(9):1254-69.
56. Libby P, Sukhova G, Lee RT, Liao JK. Molecular biology of atherosclerosis. Int J Cardiol. 1997 Dec 31;62 Suppl 2:S23-9.
57. Schwartz SM. Perspectives series: cell adhesion in vascular biology. Smooth muscle migration in atherosclerosis and restenosis. J Clin Invest. 1997 Jun 15;99(12):2814-6
58. Faries PL, Marin ML, Veith FJ, Ramirez JA, Suggs WD, Parsons RE, Sanchez LA, Lyon RT. Immunolocalization and temporal distribution of cytokine expression during the development of vein graft intimal hyperplasia in an experimental model. J Vasc Surg. 1996 Sep;24(3):463-71.
59. Tanaka H, Swanson SJ, Sukhova G, Schoen FJ, Libby P. Smooth muscle cells of the coronary arterial tunica media express tumor necrosis factor-alpha and proliferate during acute rejection of rabbit cardiac allografts. Am J Pathol. 1995 Sep;147(3):617-26
60. Ikeda U, Ikeda M, Oohara T, Kano S, Yaguinuma T. Mitogenic action of interleukin-1β on vascular smooth muscle cells mediated by PDGF. Atherosclerosis 1990; 84: 183–8.

61. Nathe TJ, Deou J, Walsh B, Bourns B, Clowes AW, Daum G. Interleukin-1beta inhibits expression of p21(WAF1/CIP1) and p27(KIP1) and enhances proliferation in response to platelet-derived growth factor-BB in smooth muscle cells. Arterioscler Thromb Vasc Biol. 2002 Aug 1;22(8):1293-8
62. Clemmons DR. Interaction of circulating cell-derived and plasma growth factors in stimulating plasma smooth muscle cell replication. J Cell Physiol 1984;121:425.
63. Pfeifle B, Ditschuneit H. Binding and biological actions of insulin-like growth factors on human smooth muscle cells. Horm Metab Res 1982;14:409.
64. Clemmons DR. Interaction of circulating cell-derived and plasma growth factors in stimulating plasma smooth muscle cell replication. J Cell Physiol 1984;121:425.
65. Fujiwara Y, Kaji T. Zinc potentiates the stimulation by basic and acidic fibroblast growth factors on the proliferation of cultured vascular smooth muscle cells. Res Commun Mol Pathol Pharmacol. 1997 Jul;97(1):95-106
66. Lindner V, Lappi DA, Baird A, Majack RA, Reidy MA. Role of basic fibroblast growth factor in vascular lesion formation. Circ Res. 1991 Jan;68(1):106-13
67. Chen Z, Lee FY, Bhalla KN, Wu J. Potent inhibition of platelet-derived growth factor-induced responses in vascular smooth muscle cells by BMS-354825 (dasatinib). Mol Pharmacol. 2006 May;69(5):1527-33. Epub 2006 Jan 25.
68. Jawien A, Bowen-Pope DF, Lindner V, Schwartz SM, Clowes AW. Platelet-derived growth factor promotes smooth muscle migration and intimal thickening in a rat model of balloon angioplasty. J Clin Invest. 1992 Feb;89(2):507-11.
69. Motomura N, Lou H, Maurice P, Foegh ML. Acceleration of arteriosclerosis of the rat aorta allograft by insulin growth factor-I. Transplantation. 1997 Apr 15;63(7):932-6.
70. Wolff RA, Ryomoto M, Stark VE, Malinowski R, Tomas JJ, Stinauer MA, Hullett DA, Hoch JR. Antisense to transforming growth factor-beta1 messenger RNA reduces vein graft intimal hyperplasia and monocyte chemotactic protein 1. J Vasc Surg. 2005 Mar;41(3):498-508
71. Selzman CH, Shames BD, Reznikov LL *et al.* Liposomal delivery of purified inhibitory-κBα inhibits tumor necrosis factor-α-induced human vascular smooth muscle proliferation. Circ. Res. 1999; 84: 867–75.
72. Zimmerman MA, Selzman CH, Reznikov LL, Miller SA, Raeburn CD, Emmick J, Meng X, Harken AH. Lack of TNF-alpha attenuates intimal hyperplasia after mouse carotid artery injury. Am J Physiol Regul Integr Comp Physiol. 2002 Aug;283(2):R505-12
73. Neschis DG, Safford SD, Hanna AK, Fox JC, Golden MA. Antisense basic fibroblast growth factor gene transfer reduces early intimal thickening in a rabbit femoral artery balloon injury model. J Vasc Surg. 1998 Jan;27(1):126-34.
74. Clowes AW, Clowes MM, Reidy MA. Kinetics of cellular proliferation after arterial injury. III. Endothelial and smooth muscle growth in chronically denuded vessels. Lab Invest. 1986 Mar;54(3):295-303.
75. Hasenstab D, Forough R, Clowes AW. Plasminogen activator inhibitor type 1 and tissue inhibitor of metalloproteinases-2 increase after arterial injury in rats. Circ Res. 1997 Apr;80(4):490-6.
76. Bendeck MP, Zempo N, Clowes AW, Galardy RE, Reidy MA. Smooth muscle cell migration and matrix metalloproteinase expression after arterial injury in the rat. Circ Res. 1994 Sep;75(3):539-45.

77. McNamara DB, Bedi B, Aurora H et al. L-arginine inhibits balloon catheter-induced intimal hyperplasia. Biochem Biophys Res Commun 1993; 193: 291-296
78. Guo JP, Milhoan KA, Tuan RS, Lefer AM. Beneficial effect of SPM-5185, a cysteine-containing nitric oxide donor, in rat carotid artery intimal injury. Circ Res 1994 Jul;75(1):77-84
79. Marks DS, Vita JA, Folts Jd *et al*. Inhibition of neointimal proliferation in rabbits after vascular injury by a single treatment with a protein adduct of nitric oxide. J Clin Invest 1995; 96: 2630-2638.
80. Groves PH, Banning AP, Penny WJ et al. The effects of exogenous nitric oxide on smooth muscle cell proliferation following porcine carotid angioplasty. Cardiovasc Res 1995; 30: 87-96
81. J. P. Guo, M. M. Panday, P. M. Consigny, and A. M. Lefer. Mechanisms of vascular preservation by a novel NO donor following rat carotid artery intimal injury. Am J Physiol Heart Circ Physiol 1995; 269: H1122-H1131.
82. Lee JS, Adrie C, Jacob HJ, et al. Chronic inhalation of nitric oxide inhibits neointimal formation after balloon-induced arterial injury. Circ Res 1996; 78: 337-342
83. Tzeng, E., L.L. Shears, P.D. Robbins, B.R. Pitt, D.A. Geller, S.C. Watkins, R.L. Simmons, and T.R. Billiar. Vascular gene transfer of the human inducible nitric oxide synthase: characterization of activity and effects on myointimal hyperplasia. Mol. Med. 1996; 2: 211-225.
84. Shears LL 2nd, Kibbe MR, Murdock AD, Billiar TR, Lizonova A, Kovesdi I, Watkins SC, Tzeng E. Efficient inhibition of intimal hyperplasia by adenovirus-mediated inducible nitric oxide synthase gene transfer to rats and pigs in vivo. J Am Coll Surg 1998 Sep;187(3):295-306
85. Cooney R, Hynes SO, Sharif F, Howard L, O'Brien T. Effect of gene delivery of NOS isoforms on intimal hyperplasia and endothelial regeneration after balloon injury. Gene Ther. 2007 Mar;14(5):396-404. Epub 2006 Nov 2.
86. Pfeiffer T, Wallich M, Sandmann W, Schrader J, Gödecke A. Lipoplex gene transfer of inducible nitric oxide synthase inhibits the reactive intimal hyperplasia after expanded polytetrafluoroethylene bypass grafting. J Vasc Surg. 2006 May;43(5):1021-7
87. Kibbe, Melina R. MD[a]; Tzeng, Edith MD[a]; Gleixner, Susan L. BS[a]; Watkins, Simon C. PhD[b]; Kovesdi, Imre PhD[c]; Lizonova, Alena PhD[c]; Makaroun, Michel S. MD[a]; Billiar, Timothy R. MD[a]; Rhee, Robert Y. Md[a].. Adenovirus-mediated gene transfer of human inducible nitric oxide synthase in porcine vein grafts inhibits intimal hyperplasia. Journal of Vascular Surgery. 2001; 34(1): 156-165
88. Lee, Paul C.5 6; Wang, Zhi Liang2; Qian, Shiguang2; Watkins, Simon C.3; Lizonova, Alena4; Kovesdi, Imre4; Tzeng, Edith6; Simmons, Richard L.6; Billiar, Timothy R.6; Shears, Larry L. II6. Endothelial nitric oxide synthase protects aortic allografts from the development of transplant arteriosclerosis. Transplantation 2000; 69(6): 1186-1192
89. Shears, Larry L. II; Kawaharada, Nobuyoshi; Tzeng, Edith; Billiar, Timothy R.; Watkins, Simmon C.; Kovesdi, Imre; Lizonova, Alena; Pham, Si M. Inducible Nitric Oxide Synthase Suppresses the Development of Allograft Arteriosclerosis. The Journal of Clinical Investigation, Volume 100(8), 1997: 2035-2042

90. Fulton GJ, Davies MG, Barber L, Gray JL, Svendsen E, Hagen PO. Local effects of nitric oxide supplementation and suppression in the development of intimal hyperplasia in experimental vein grafts. Eur J Vasc Endovasc Surg. 1998 Apr;15(4):279-89.
91. Chaux A, Ruan XM, Fishbein MC, Ouyang Y, Kaul S, Pass JA, Matloff JM. Perivascular delivery of a nitric oxide donor inhibits neointimal hyperplasia in vein grafts implanted in the arterial circulation. J Thorac Cardiovasc Surg. 1998 Mar;115(3):604-12.
92. Kibbe MR, Nie S, Yoneyama T, Hatakeyama K, Lizonova A, Kovesdi I, Billiar TR, Tzeng E. Optimization of ex vivo inducible nitric oxide synthase gene transfer to vein grafts. Surgery. 1999 Aug;126(2):323-9.
93. Kown MH, Lijkwan MA, Jahncke CL, Murata S, Rothbard JB, Robbins RC. L-Arginine polymers enhance coronary flow and reduce oxidative stress following cardiac transplantation in rats. J Thorac Cardiovasc Surg. 2003 Oct;126(4):1065-70.
94. West NE, Qian H, Guzik TJ, Black E, Cai S, George SE, Channon KM. Nitric oxide synthase (nNOS) gene transfer modifies venous bypass graft remodeling: effects on vascular smooth muscle cell differentiation and superoxide production. Circulation. 2001 Sep 25;104(13):1526-32.
95. Ziche M, Morbidelli L, Masini E, Amerini S, Granger HJ, Maggi CA, Geppetti P, Ledda F. Nitric oxide mediates angiogenesis in vivo and endothelial cell growth and migration in vitro promoted by substance P. J Clin Invest. 1994 Nov;94(5):2036-44
96. Tzeng E, Billiar TR, Williams DL, Li J, Lizonova A, Kovesdi I, Kim YM. Adenovirus-mediated inducible nitric oxide synthase gene transfer inhibits hepatocyte apoptosis. Surgery. 1998 Aug;124(2):278-83.
97. Lou H, Kodama T, Wang YN, et al. L-arginine prevents heart transplant arteriosclerosis by modulating the vascular cell proliferative response to insulin-like growth factor-I and interleukin-6. J. Heart Lung Transplant. 1996; 15: 1248
98. Kown MH, van Der Steenhoven T, Uemura S, Jahncke CL, Hoyt GE, Rothbard JB, Robbins RC. L-arginine polymer mediated inhibition of graft coronary artery disease after cardiac transplantation. Transplantation. 2001 Jun 15;71(11):1542-8.
99. J. Koglin, J.S. Mudgett and M.E. Russell. Exacerbated Transplant Arteriosclerosis in Inducible Nitric Oxide-Deficient Mice. Circulation, 1998; 97(20): 2059-65
100. Kochanek S, Clemens PR, Mitani K, Chen HH, Chan S, Caskey CT. A new adenoviral vector: Replacement of all viral coding sequences with 28 kb of DNA independently expressing both full-length dystrophin and beta-galactosidase. : Proc Natl Acad Sci U S A 1996 Jun 11;93(12):5731-6
101. Kumar-Singh R, Chamberlain JS. Encapsidated adenovirus minichromosomes allow delivery and expression of a 14 kb dystrophin cDNA to muscle cells. Hum Mol Genet 1996 Jul;5(7):913-21
102. Parks RJ, Chen L, Anton M, Sankar U, Rudnicki MA, Graham FL. A helper-dependent adenovirus vector system: removal of helper virus by Cre-mediated excision of the viral packaging signal. Proc Natl Acad Sci U S A 1996 Nov 26;93(24):13565-70
103. Alemany R, Dai Y, Lou YC, Sethi E, Prokopenko E, Josephs SF, Zhang WW. Complementation of helper-dependent adenoviral vectors: size effects and titer fluctuations. J Virol Methods 1997 Nov;68(2):147-59
104. Hardy S, Kitamura M, Harris-Stansil T, Dai Y, Phipps ML. Construction of adenovirus vectors through Cre-lox recombination. J Virol 1997 Mar;71(3):1842-9

105. Shah AM, Spurgeon HA, Sollott SJ, Talo A, Lakatta EG. 8-bromo-cGMP reduces the myofilament response to Ca2+ in intact cardiac myocytes. Circ Res 1994 May;74(5):970-8
106. Mohan P, Brutsaert DL, Paulus WJ, Sys SU. Myocardial contractile response to nitric oxide and cGMP. Circulation 1996 Mar 15;93(6):1223-9
107. G. Kojda, K. Kottenberg and E. Noack, Inhibition of NO-synthase and soluble guanylate cyclase induces cardiodepressive effects in normal rat hearts. Eur J Pharmacol 1997; 334: 181–190.
108. W.K. Raff, U. Drechsel, J. Scholtholt and W. Lochner, Herzwirkung des Nitroglycerins. Pflug Arch Eur J Physiol 1970; 317:336–343.
109. Strauer and A. Scherpe, Ventricular function and coronary hemodynamics after intravenous nitroglycerin in coronary artery disease. Am Heart J 1978; 95: 210–219.
110. Preckel, G. Kojda, W. Schlack *et al.* Inotropic effects of glyceryl trinitrate and spontaneous NO-donors in the dog heart. Circulation 1997; 96: 2675–2682.
111. Finkel MS, Odis CV, Jacob TD, Watkins SC, Hattler BG, Simmons RL. Negative inotropic effects of cytokines on the heart mediated by nitric oxide. Science. 1992;257:387-389.
112. Roberts AB, Vodovotz Y, Roche NS, Sporn MB, Nathan CF. Role of nitric oxide in antagonistic effects of transforming growth factor-beta and interleukin-1 beta on the beating rate of cultured cardiac myocytes. Mol Endocrinol. 1992 Nov;6(11):1921-30.
113. Adrian J.B. Brady, Philip A. Poole-Wilson, Sian E. Harding, and John B. Warren. Nitric oxide production within cardiac myocytes reduces their contractility in endotoxemia. Nitric Oxide production within cardiac myocytes reduces their contractility in endothoxemia. The American J. Physiology. Vol. 32, 1992:H1963-H1966.
114. Balligand JL, Ungureanu D, Kelly RA, Kobzik L, Pimental D, Michel T, Smith TW. Abnormal contractile function due to induction of nitric oxide synthesis in rat cardiac myocytes follows exposure to activated macrophage-conditioned medium. J Clin Invest. 1993; 91(5): 2314-2319.
115. J.-L. Balligand, D. Ungureanu-Longrois, W.W. Simmons *et al.*, Cytokine-inducible nitric oxide synthase (iNOS) expression in cardiac myocytes. Characterization and regulation of iNOS expression and detection of iNOS activity in single cardiac myocytes in vitro. J Biol Chem 1994; 269: 27580–27588.
116. Pinsky DJ, Cai B, Yang, X, Rodriguez C, sciacca RR, Cannon PJ. The lethal effects of cytokine-induced nitric oxide on cardiac myoctyes are blocked by nitric oxide synthase antagonism or transforming growth factor β. J. Clin Invest 1995; 95: 677-685
117. Mungrue, Imran N. 1,2,3. Gros, Robert 1,2. You, Xiaomang 1,2. Pirani, Asif 2. Azad, Azar 4. Csont, Tamas 5. Schulz, Richard 5. Butany, Jagdish 1. Stewart, Duncan J. 1,3,4. Husain, Mansoor 1,2,3. Cardiomyocyte overexpression of iNOS in mice results in peroxynitrite generation, heart block, and sudden death. J. Clin. Invest. 2002; 109(6): 735-743
118. Yang, Xiaochun; Chowdhury, Nepal; Cai, Bolin; Brett, Jerold; Marboe, Charles; Sciacca, Robert R.; Michler, Robert E.; Cannon, Paul J. Induction of Myocardial Nitric Oxide Synthase by Cardiac Allograft Rejection. 1994; Vol. 94(2): 714-721
119. M. Szabolcs, R.E. Michler, X. Yang *et al*. Cellular and Molecular Cardiovascular Disease: Apoptosis of Cardiac Myocytes During Cardiac Allograft Rejection: Relation to Induction of Nitric Oxide Synthase. Circulation 1996; 94: 1665

120. Lewis, Neil P. MB MPhil, MD, MRCP. Tsao, Philip S. PhD. Rickenbacher, Peter R. MD. Xue, Chun MD PhD. Johns, Roger A. MD. Haywood, Guy A. MB MD, MRCP. von der Leyen, Heiko MD. Trindade, Pedro T. MD. Cooke, John P. MD PhD. Hunt, Sharon A. MD. Billingham, Margaret E. MB FRCPath. Valantine, Hannah A. MB MD, MRCP. Fowler, Michael B. MB MRCP. Induction of Nitric Oxide Synthase in the Human Cardiac Allograft Is Associated With Contractile Dysfunction of the Left Ventricle. Circulation, 1996; 93(4): 720-729
121. Paulus, Walter J. MD, PhD; Kastner, Stefanie BS; Pujadas, Penelope MD; Shah, Ajay M. MD, MRCP; Drexler, Helmut MD; Vanderheyden, Marc MD, Left Ventricular Contractile Effects of Inducible Nitric Oxide Synthase in the Human Allograft. Circulation, 1997; 96(10): 3436-3442
122. NK Worrall, WD Lazenby, TP Misko, TS Lin, CP Rodi, PT Manning, RG Tilton, JR Williamson, and TB Ferguson, Jr. Modulation of in vivo alloreactivity by inhibition of inducible nitric oxide synthase. J. Exp. Med. 1995 181: 63-70.
123. Worrall NK, Misko TP, Sullivan PM, Hui JJ, Ferguson TB Jr. Inhibition of inducible nitric oxide synthase attenuates established acute cardiac allograft rejection. Ann Thorac Surg 1996 Aug;62(2):378-85
124. Worrall NK, Pyo RT, Botney MD, Misko TP, Sullivan PM, Alexander DG, Lazenby WD, Ferguson TB. Inflammatory cell-derived NO modulates cardiac allograft contractile and electrophysiological function. Am J Physiol 1997 Jul;273(1 Pt 2):H28-37
125. Soto PF, Jia CX, Rabkin DG, Hart JP, Carter YM, Sardo MJ, Hsu DT, Fisher PE, Pinsky DJ, Spotnitz HM. Improvement of rejection-induced diastolic abnormalities in rat cardiac allografts with inducible nitric oxide synthase inhibition. J Thorac Cardiovasc Surg 2000 Jul;120(1):39-46
126. Szabolcs MJ, Ma N, Athan E, Zhong J, Ming M, Sciacca RR, Husemann J, Albala A, Cannon PJ. Acute cardiac allograft rejection in nitric oxide synthase-2(-/-) and nitric oxide synthase-2(+/+) mice: effects of cellular chimeras on myocardial inflammation and cardiomyocyte damage and apoptosis. Circulation 2001 May 22;103(20):2514-20
127. Hajitou A, Pasqualini R, Arap W. Vascular targeting: recent advances and therapeutic perspectives. Trends Cardiovasc Med. 2006 Apr;16(3):80-8
128. Schlaeger TM, Bartunkova S, Lawitts JA, Teichmann G, Risau W, Deutsch U, Sato TN. Uniform vascular-endothelial-cell-specific gene expression in both embryonic and adult transgenic mice. Proc Natl Acad Sci U S A 1997 Apr 1;94(7):3058-63
129. Cowan PJ, Shinkel TA, Witort EJ, Barlow H, Pearse MJ, d'Apice AJ. Targeting gene expression to endothelial cells in transgenic mice using the human intercellular adhesion molecule 2 promoter. Transplantation 1996 Jul 27;62(2):155-60
130. Aird WC, Jahroudi N, Weiler-Guettler H, Rayburn HB, Rosenberg RD. Human von Willebrand factor gene sequences target expression to a subpopulation of endothelial cells in transgenic mice. Proc Natl Acad Sci U S A. 1995 May 9;92(10):4567-71.
131. Gory S, Vernet M, Laurent M, Dejana E, Dalmon J, Huber P. The vascular endothelial-cadherin promoter directs endothelial-specific expression in transgenic mice. Blood 1999 Jan 1;93(1):184-92
132. Harats D, Kurihara H, Belloni P, Oakley H, Ziober A, Ackley D, Cain G, Kurihara Y, Lawn R, Sigal E. Targeting gene expression to the vascular wall in transgenic mice using the murine preproendothelin-1 promoter. J Clin Invest. 1995 Mar;95(3):1335-44

133. Shindo T, Kurihara H, Maemura K, Kurihara Y, Kuwaki T, Izumida T, Minamino N, Ju KH, Morita H, Oh-hashi Y, Kumada M, Kangawa K, Nagai R, Yazaki Y. Hypotension and resistance to lipopolysaccharide-induced shock in transgenic mice overexpressing adrenomedullin in their vasculature. Circulation. 2000 May 16;101(19):2309-16
134. Madsen CS, Regan CP, Hungerford JE, White SL, Manabe I, Owens GK. Smooth muscle-specific expression of the smooth muscle myosin heavy chain gene in transgenic mice requires 5'-flanking and first intronic DNA sequence. Circ Res 1998 May 4;82(8):908-17
135. Wolfgang M. Franz, Oliver J. Mueller, Michaela Fleischmann, Philip Babij, Norbert Frey, Matthias Mueller, Urban Besenfelder, Antoon F. M. Moorman, Gottfried Brem and Hugo A. Katus The 2.3 kb smooth muscle myosin heavy chain promoter directs gene expression into the vascular system of transgenic mice and rabbits. Cardiacvascular Research; 43(4): 1040-1048
136. Kim, S., H.S. Ip, M.M. Lu, C. Clendenin, and M.S. Parmacek. A serum response factor-dependent transcriptional regulatory program identifies distinct smooth muscle cell sublineages. Mol. Cell. Biol. 1997;17:2266-2278.
137. Kaoru Morishita, Daniel E. Johnson, and Lewis T. Williams. A novel promoter for vascular endothelial growth factor receptor (flt-1) that confers endothelial-specific gene expression. J Biol Chem. 1995 Nov 17;270(46):27948-53.
138. Nicklin SA, Reynolds PN, Brosnan MJ, White SJ, Curiel DT, Dominiczak AF, Baker AH. Analysis of cell-specific promoters for viral gene therapy targeted at the vascular endothelium. Hypertension. 2001 Jul;38(1):65-70.
139. Reynolds PN, Nicklin SA, Kaliberova L, Boatman BG, Grizzle WE, Balyasnikova IV, Baker AH, Danilov SM, Curiel DT. Combined transductional and transcriptional targeting improves the specificity of transgene expression in vivo. Nat Biotechnol. 2001 Sep;19(9):838-42.131.
140. Shenk, T. Adenoviridae: the viruses and their replication. 1996. In B.N. Fields et al. (ed.), Fields virology. Raven Press, New York, N.Y. 2111-2148
141. Hill, M., Bett, A. J. , Addison, C.L., Prevec, L. & Graham, F.L. (1995) in Methods in Molecular Genetics, ed. Adolph, K.W. (Academic, San Diego), Vol 7, pp. 13-30
142. Brody, S.L. & Crystal, R.G. Adenovirus-mediated in vivo gene transfer. Ann. N.Y. Acad. Sci 1994; 716: 90-101
143. Bramson, J.L., Graham, F.L. & Gauldie, J. Cur. Opin. Biotechnol. 1995; 6: 590-595
144. McGuire SE, Roman G, Davis RL. Gene expression system in Drosophila: a synthesis of time and space. Trends in Genetics. 2004, August; 20 (8): 384-391
145. Bockamp E, Maringer M, Spangenberg C, Fees S, Fraser S, Eshkind L, Oesch F, Zabel B. Of mice and models: improved animal models for biomedical research. Physiol Genomics. 2002, Dec.3; 11 (3); 115-32. Epub 2002 Dec 3
146. Osterwalder T, Yoon KS, White BH, Keshishian H. A conditional tissue-specific transgene expression system using inducible GAL4. Proc Natl Acad Sci U S A. 2001 Oct 23;98(22):12596-601.
147. Bo J, Yu W, Zhang YM, Demayo FJ, Wei L. Cardiac-specific and ligand-inducible target gene expression in transgenic mice.J Mol Cell Cardiol. 2005 Apr;38(4):685-91.
148. Babij P, Psaltis G, Song D, Kulik J, Mollova N, Abruzzese RV, Nordstrom JL. Blue heart": characterization of a mifepristone-dependent system for conditional gene

expression in genetically modified animals. Biochim Biophys Acta. 2003 May 13;1627(1):15-25.
149. Nordstorm JL. The anti-progestin dependent geneswitch system for regulated gene therapy. Steroids. 2003; 68: 1085-1094
150. Sipo I, Pico AH, Wang X, Eberle J, Petersen I, Weger S, Poller W and Fechner H. J Mol Med, 2006; 84: 215–225
151. Jiang L, Rampalli S, George D, Press C, Bremer EG, O'Gorman MR, Bohn MC. Tight regulation from a single tet-off rAAV vector as demonstrated by flow cytometry and quantitative, real-time PCR. Gene Therapy. 2004 Jul;11(13):1057-67.
152. Oparil S, Levine RL, Chen SJ, Durand J, Chen YF. Sexually dimorphic response of the balloon-injured rat carotid artery to hormone treatment. Circulation. 1997 Mar 4;95(5):1301-7.
153. Inhibition of the protective effect of estrogen by progesterone in experimental atherosclerosis. Atherosclerosis. 1996 Mar;121(1):129-38.
154. Hanke H, Hanke S, Finking G, Muhic-Lohrer A, Muck AO, Schmahl FW, Haasis R, Hombach V. Different effects of estrogen and progesterone on experimental atherosclerosis in female versus male rabbits. Quantification of cellular proliferation by bromodeoxyuridine. Circulation.1996 Jul15;94(2):175-81.
155. Adams MR, Register TC, Golden DL, Wagner JD, Williams JK. Medroxyprogesterone acetate antagonizes inhibitory effects of conjugated equine estrogens on coronary artery atherosclerosis. Arterioscler Thromb Vasc Biol. 1997 Jan;17(1):217-21.
156. Lutucuta S, Tsybouleva N, Ishiyama M, Defreitas G, Wei L, Carabello B, Marian AJ. J Am Coll Cardiol. 2004 Dec 7;44(11):2221-30.
157. von der Leyen HE, Gibbons GH, Morishita R, Lewis NP, Zhang L, Nakajima M, Kaneda Y, Cooke JP, Dzau VJ. Gene therapy inhibiting neointimal vascular lesion: in vivo transfer of endothelial cell nitric oxide synthase gene. Proc Natl Acad Sci U S A 1995 Feb 14;92(4):1137-41
158. Iwata A, Sai S, Nitta Y, Chen M, de Fries-Hallstrand R, Dalesandro J, Thomas R, Allen MD. Liposome-mediated gene transfection of endothelial nitric oxide synthase reduces endothelial activation and leukocyte infiltration in transplanted hearts. Circulation. 2001 Jun 5;103(22):2753-9.
159. van Haperen R, de Waard M, van Deel E, Mees B, Kutryk M, van Aken T, Hamming J, Grosveld F, Duncker DJ, de Crom R. Reduction of blood pressure, plasma cholesterol, and atherosclerosis by elevated endothelial nitric oxide. J Biol Chem. 2002 Dec 13;277(50):48803-7. Epub 2002 Oct 2.
160. Ono K, Lindsey ES. Improved technique of heart transplantation in rats. J Thorac Cardiovasc Surg 1969; 57: 225161. Cowan PJ, Shinkel TA, Witort EJ, Barlow H, Pearse MJ, d'Apice AJ.Targeting gene expression to endothelial cells in transgenic mice using the human intercellular adhesion molecule 2 promoter. Transplantation. 1996 Jul 27;62(2):155-60. 162. Cowan PJ, Tsang D, Pedic CM, Abbott LR, Shinkel TA, d'Apice AJ, Pearse MJ. The human ICAM-2 promoter is endothelial cell-specific in vitro and in vivo and contains critical Sp1 and GATA binding sites. J Biol Chem. 1998 May 8;273(19):11737-44. 163. Shinkel TA, Cowan PJ, Barlow H, Aminian A, Romanella M, Lublin DM, Pearse MJ, d'Apice AJ. Expression and functional analysis of glycosyl-phosphatidyl inositol-linked CD46 in transgenic mice. Transplantation. 1998 Dec

15;66(11):1401-6.164. Velasco B, Ramirez JR, Relloso M, Li C, Kumar S, Lopez-Bote JP, Perez-Barriocanal F, Lopez-Novoa JM, Cowan PJ, d'Apice AJ, Bernabeu C. Vascular gene transfer driven by endoglin and ICAM-2 endothelial-specific promoters. Gene Ther. 2001 Jun;8(12):897-904.
165. Cowan PJ, Shinkel TA, Fisicaro N, Godwin JW, Bernabeu C, Almendro N, Rius C, Lonie AJ, Nottle MB, Wigley PL, Paizis K, Pearse MJ, d'Apice AJ. Targeting gene expression to endothelium in transgenic animals: a comparison of the human ICAM-2, PECAM-1 and endoglin promoters. Xenotransplantation. 2003 May;10(3):223-31.
166. R. Schulz, D.L. Panas, R. Catena *et al.*, The role of nitric oxide in cardiac depression induced by interleukin-1β and tumour necrosis factor-α. Br J Pharmacol 1995; 114: 27–34
167. Oh P, Li Y, Durr E, Krasinska KM, Carver LA, Testa JE and Schnitzer JE. Subtractive proteomic mapping of the endothelial surface in lung solid tumours for tissue-specific therapy. Nature, vol. 429, June 2004; 629-635
168. Jahroudi N, Schmaier A, Srikanth S, Mahdi F, Lutka FA, Bowser R. Von Willebrand factor promoter targets the expression of amyloid beta protein precursor to brain vascular endothelial cells of transgenic mice. J Alzheimers Dis. 2003 Apr;5(2):149-58.
169. Minami T, Donovan DJ, Tsai JC, Rosenberg RD, Aird WC. Differential regulation of the von Willebrand factor and Flt-1 promoters in the endothelium of hypoxanthine phosphoribosyltransferase-targeted mice. Blood. 2002 Dec 1;100(12):4019-25. Epub 2002 Aug 1.
170. Gojo S, Niwaya K, Taniguchi S, Nishizaki K, Kitamura S. Gene transfer into the donor heart during cold preservation for heart transplantation. Ann Thorac Surg. 1998 Mar;65(3):647-52.
171. Kypson AP, Peppel K, Akhter SA, Lilly RE, Glower DD, Lefkowitz RJ, Koch WJ. Ex vivo adenovirus-mediated gene transfer to the adult rat heart. J Thorac Cardiovasc Surg. 1998 Mar;115(3):623-30.
172. Yap J, Pellegrini C, O'Brien T, Tazelaar HD, McGregor CG. Conditions of vector delivery improve efficiency of adenoviral-mediated gene transfer to the transplanted heart. Eur J Cardiothorac Surg. 2001 May;19(5):702-7.
173. Adlam D, Bendall JK, De Bono JP, Alp NJ, Khoo J, Nicoli T, Yokoyama M, Kawashima S, Channon KM. Relationships between nitric oxide-mediated endothelial function, eNOS coupling and blood pressure revealed by eNOS-GTP cyclohydrolase 1 double transgenic mice. Exp Physiol. 2007 Jan;92(1):119-26. Epub 2006 Sep 28
174. Uehara S, Chase CM, Cornell LD, Madsen JC, Russell PS, Colvin RB. Chronic cardiac transplant arteriopathy in mice: relationship of alloantibody, C4d deposition and neointimal fibrosis. Am J Transplant. 2007 Jan;7(1):57-65.
175. Demetris AJ, Murase N, Ye Q, Galvao FH, Richert C, Saad R, Pham S, Duquesnoy RJ, Zeevi A, Fung JJ, Starzl TE. Analysis of chronic rejection and obliterative arteriopathy. Possible contributions of donor antigen-presenting cells and lymphatic disruption. Am J Pathol. 1997 Feb;150(2):563-78.
176. Ozaki M, Kawashima S, Yamashita T, Hirase T, Namiki M, Inoue N, Hirata K, Yasui H, Sakurai H, Yoshida Y, Masada M, Yokoyama M. Overexpression of endothelial nitric oxide synthase accelerates atherosclerotic lesion formation in apoE-deficient mice. J Clin Invest. 2002 Aug;110(3):331-40.

177. Hurshman AR, Krebs C, Edmondson DE, Huynh BH, Marletta MA. Formation of a pterin radical in the reaction of the heme domain of inducible nitric oxide synthase with oxygen. Biochemistry. 1999 Nov 30;38(48):15689-96.
178. Bendall JK, Alp NJ, Warrick N, Cai S, Adlam D, Rockett K, Yokoyama M, Kawashima S, Channon KM. Stoichiometric relationships between endothelial tetrahydrobiopterin, endothelial NO synthase (eNOS) activity, and eNOS coupling in vivo: insights from transgenic mice with endothelial-targeted GTP cyclohydrolase 1 and eNOS overexpression. Circ Res. 2005 Oct 28;97(9):864-71. Epub 2005 Sep 22
179. Alp NJ, McAteer MA, Khoo J, Choudhury RP, Channon KM. Increased endothelial tetrahydrobiopterin synthesis by targeted transgenic GTP-cyclohydrolase I overexpression reduces endothelial dysfunction and atherosclerosis in ApoE-knockout mice. Arterioscler Thromb Vasc Biol. 2004 Mar;24(3):445-50. Epub 2004 Jan 5.
180. Alp N, Channon KM. Regulation of endothelial nitric oxide synthase by tetrahydrobiopterin in vascular disease. Aterioscler Thromb Vasc Biol. 2004; 24: 413-420
181. Feldman, P.L., Griffith, O.W. and Stuehr, D.J. (1993) "The surprising life of nitric oxide", Chem. Eng. News December 20, 26–38
182. Jonas M, Fang JC, Wang JC, Giri S, Elian D, Har-Zahav Y, Ly H, Seifert PA, Popma JJ, Rogers C. In-stent restenosis and remote coronary lesion progression are coupled in cardiac transplant vasculopathy but not in native coronary artery disease. J Am Coll Cardiol. 2006 Aug 1;48(3):453-61. Epub 2006 Jul 12.
183. Atkinson C, Southwood M, Pitman R, Phillpotts C, Wallwork J, Goddard M. Angiogenesis occurs within the intimal proliferation that characterizes transplant coronary artery vasculopathy. J Heart Lung Transplant. 2005 May;24(5):551-8.
184. Krasnykh V, Dmitriev I, Mikheeva G, Miller CR, Belousova N, Curiel DT. Characterization of an adenovirus vector containing a heterologous peptide epitope in the HI loop of the fiber knob. J Virol 1998 Mar;72(3):1844-52
185. Emmanuelle Vigne, Irene Mahfouz, Jean-Francois Dedieu, Anne Brie, Michel Perricaudet, and Patrice Yeh. RGD Inclusion in the Hexon Monomer Provides Adenovirus Type 5-Based Vectors with a Fiber Knob-Independent Pathway for Infection. Journal of Virology 1999; 73 (6): 5156-5161.
186. TJ Wickham, DM Segal, PW Roelvink, ME Carrion, A Lizonova, GM Lee, and I Kovesdi. Targeted adenovirus gene transfer to endothelial and smooth muscle cells by using bispecific antibodies. J. Virol. 1996 70: 6831-6838.
187. Harari OA, Wickham TJ, Stocker CJ, Kovesdi I, Segal DM, Huehns TY, Sarraf C, Haskard DO. Targeting an adenoviral gene vector to cytokine-activated vascular endothelium via E-selectin. Gene Ther 1999 May;6(5):801-7
188. Reynolds PN, Zinn KR, Gavrilyuk VD, Balyasnikova IV, Rogers BE, Buchsbaum DJ, Wang MH, Miletich DJ, Grizzle WE, Douglas JT, Danilov SM, Curiel DT. A targetable, injectable adenoviral vector for selective gene delivery to pulmonary endothelium in vivo. Mol Ther. 2000 Dec;2(6):562-78.
189. Rodriguez ER; International Society for Heart and Lung Transplantation. The pathology of heart transplant biopsy specimens: revisiting the 1990 ISHLT working formulation. J Heart Lung Transplant. 2003 Jan;22(1):3-15.
190. Dhaliwal A, Thohan V. Cardiac allograft vasculopathy: the Achilles' heel of long-term survival after cardiac transplantation. Curr Atheroscler Rep. 2006 Mar;8(2):119-30

191. Billingham, ME. Cardiac transplant atherosclerosis. *Transplant Proc* 1987, 4(suppl 5),19-25
192. Ramzy D, Rao V, Brahm J, Miriuka S, Delgado D, Ross HJ. Cardiac allograft vasculopathy: a review. Can J Surg. 2005 Aug;48(4):319-27
193. Lim TT, Liang DH, Botas J, Schroeder JS, Oesterle SN, Yeung AC. Role of compensatory enlargement and shrinkage in transplant coronary artery disease. Serial intravascular ultrasound study. Circulation. 1997 Feb 18;95(4):855-9.
194. Tsutsui H, Ziada KM, Schoenhagen P, Iyisoy A, Magyar WA, Crowe TD, Klingensmith JD, Vince DG, Rincon G, Hobbs RE, Yamagishi M, Nissen SE, Tuzcu EM. Lumen loss in transplant coronary artery disease is a biphasic process involving early intimal thickening and late constrictive remodeling: results from a 5-year serial intravascular ultrasound study. Circulation. 2001 Aug 7;104(6):653-7.
195. Labarrere CA, Nelson DR, Miller SJ, Nieto JM, Conner JA, Pitts DE, Kirlin PC, Halbrook HG. Value of serum-soluble intercellular adhesion molecule-1 for the noninvasive risk assessment of transplant coronary artery disease, posttransplant ischemic events, and cardiac graft failure. Circulation. 2000 Sep 26;102(13):1549-55
196. Rabin BS, Griffith BP, Hardesty RL. Vascular endothelial cell HLA-DR antigen and myocyte necrosis in human allograft rejection. J Heart Transplant. 1985 May;4(3):293-5
197. Zhao XM, Hu Y, Miller GG, Mitchell RN, Libby P. Association of thrombospondin-1 and cardiac allograft vasculopathy in human cardiac allografts. Circulation. 2001 Jan 30;103(4):525-31
198. Shoskes DA, Parfrey NA, Halloran PF. Increased major histocompatibility complex antigen expression in unilateral ischemic acute tubular necrosis in the mouse. Transplantation. 1990 Jan;49(1):201-7.
199. Radovancevic B, Birovljev S, Vega JD, Lonquist JL, Sweeney MS, Vasiljevic JD, Van Buren CT, Kerman RH, Frazier OH. Inverse relationship between human leukocyte antigen match and development of coronary artery disease. Transplant Proc. 1991 Feb;23(1 Pt 2):1144-5.
200. Costanzo-Nordin MR. Cardiac allograft vasculopathy: relationship with acute cellular rejection and histocompatibility. J Heart Lung Transplant. 1992 May-Jun;11(3 Pt 2):S90-103.
201. Hammond EH, Yowell RL, Price GD, Menlove RL, Olsen SL, O'Connell JB, Bristow MR, Doty DB, Millar RC, Karwande SV, et al. Vascular rejection and its relationship to allograft coronary artery disease. J Heart Lung Transplant. 1992 May-Jun;11(3 Pt 2):S111-9.
202. Costanzo-Nordin MR. Cardiac allograft vasculopathy: relationship with acute cellular rejection and histocompatibility. J Heart Lung Transplant. 1992 May-Jun;11(3 Pt 2):S90-103.
203. Uretsky BF, Murali S, Reddy PS, Rabin B, Lee A, Griffith BP, Hardesty RL, Trento A, Bahnson HT. Circulation. Development of coronary artery disease in cardiac transplant patients receiving immunosuppressive therapy with cyclosporine and prednisone. 1987 Oct;76(4):827-34.
204. Schütz A, Kemkes BM, Kugler C, Angermann C, Schad N, Rienmüller R, Fritsch S, Anthuber M, Neumaier P, Gokel JM. The influence of rejection episodes on the development of coronary artery disease after heart transplantation. Eur J Cardiothorac Surg. 1990;4(6):300-7; discussion 308

205. Mehra MR, Ventura HO, Chambers R, Collins TJ, Ramee SR, Kates MA, Smart FW, Stapleton DD. Predictive model to assess risk for cardiac allograft vasculopathy: an intravascular ultrasound study. J Am Coll Cardiol. 1995 Nov 15;26(6):1537-44.
206. Gohra H, McDonald TO, Verrier ED, Aziz S. Endothelial loss and regeneration in a model of transplant arteriosclerosis. Transplantation. 1995 Jul 15;60(1):96-102.
207. Grattan MT, Moreno-Cabral CE, Starnes VA, Oyer PE, Stinson EB, Shumway NE. Cytomegalovirus infection is associated with cardiac allograft rejection and atherosclerosis. JAMA. 1989 Jun 23-30;261(24):3561-6
208. Weis M, Kledal TN, Lin KY, Panchal SN, Gao SZ, Valantine HA, Mocarski ES, Cooke JP. Cytomegalovirus infection impairs the nitric oxide synthase pathway: role of asymmetric dimethylarginine in transplant arteriosclerosis. Circulation. 2004 Feb 3;109(4):500-5. Epub 2004 Jan 19.
209. Costanzo MR, Naftel DC, Pritzker MR, Heilman JK 3rd, Boehmer JP, Brozena SC, Dec GW, Ventura HO, Kirklin JK, Bourge RC, Miller LW. Heart transplant coronary artery disease detected by coronary angiography: a multiinstitutional study of preoperative donor and recipient risk factors. Cardiac Transplant Research Database. J Heart Lung Transplant. 1998 Aug;17(8):744-53.
210. Rickenbacher PR, Kemna MS, Pinto FJ, Hunt SA, Alderman EL, Schroeder JS, Stinson EB, Popp RL, Chen I, Reaven G, Valantine HA. Coronary artery intimal thickening in the transplanted heart. An in vivo intracoronary untrasound study of immunologic and metabolic risk factors. Transplantation. 1996 Jan 15;61(1):46-53.
211. Kobashigawa JA, Katznelson S, Laks H, Johnson JA, Yeatman L, Wang XM, Chia D, Terasaki PI, Sabad A, Cogert GA et al. Effect of pravastatin on outcomes after cardiac transplantation. N Engl J Med. 1995 Sep 7;333(10):621-7.
212. Berger PB, Jones JD, Olson LJ, Edwards BS, Frantz RP, Rodeheffer RJ, Kottke BA, Daly RC, McGregor CG. Increase in total plasma homocysteine concentration after cardiac transplantation. Mayo Clin Proc. 1995 Feb;70(2):125-31.
213. Arnadottir M, Hultburg B, Vladov V, Nilsson-Ehle P, Thysell H. Hyperhomocysteinemia in cyclosporing-treated renal transplant recipients. Transplantation. 199 Feb 15; 61(3):509-12
214. Ambrosi P, Garçon D, Riberi A, Habib G, Barlatier A, Kreitmann B, Rolland PH, Bouvenot G, Luccioni R, Métras D. Association of mild hyperhomocysteinemia with cardiac graft vascular disease. Atherosclerosis. 1998 Jun;138(2):347-50
215. Gupta A, Moustapha A, Jacobsen DW, Goormastic M, Tuzcu EM, Hobbs R, Young J, James K, McCarthy P, van Lente F, Green R, Robinson K. High homocysteine, low folate, and low vitamin B6 concentrations: prevalent risk factors for vascular disease in heart transplant recipients. Transplantation. 1998 Feb 27;65(4):544-50.
216. Valantine H, Rickenbacker P, Kemna M, Hunt S, Chen YD, Reaven G, Stinson EB. Metabolic abnormalities characteristic of dysmetabolic syndrome predict the development of transplant coronary artery disease: a prospective study. Circulation. 2001 May 1;103(17):2144-52.
217. Day JD, Rayburn BK, Gaudin PB, Baldwin WM 3rd, Lowenstein CJ, Kasper EK, Baughman KL, Baumgartner WA, Hutchins GM, Hruban RH. Cardiac allograft vasculopathy: the central pathogenetic role of ischemia-induced endothelial cell injury. J Heart Lung Transplant. 1995 Nov-Dec;14(6 Pt 2):S142-9.

218. Behrendt D, Ganz P, Fang JC. Cardiac allograft vasculopathy. Curr Opin Cardiol. 2000 Nov;15(6):422-9.
219. Okada K, Nishida Y, Murakami H, Sugimoto I, Kosaka H, Morita H, Yamashita C, Okada M. Role of endogenous endothelin in the development of graft arteriosclerosis in rat cardiac allografts: antiproliferative effects of bosentan, a nonselective endothelin receptor antagonist. Circulation. 1998 Jun 16;97(23):2346-51.
220. Yamaguchi A, Miniati DN, Hirata K, Hoyt EG, Robbins RC. Ex vivo blockade of endothelin-1 inhibits graft coronary artery disease in a rodent cardiac allograft model. J Heart Lung Transplant. 2002 Apr;21(4):417-24.
221. Calabró P, Willerson JT, Yeh ET. Inflammatory cytokines stimulated C-reactive protein production by human coronary artery smooth muscle cells. Circulation. 2003 Oct 21;108(16):1930-2. Epub 2003 Oct 6.
222. Verma S, Wang CH, Li SH, Dumont AS, Fedak PW, Badiwala MV, Dhillon B, Weisel RD, Li RK, Mickle DA, Stewart DJ. A self-fulfilling prophecy: C-reactive protein attenuates nitric oxide production and inhibits angiogenesis. Circulation. 2002 Aug 20;106(8):913-9.
223. Wang CH, Li SH, Weisel RD, Fedak PW, Dumont AS, Szmitko P, Li RK, Mickle DA, Verma S. C-reactive protein upregulates angiotensin type 1 receptors in vascular smooth muscle. Circulation. 2003 Apr 8;107(13):1783-90. Epub 2003 Mar 17.
224. Tsukioka K, Suzuki J, Kawauchi M, Wada Y, Zhang T, Nishio A, Koide N, Endoh M, Takayama K, Takamoto S, Isobe M, Amano J. Expression of membrane-type 1 matrix metalloproteinase in coronary vessels of allotransplanted primate hearts. J Heart Lung Transplant. 2000 Dec;19(12):1193-8.
225. Yamani MH, Tuzcu EM, Starling RC, Ratliff NB, Yu Y, Vince DG, Powell K, Cook D, McCarthy P, Young JB. Myocardial ischemic injury after heart transplantation is associated with upregulation of vitronectin receptor (alpha(v)beta3), activation of the matrix metalloproteinase induction system, and subsequent development of coronary vasculopathy. Circulation. 2002 Apr 23;105(16):1955-61
226. Tsukioka K, Suzuki J, Fujimori M, Wada Y, Yamaura K, Ito K, Morishita R, Kaneda Y, Isobe M, Amano J. Expression of matrix metalloproteinases in cardiac allograft vasculopathy and its attenuation by anti MMP-2 ribozyme gene transfection. Cardiovasc Res. 2002 Dec;56(3):472-8.
227. Meliss RR, Pethig K, Schmidt A, Heublein B, Harringer W, Karck M, Choritz H, Haverich A. Cardiac allograft vasculopathy: adventitial immunoreactivity for PDGF-B and PDGFr-beta in extra- versus intramural coronary arteries. Transplant Proc. 2001 Feb-Mar;33(1-2):1579-80.
228. Aziz T, Hasleton P, Hann AW, Yonan N, Deiraniya A, Hutchinson IV. Transforming growth factor beta in relation to cardiac allograft vasculopathy after heart transplantation. J Thorac Cardiovasc Surg. 2000 Apr;119(4 Pt 1):700-8.
229. Bendeck MP, Zempo N, Clowes AW, Galardy RE, Reidy MA. Smooth muscle cell migration and matrix metalloproteinase expression after arterial injury in the rat. Circ Res. 1994 Sep;75(3):539-45.
230. Smith JD, Danskine AJ, Rose ML, Yacoub MH. Specificity of lymphocytotoxic antibodies formed after cardiac transplantation and correlation with rejection episodes. Transplantation. 1992 Jun;53(6):1358-62.

231. Petrossian GA, Nichols AB, Marboe CC, Sciacca R, Rose EA, Smith CR, Cannon PJ, Reemtsma K, Powers ER. Relation between survival and development of coronary artery disease and anti-HLA antibodies after cardiac transplantation. Circulation. 1989 Nov;80(5 Pt 2):III122-5.
232. Rose EA, Pepino P, Barr ML, Smith CR, Ratner AJ, Ho E, Berger C. Relation of HLA antibodies and graft atherosclerosis in human cardiac allograft recipients. J Heart Lung Transplant. 1992 May-Jun;11(3 Pt 2):S120-3.
233. Reed EF, Hong B, Ho E, Harris PE, Weinberger J, Suciu-Foca N. Monitoring of soluble HLA alloantigens and anti-HLA antibodies identifies heart allograft recipients at risk of transplant-associated coronary artery disease. Transplantation. 1996 Feb 27;61(4):566-72.
234. Rose EA, Smith CR, Petrossian GA, Barr ML, Reemtsma K. Humoral immune responses after cardiac transplantation: correlation with fatal rejection and graft atherosclerosis. Surgery. 1989 Aug;106(2):203-7; discussion 207-8.
235. Fredrich R, Toyoda M, Czer LS, Galfayan K, Galera O, Trento A, Freimark D, Young S, Jordan SC. The clinical significance of antibodies to human vascular endothelial cells after cardiac transplantation. Transplantation. 1999 Feb 15;67(3):385-91.
236. B. Stein, P. Frank, W. Schmitz, H. Scholz and M. Thoenes. Endotoxin and cytokines induce direct cardiodepressive effects in mammalian cardiomyocytes via induction of nitric oxide synthase. J Mol Cell Cardiol 1996; 28: 1631–1639.
237. Tan Y, Liu F, Li Z, Li S, Huang L. Sequential injection of cationic liposome and plasmid DNA effectively transfects the lung with minimal inflammatory toxicity.
Mol Ther. 2001 May;3(5 Pt 1):673-82.
238. Ma Z, Mi Z, Wilson A, Alber S, Robbins PD, Watkins S, Pitt B, Li S. Redirecting adenovirus to pulmonary endothelium by cationic liposomes. Gene Ther. 2002 Feb;9(3):176-82.
239. Ravalli S, Szabolcs M, Albala A, Michler RE, Cannon PJ. Increased immunoreactive endothelin-1 in human transplant coronary artery disease. Circulation. 1996 Nov 1;94(9):2096-102.